

# DRYMASS project

Progress Report – Year 3 (1 February 2012 to 31 January 2013)

## Summary of the work (max 6000 characters, with spaces)

Briefly describe the activities undertaken in the reporting period and the results achieved.  
Specifically refer to the tasks under execution in that period.

Website of the project: <http://www-ext.lnec.pt/drymass/> (login: drymass; password: Xtv7iqaX).

### Task T1 – Management and coordination

The 4th project meeting took place on 22 June 2012 with the consultant Dr. Leo Pel. The minutes can be found at the website of the project.

In July 2012, a second proposal for reformulation of the project, due to the withdrawal of the initial partner FCT/UNL, had to be submitted because the first, submitted in June 2011, had lost validity. The new proposal (Annex I) was approved by the FCT in October 2012. It is based on: (i) extension of the project for another year; (ii) allocation to LNEC of the funds originally attributed to the FCT/UNL.

The international workshop CRYSPOM III was prepared and took place from 4 to 7 September 2012, in Tróia, as a joint organization of LNEC and the Technical University of Eindhoven (TUE). It had 45 participants from 11 countries. There were 29 oral presentations and 6 posters. The sessions were always full. The presentations had excellent quality and were widely discussed. The program and book of abstracts are attached (Annex II), as well as a summary report by Dr. Leo Pel (Annex III). Further information can be found at <http://www.phys.tue.nl/nfcmr/cryspom/cryspommain.html>.

Two competitive calls were launched in January 2013 for project grants (BI, Licentiate/Master) of 10 and 6 months, respectively.

### Task T3 – Material properties

New drying tests were carried out at four different RH on eleven materials, now including two calcium silicate materials with 80% capillary porosity, and free water surfaces. It was found that the relationship between the CDRP drying rate and porosity is well described, as a first order approximation, by an inverted parabolic function: the drying rate first increases with increasing porosity, and then decreases until the situation of a free water surface (100% porosity) is reached.

The surface morphology of the materials continued to be studied with the 3D optical profilometer. The aim was to verify whether the drying rate could be explained by the dimension of the effective evaporation surface.

These results were presented at the Crispom III meeting. The abstract of the presentation [5] can be found in Annex II (page 61). Further analysis of the results is currently being carried out.

Meanwhile, experience was acquired in the application of 3D optical profilometry to porous building materials. An abstract [1] on some of its possibilities and limitations was submitted to the conference Built Heritage 2013, under the topic "Cutting edge technologies for materials and structural diagnostic". This abstract is included in Annex IV.

#### Task T4 – Soluble salts

The measurement of the vapour permeability of NaCl or NaNO<sub>3</sub> efflorescence-covered specimens of the Ançã limestone, grey limestone and Bentheimer sandstone finished.

A global analysis of all the experimental results (vapour permeability, capillary absorption, drying and vapour pressure) allowed reaching the following main conclusions:

- The influence of the salts on liquid transport can be very relevant and it is due to their effect on the surface tension ( $\sigma$ ) and viscosity ( $\eta$ ) of the solution.
- The obstruction that efflorescence can pose to vapour transport depends on their morphology and is often negligible. Morphology varied with the type of stone and of salt, but showed that it incorporates also a significant component of unpredictability.
- The unsaturated solutions reach saturation at the evaporation front early in the drying process. This means that the slower drying the materials depict for higher salt concentrations cannot be explained by the lower vapour pressure of the initial solution.

A first presentation of these results was carried out at the Crispom III meeting. The corresponding abstract [6] can be found in Annex II (page 29). Afterwards, an article was elaborated and submitted to the journal Transport in Porous Media. The submitted version of the article [4], which is currently under revision, is included in Annex V.

The Na<sub>2</sub>SO<sub>4</sub>-contaminated specimens developed different decay patterns during drying: exfoliation of the Ançã (multilayer), delamination of the grey limestone (unilayer) and efflorescence on the Bentheimer. Some of the experiments were then repeated to try to monitor these alterations in surface morphology by optical profilometry, which is being successfully achieved, as seen in the example presented in Figs. 1 and 2 (Annex IV). An abstract [3] was submitted to the 2013 EGU meeting for presentation and further discussion of the first results, and was accepted. It is included in Annex IV.

The thermal dilation of salt laden samples was measured and a first analysis of the results carried out. It was decided to repeat some of the tests, which is currently being done.

#### Task T5 – Surface layers

The tests on the possible enhancement of the drying rate of porous building materials by the use of coatings were started. The first experiments addressed the influence of one artisanal lime paint in the drying of the lime mortar, the Ançã, the grey limestone, the Bentheimer, one of the calcium silicate materials, and a new stone, the Maastricht limestone, with 42% capillary porosity. The water/lime ratio of the lime paint was selected from preliminary tests which showed how the porosity of the hardened paste varied with its initial water content. The formulation which gave rise to the highest possible porosity was chosen. The subsequent experimental results showed that this lime paint was indeed able to accelerate the drying of some substrate materials.

An abstract on this first work was submitted to the HMC 2013 conference and was accepted. The full article is currently in preparation. The abstract [2] can be found at Annex IV.

#### Task T7 – Dissemination of results

Two presentations [5, 6] were carried out. One journal article [4] and three conference abstracts [1, 2, 3] were submitted.

## **Deviations from the Approved Proposal** (max 4000 characters, with spaces)

If there were deviations in relation to the approved proposal, both from a scientific or financial viewpoint, indicate and justify them. Indicate also major difficulties in implementing the approved work plan, and how they will be overcome. Mention any fund transfers between items (whether or not they require authorization from the FCT) and indicate their reasons.

#### Task T1 – Management and coordination

A fund transfer between the items Consultants (+1500 EUR), Missions (-1000 EUR) and Service Procurement and Acquisitions (-500 EUR) was requested in July 2012 and was subsequently approved by the FCT. It allowed supporting the participation in the CRYSPOM III workshop of three guest speakers.

However, the major deviations from the approved proposal are related to the withdrawal of the FCT/UNL team and the consequent reformulation of the project.

The reformulation proposal was approved by the FCT in October 2012, i.e., in the second half of this 3<sup>rd</sup> year of the project. It can be found at Annex I together with an updated timeline (which had now slight corrections).

With the reformulation, the original funds of the FCT/UNL were transferred to the same items of LNEC's budget. A new fund transfer between items was therefore necessary and was requested to the FCT in November 2012, so that LNEC's budget was in accordance with the reformulation proposal. This fund transfer was authorized a few days later and involved the following items: Human Resources (+8200 EUR); Missions (-7500 EUR); Consultants (+1000 EUR); Service Procurement and Acquisitions (-3700 EUR); Equipment (+2000 EUR).

In the reformulation proposal it was foreseen to extend the current project grant until January 2014. Following clarification from the FCT that it could not be extended beyond 36-months, it was decided to attribute a new grant for the remaining 10 months

The limitations in the experimental support to the project, due to the departure and non-replacement of laboratory technicians, remained this year. This situation is expected to improve in the next year, with the on-going organizational restructuring of LNEC, extension of the project for another year and reinforcement of the research team with the new 6 month grant.

As mentioned, competitive calls for the 10 month and 6 month grants were launched in January 2013.

### Task T3 – Material properties

A definitive causal link was not yet established between the high drying rate that some porous materials show, and the fact that their surface has fractal properties, hence, a much higher effective surface area than the projected surface. This issue is under analysis and the use of complementary experimental techniques, such as BET, is being considered.

One master thesis on the theme of evaporative cooling will be held at LNEC during the next year. It is foreseen to include a practical application of some of the results obtained in task T3 to the subject, currently so relevant, of energy saving.

### Task T6 – Nuclear magnetic resonance

This task had no activity because the NMR equipment of FCT/UNL ceased to be available to this project. It is foreseen to perform work on this subject over the next year at the Technical University of Eindhoven (TUE), in collaboration with the consultant Dr. Leo Pel, as stated in the reformulation proposal. However, the viability, timing and duration of the work depend on the availability at TUE.

## **Publications/presentations**

Mention the situation:

- Published / Presented
- Accepted (for publication / presentation)
- Submitted

For those accepted for presentation or publication, the date of acceptance shall be stated in the description field.

For those that have been published or presented, the URL should be indicated.

[1] Submitted - T. Diaz Gonçalves, V. Brito, "Possibilities and limitations of optical 3D profilometry in the study of porous building materials of the architectural heritage", Abstract submitted to the International Conference Built Heritage 2013 Monitoring Conservation Management, Politecnico di Milano, 18-20 November 2013.

[2] Accepted - Vânia Brito, Teresa Diaz Gonçalves, "Artisanal lime paints and their influence on moisture transport during drying", abstract accepted (December 2012), HMC13 - 3rd Historic Mortars Conference, Glasgow, 11-14 September 2013, full article in preparation.

[3] Accepted - V. Brito, T. Diaz Gonçalves, "Decay patterns of natural stones during drying due to sodium sulphate crystallization: monitoring by a 3D optical technique", Abstract accepted (January 2013), EGU 2013, Session GI3.4 - From Artefact to Historical Site: Geoscience and Non-Invasive Methods for the Study and Conservation of Cultural Heritage. Vienna, 7-12 April 2013.

[4] Submitted, under review - Vânia Brito, Teresa Diaz Gonçalves, "Drying kinetics of porous stones in the presence of NaCl and NaNO<sub>3</sub>. An assessment of the factors affecting liquid and vapour transport", submitted (September 2012) to Transport in Porous Media.

[5] Presented - Teresa Diaz Gonçalves, Vânia Brito, Leo Pel, José Delgado Rodrigues (2012) "Magnitude of the stage I drying rate of porous building materials with different porosity". Workshop CRYSPOM III - Crystallization in Porous Media, joint organization TU/e-LNEC. Tróia, Portugal, September 4-7 (oral). URL: <http://www.phys.tue.nl/nfcmr/cryspom/2012-CryspomIII-abstracts.pdf>.

[6] Presented - Vânia Brito, Teresa Diaz Gonçalves (2012) "Effects of NaCl and NaNO<sub>3</sub> on the capillary suction, drying kinetics and vapour permeability of three building stones". Workshop CRYSPOM III - Crystallization in Porous Media, joint organization TU/e-LNEC. Tróia, Portugal, September 4-7 (oral). URL: <http://www.phys.tue.nl/nfcmr/cryspom/2012-CryspomIII-abstracts.pdf>.

## Annex files

Max 5 files with a total of 10MB

- Annex I – 2<sup>nd</sup> reformulation proposal with updated timeline
- Annex II – Cryspom III - Book of abstracts and conference program
- Annex III – Summary report on Cryspom III
- Annexe IV – Figures and abstracts
- Annexe V – Article submitted to Transport in Porous Media

## Reformulation of the project (2<sup>nd</sup> proposal)

### 1 - Introduction

The DRYMASS project addresses the drying of porous building materials potentially contaminated with soluble salts, and is based on research with a strong experimental component. The Laboratório Nacional de Engenharia Civil (LNEC) is the Principal Contractor and the Faculdade de Ciências e Tecnologia da Universidade Nova de Lisboa (FCT/UNL) the Participating Institution.

The project started on February 2010. Since then, the FCT/UNL team decided to step down, which makes it necessary to reformulate the initial plan. Such reformulation is presented in the following sections and has two main strands:

- (i) extension of the project for one year, to allow compensating the loss of scientific potential and of time due to the absence of the FCT/UNL and to the consequent need to reformulate the project
- (ii) attribution to LNEC of the funds initially allocated to the FCT/UNL, which will be used to finance the project activities during the extra year

The reformulation is aimed at ensuring that the objectives of the project will still be, as much as possible, fulfilled, thereby justifying also the considerable investment already made by LNEC, FCT and the external consultant.

### 2 - Impact on the original objectives of the project

The DRYMASS project has two main technical/scientific objectives and two strategic objectives, as described below.

#### Technical/scientific objectives

- (i) Improve the state-of-the-art knowledge on drying of porous building materials
- (ii) Evaluate the possibility of enhancing the drying of these materials by means of a surface layer that promotes evaporation

#### Strategic objectives

- (iii) Contribute to the implementation of the use of nuclear magnetic resonance (NMR) in Portugal, for the study of civil engineering materials
- (iv) Promote an effective dissemination of results, not only within the international scientific community, but also within the national technical community, hence contributing to the implementation of better conservation practices in Portugal

The reformulation will not affect the two technical/scientific objectives. It will also not affect the second strategic objective which concerns the dissemination of results.

However, the first strategic objective (iii) is significantly impacted by the leaving of the FCT/UNL because it depends on the NMR equipment of this university, which will be no longer available to the project. The proposed reformulation will try to minimize this impact, by promoting, if possible, the training of a young researcher on NMR techniques suitable for building materials. But, in fact, it will not be possible to fully

compensate the losses in this strategic objective. To minimize the effects on the whole project, the importance of the two technical-scientific objectives will be reinforced.

### **3 – Main changes to the project tasks**

#### **3.1 – Tasks T3 and T5**

MIP measurements carried out with the Micromeritics Autopore VI porosimeter of FCT/UNL were foreseen in Tasks T3 and T5. Since this equipment will no longer be available, MIP measurements will be performed with the Quantachrome porosimeter of LNEC. This is a much older equipment (installed in 1992) but it provides reliable information about the pores up to 5  $\mu\text{m}$ . In fact, as the FCT/UNL informed that they had not personnel available to operate its porosimeter, LNEC's equipment had to be used right from the beginning of the project for the measurements made within Task T3, as indicated in the first and second year reports.

#### **3.2 – Task T6**

The main changes concern task T6 (Nuclear Magnetic Resonance) that was to be carried out under the responsibility of FCT/UNL using its new NMR equipment.

To overcome the unavailability of the NMR equipment of FCT/UNL, NMR-monitored drying experiments will be, if possible, carried out at the Technical University of Eindhoven (TUE). For that, the grant holder of the DRYMASS project will stay with the Group Transport in Permeable Media (GTPM) of the Centre for Material Research with Magnetic Resonance – Department of Applied Physics of TUE (<http://www.phys.tue.nl/nfcmr/cmrmmain.html>). The work at TUE will be carried out under the supervision of Dr. Leo Pel, consultant to the DRYMASS project. It is expected that the stay in the Netherlands will last approximately one month. However, it must be noted that the possibility of its realization, as well as the corresponding dates depend on the availability from the GTPM. Because the group is moving facilities, the stay will have to be scheduled later.

The new task T6 will include: (i) study of the fundamentals of NMR; (ii) planning of the NMR-monitored experiments; (iii) stay of the grant holder at TUE; (iv) analysis and treatment of results.

### **4 - Impact on the expected indicators**

Two of the expected indicators of the project concern the work that will no longer be done by the FCT/UNL:

- one paper (international journal) that would be elaborated under task T6;
- the master thesis that would be carried out in the framework of the grant attributed by the FCT/UNL during the first year of the project (said grant was never attributed).

These losses will be compensated by the enhanced importance of the two technical-scientific objectives and a consequent greater effort put in tasks T3 (Materials) and T4 (Soluble Salts), with a corresponding increase of their output results. Overall, it is expected to achieve in these tasks one more paper in an international journal and one more communication to an international conference. Therefore, in quantitative terms, the expected indicators will suffer only a minor change.

### **5 - Budget and justification**

It is proposed, as explained above, to extend the project for one more year and to attribute to LNEC the funds initially allocated to the FCT/UNL (€ 25 736,00). These funds will be redistributed within the extra year (Year 4) of the project.

The reformulated budget of LNEC is presented in the following table. The justification for the new funds is given immediately below the table.

Table - Reformulated budget of LNEC

Description	Original budget (€)			Redistribution of the funds originally allocated to the FCT/UNL (€)	Total (€)
	Year 1	Year 2	Year 3	Year 4	
Human resources	12767	12797	12828	18146	56511
Missions	3500	4000	3000	0	10500
Consultants	1000	1000	2000	1000	5000
Service procurement and acquisitions	1500	1500	1000	300	4300
Patent registration	0	0	0	0	0
Adaptation of buildings and facilities	0	0	0	0	0
Equipment	87275	0	0	2000	89303
<b>TOTAL CURRENT EXPENSES</b>	<b>106042</b>	<b>19297</b>	<b>18828</b>	<b>21446</b>	<b>165614</b>
Overheads	21208	3859	3766	4289	33123
<b>TOTAL</b>	<b>127250</b>	<b>23157</b>	<b>22594</b>	<b>25735</b>	<b>198737</b>

Note: As far as we know, the FCT/UNL never made any expenses within the project. It returned to LNEC, in full, the initial tranche.

### Human resources

The proposed value concerns two grants, in a total of 18 months distributed as follows:

- Prolongation of the current project grant for 12 months (it is convenient to maintain the person presently working in the project, to avoid further losses of scientific potential).
- Attribution of a new 6 month grant (Mestre). The new grant holder will also be engaged in the project as full-time collaborator. He/she should preferably have a background in civil or materials engineering.

In principle, the new grant holder will work mostly in tasks T3 and T5, with pure water. The current grant holder will continue to work with salt solutions, which has greater complexity and requires specific background she has already acquired in the course of the project.

The costs were calculated considering a monthly value of € 980,00 (for the grant) plus € 115.29 (for the voluntary social insurance). The existing positive balance of € 1597,03 in the Human Resources rubric was taken into consideration, as well as an additional of € 28,00 for rounding purposes.

### Missions

The Missions rubric has presently a positive balance of € 7064.29, so it is not necessary to use the new funds in this item. The value still available is, in principle, sufficient to finance any conference missions that come to be necessary, as well as the stay of the grant holder at TUE.

### Consultants

One more visit of Dr. Leo Pel to Portugal is foreseen to help discussing the methods and results of the project. The cost of the visit is estimated in € 1000,00, which includes travel expenses, accommodation and meals.

### Service procurement and acquisitions

The experimental work requires acquisition of materials, laboratory consumables and reagents. These will be necessary for tasks T3, T4, T5 and T6.



## Equipment

- Components and equipment (including a digital camera and a small balance) to assemble a device for simultaneous time-lapse photography and weight monitoring. The device will be used to monitor salt decay processes occurring during drying, for instance, the stone delamination due to sodium sulphate crystallization observed within task T4 in steady state conditions (which is striking, for delamination is usually attributed to the occurrence of wet/dry cycles): € 800,00
- Portable thermohygrometer (Rotronic) to replace older equipment: € 400,00
- Portable computer to be utilized in the course of the project by one of the grant holders (the other will use an available computer): € 600,00
- Acrylic glass boxes with approximate dimensions of 5 cm x 5 cm x 3 cm to use in vapour permeability tests on small samples of porous building materials. LNEC has only 18 of these boxes available, which makes it difficult to schedule and accomplish the tests in a reasonable period of time: € 200,00 (around 20 boxes)

## 6 - New timeline

date: 25 February 2013

Tasks	Person *month	2010												2011												2012												2013												2014
		Feb	Mar	Apr	May	Jun	Jul	Aug	Sep	Oct	Nov	Dec	Jan	Feb	Mar	Apr	May	Jun	Jul	Aug	Sep	Oct	Nov	Dec	Jan	Feb	Mar	Apr	May	Jun	Jul	Aug	Sep	Oct	Nov	Dec	Jan													
T1 - Management and coordination	10	[shaded]												[shaded]												[shaded]												[shaded]												[shaded]
T2 - Preliminary testing of new equipment	2	[shaded]												[shaded]												[shaded]												[shaded]												[shaded]
T3 - Material properties	24	[shaded]												[shaded]												[shaded]												[shaded]												[shaded]
T4 - Soluble salts	16	[shaded]												[shaded]												[shaded]												[shaded]												[shaded]
T5 - Surface layers	18	[shaded]												[shaded]												[shaded]												[shaded]												[shaded]
T6 - Nuclear Magnetic Resonance (NMR)	0	[shaded]												[shaded]												[shaded]												[shaded]												[shaded]
T7 - Dissemin of results	18	[shaded]												[shaded]												[shaded]												[shaded]												[shaded]
Total:	88	[shaded]												[shaded]												[shaded]												[shaded]												[shaded]

1st Progress Report                      2nd Progress Report                      3rd Progress Report                      Final Report

Date: 19 July 2012 (the timeline had corrections in February 2013)

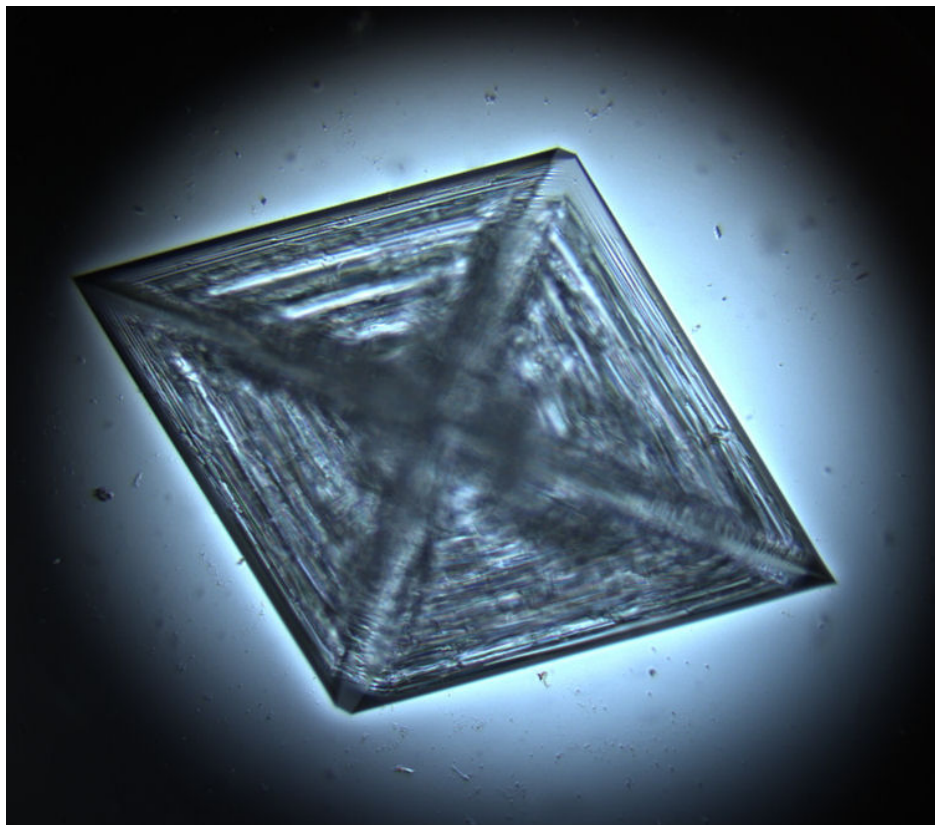
*Teresa Drey Foucalves*

PhD, Principal Investigator of the DRYMASS project

Workshop

# CRYSPOM III

Crystallization in porous media



Tróia, Portugal

4-7 September 2012

### **Workshop Chair**

Leo Pel (TU/e) and Teresa Diaz Gonçalves (LNEC)

### **Organizing committee**

*Department of Applied Physics, Eindhoven University of Technology, The Netherlands*

Leo Pel

Sonia Gupta

*Laboratório Nacional de Engenharia Civil, Lisbon, Portugal*

Teresa Diaz Gonçalves

Vânia Brito

João Manuel Mimoso

Dória Costa

### **Scientific committee**

Leo Pel - TU/e (Netherlands)

Teresa Diaz Gonçalves - LNEC (Portugal)

Jan Carmeliet - ETH (Switzerland)

Noushine Shahidzadeh-Bonn - UVA (Netherlands)

Rosa M. Espinosa-Marzal - ETH (Switzerland)

Wednesday, September 05, 2012

8 : 3 0 – 8 : 4 5	Opening (Leo Pel / Teresa Diaz Gonçalves)	
8 : 4 5 – 9 : 2 5	<u>Jan Carmeliet</u> , Dominique Derome, Hannelore Derluyn, Robert Guyer, Sergey Churakov	Keynote lecture 1 - Sorption and crystallization induced deformation: from molecular dynamics to macroscopic modeling
9 : 2 5 – 9 : 5 0	<u>Andrea Hamilton</u> and Christopher Hall	Atomic Strain Produced From Mirabilite Crystallisation In Sandstone And Calcium Silicate.
9 : 5 0 – 1 0 : 1 5	<u>Francesco Caruso</u> and Robert J. Flatt	A “new” Correns’ experiment
1 0 : 1 5 – 1 0 : 4 0	Julie Desarnaud and <u>Noushine Shahidzadeh-Bonn</u>	Study of the kinetics of salt crystallization during rewetting/drying and humidity cycling
1 0 : 4 0 – 1 1 : 1 0	Coffee break	
1 1 : 1 0 – 1 1 : 5 0	<u>George W. Scherer</u> <sup>1</sup> and Rosa M. Espinosa-Marzal <sup>1,2</sup>	Keynote lecture 2 - Kinetics of crystallization in pores
1 1 : 5 0 – 1 2 : 1 5	Hannelore Derluyn, <u>Dominique Derome</u> , Iwan Jerjen, Jan Dewanckele, Veerle Cnudde, Eberhard Lehmann and Jan Carmeliet	Characterizing salt transport and crystallization damage in porous limestone with neutron radiography and X-ray micro-tomography
1 2 : 1 5 – 1 2 : 4 0	Hannelore Derluyn, Peter Moonen and Jan Carmeliet	Numerical modeling of crystallization induced damage processes
1 2 : 4 0 – 1 3 : 0 5	<u>Eduardo E. Alonso</u> and Anna Ramon	Gypsum crystal growth under bridge foundations
1 3 : 0 5 – 1 4 : 0 5	Lunch	
1 4 : 0 5 – 1 4 : 4 5	<u>Marc Prat</u>	Keynote lecture 3 - How to make crusty or patchy efflorescence
1 4 : 4 5 – 1 5 : 1 0	<u>Sonia Gupta</u> , Henk Huinink and Leo Pel	Effect of ferrocyanide ions on the drying behavior of NaCl contaminated porous material
1 5 : 1 0 – 1 5 : 3 5	<u>Barbara Lubelli</u> , Timo G. Nijland and Rob P.J. van Hees	Effect of inhibitors on sodium sulfate crystallization
1 5 : 3 5 – 1 6 : 0 0	<u>J.M.P.Q. Delgado</u> , A.S. Guimarães and V.P. de Freitas	Salt Transport in Porous Media: Preliminary Experimental and Theoretical Analysis of Salt Diffusion
1 6 : 0 0 – 1 6 : 3 0	Coffee break	
1 6 : 3 0 – 1 6 : 5 5	<u>J. Dewanckele</u> , W. de Boever, T. de Kock, M.A. Boone, M.N. Boone, L. Brabant, G. Fronteau, L. Van Hoorebeke, V. Cnudde and P. Jacobs	Influence of limestone microstructure on gypsum crystallization
1 6 : 5 5 – 1 7 : 2 0	<u>Vânia Brito</u> , Teresa Diaz Gonçalves	Effects of NaCl and NaNO <sub>3</sub> on the capillary suction, drying kinetics and vapour permeability of three building stones

17 : 20 - 18 : 20	<p>Poster Session:</p> <ul style="list-style-type: none"> <li>• <u>J.M.P.Q. Delgado</u>, A.S. Guimarães and V.P. de Freitas - Salt Degradation in Stone of Historical Buildings: The Importance of Water Absorption Coefficient</li> <li>• Jorge Feijoo Conde<sup>1</sup>, Teresa Rivas Brea<sup>1</sup>, Nóvoa X.R.<sup>2</sup>, <u>Iván de Rosario Amado</u><sup>1</sup> and Javier Taboada<sup>1</sup> - Extraction of sulphates by electromigration in two different granites</li> <li>• <u>Jacek Chwast</u> and Jan Elsen - Gypsum efflorescence on clay brick masonry</li> <li>• <u>Nadine Lindström</u>, Nicole Heitmann, Kirsten Linnow and Michael Steiger - Crystallization behavior of NaNO<sub>3</sub>-Na<sub>2</sub>SO<sub>4</sub> salt mixtures in sandstone and comparison to single salt behavior</li> <li>• <u>Paulina Faria</u>, Vitor Silva - Capillary and drying of natural hydraulic lime and of air lime based mortars</li> <li>• Maria Idália Gomes, <u>Teresa Diaz Gonçalves</u>, Paulina Faria - Capillary water absorption of unstabilized and stabilized earth materials: anomalous time scaling behavior</li> <li>• <u>S.Gupta</u>, L.Pel, Michael Steiger - Influence of ferrocyanide ions on NaCl crystallization in the mixture of salts</li> </ul>
19 : 30	Porto wine at the penthouse (sunset is at 20:00)
20 : 30	Dinner

## KEYNOTE LECTURE

### Sorption and crystallisation induced deformation: from molecular dynamics to macroscopic modeling

Jan Carmeliet<sup>1,2</sup>, Dominique Derome<sup>2</sup>, Hannelore Derluyn<sup>2</sup>, Robert Guyer<sup>3</sup>, Sergey Churakov<sup>4</sup>

<sup>1</sup>ETH Zürich, Chair of Building Physics, Zürich, Switzerland

<sup>2</sup>EMPA, Swiss Federal Laboratories for Materials Science and Technology, Laboratory for Building Science and Technology, Dübendorf, Switzerland

<sup>3</sup>LANL/University of Nevada, USA

<sup>4</sup>Paul Scherrer Institute, Switzerland

#### ABSTRACT

Adsorption originates at the molecular scale from the interactions between the atoms of the solid skeleton and the molecules of the fluid. When the size of the pores is in the order of the range of the molecular interactions (micro or nanoporous materials), a mechanical pressure arises orthogonal to the porous interface leading to sorption induced deformations (swelling). To study sorption induced deformations in microporous materials, a poromechanical approach is used taking into account explicitly solid-fluid interactions arising in complex random microporous materials. To determine the mechanical effects of adsorption, the amount of adsorbed fluid in the medium has to be known in function of both the chemical potential of the fluid and the volumetric strain of the porous medium. This information can be gained by experiments and modeling.

In this presentation, we present different approaches to determine the macroscopic material properties including coupling coefficients: molecular dynamics, coarse grain simulation and the dependent domain approach to link different scales in hierarchical materials. In the dependent domain theory, the global material behavior results from the interaction of basic elements situated at different scales and characterized by statistical distributions. Upscaling is taking into account for hierarchical materials, showing geometric disorder and anisotropic behavior at lower scales. Towards developing a framework for the determination of sorption induced deformations using dependent domain theory and computational upscaling, which allows to determine nonlinear coupling coefficient and the hysteretic coupled behavior, we observe experimentally by high resolution X-ray tomography different microstructures containing microporous materials. In particular, we study hierarchical materials like wood, which can be used to develop our understanding of shape memory effects upon moistening.

Finally we will extend the approach towards chemical induced deformations. In particular we discuss as an example the state and dynamics of water and cations in pure and mixed Na-Cs-montmorillonite as a function of the interlayer water content using Monte Carlo and classical, molecular-dynamics methods.



## **Atomic strain produced from mirabilite crystallisation in sandstone and calcium silicate**

Andrea Hamilton<sup>1</sup> and Christopher Hall<sup>1</sup>,

<sup>1</sup>University of Edinburgh, UK, Andrea.hamilton@ed.ac.uk

### **ABSTRACT**

We show the evolution of atomic level strain from mirabilite crystallisation in Berea sandstone and calcium silicate plate during cooling. Using white beam synchrotron X-ray diffraction we can measure face specific displacements in lattice d-spacing and show how mirabilite compression varies according to crystallographic face being compressed. We present for the first time, a view of in pore crystallisation that sees the crystal as a faceted object. We compare this to hydrostatic compression of mirabilite in a diamond anvil cell and show that in this environment, mirabilite loses crystallinity at room temperature and ~5.7 kbar of pressure. We examine different pore environments provided by sandstone compared to the loosely packed xonotlite needles in calcium silicate board. We also show how quartz, kaolinite and xonotlite d spacings vary with temperature and crystallisation pressure from mirabilite.





## A “new” Correns’ experiment

Francesco Caruso<sup>1</sup>, Robert J. Flatt<sup>1</sup>

<sup>1</sup>Institut für Baustoffe (IfB), ETH Zürich, Schafmattstrasse 6, HIF B60.2 and E11, 8093 Zurich (Switzerland).

### ABSTRACT

The growth of salt crystals within the porous network of stones is the single most important cause for their decay [1,2,3]. Such growth can cause stresses sufficient to overcome the tensile strength of a stone and turn it into a powder. These stresses are directly related to the crystallization pressure. Therefore, a quantitative estimation and modeling appear to be necessary for a thorough understanding of the damage by salt crystallization.

Correns and Steinborn performed an early experiment for the determination of crystallization pressure [4,5,6]. Thanks to an ingenious optical system, they measured the vertical displacement of a loaded aluminum rod (whose end was covered with a glass socket) pushing on a potassium alum monocrystal ( $\text{KAl}(\text{SO}_4)_2 \cdot 12 \text{H}_2\text{O}$ ) in its supersaturated solutions. Then, they related such a displacement to the crystallization pressure as a function of the supersaturation ratio of the solutions. Interestingly, they obtained an incomplete equation of the crystallization pressure in good agreement with their experimental data.

The scope of this work is a study of the original experiment, recognizing and avoiding possible experimental artifacts that Correns and Steinborn probably neglected [6]. Up to now, we have considered supersaturated potassium alum solutions from  $c/c_s = 1.0$  to  $c/c_s = 1.5$ , verified their stability to nucleation and measured their pH (in an attempt to know more about aluminum speciation). Although the chemistry of aluminum at low pH values is complex [7], such stability is the main reason for continuing to work with potassium alum (probably used at Correns’ times for its ability to produce very good monocrystals). Also, we have characterized by optical profilometry the (111) surface of five commercial potassium alum crystals with  $0.1^\circ$  and  $1^\circ$  orientation accuracies. We are now working on the design and production of a stainless steel glass covered pushrod to be connected to a load cell of a universal testing machine. This will eventually be used for carrying out the crystallization pressure measurements.

### REFERENCES

- [1]G.W. Scherer, Crystallization in pores, Cement and Concrete Research, 29, 1347-1358, 1999.
- [2]G.W. Scherer, Stress from crystallization of salt, Cement and Concrete Research 34, 1613-1623, 2004.
- [3]R.M. Espinosa-Marzal, G.W. Scherer, Advances in Understanding Damage by Salt Crystallization, Accounts of Chemical Research, 43, 897-905, 2010.
- [4]C.W. Correns, W. Steinborn, Experimente zur Messung und Erklärung der sogenannten Kristallisationskraft, Zeitschrift für Kristallographie 101, 117-133, 1939.
- [5]C.W. Correns, Growth and dissolution of crystals under linear pressure, Discussion of the Faraday Society, 5, 267-271, 1949.
- [6]R.J Flatt, M. Steiger, G.W. Scherer, A commented translation of the paper by C.W. Correns and W. Steinborn on crystallization pressure, Environmental Geology, 52, 187-203, 2007.
- [7]D. Hendricks, Fundamentals of Water Treatment Unit Processes – Physical, Chemical, and Biological, CRC Press, Boca Raton, FL, 2011.



## Study of the kinetics of salt crystallization during rewetting/drying and humidity cycling

Julie Desarnaud<sup>1</sup> and Noushine Shahidzadeh-Bonn<sup>1</sup>

<sup>1</sup>Van der Waals-Zeeman Institute, IOP, University of Amsterdam, Science Park 904, 1098 XH Amsterdam, The Netherlands

### ABSTRACT

In this paper, we reveal the major role the recrystallization dynamics plays in the way different salts can cause damage to stone under different environmental conditions. There are two ways in which a salt, once crystallized, can take up water again: by bringing it in contact with liquid water (dissolution) or with water vapour (deliquescence). We compare the kinetics of salt recrystallization for different salts (NaCl, KCl, Na<sub>2</sub>SO<sub>4</sub>), after either deliquescence or dissolution followed by drying, for several cycles.

We find that deliquescence/recrystallization with humidity cycling leads to the growth of salt crystals by expelling impurities. For salts such as NaCl that have only one crystalline form, this leads to the growth of less nuclei which can achieve larger size. In this process, the solution can reach high concentration before the crystal growth. The consequence of the latter is the faster growth of a smaller number of crystals with the progression of cycles. These results can be a plausible explanation for why subsequent humidity cycling with NaCl leads to an irreversible dilation and the gradual expansion of the material.

For Na<sub>2</sub>SO<sub>4</sub> which has different crystalline forms (hydrated and anhydrous), the fact that high salt concentrations are reached after deliquescence followed by drying, favors the direct precipitation of anhydrous Na<sub>2</sub>SO<sub>4</sub>. The results show that the crystallization of the anhydrous salt generates only very small stresses that hardly damage the stone. On the contrary, with rewetting/drying sodium sulfate can lead to severe damage because the thenardite microcrystals dissolve very rapidly, and remaining crystals act as seeds to form large amount of hydrated crystals creating grape-like structures that expand rapidly. These clusters generate stresses larger than tensile strength of the stone. These results shed some light on how the kinetic pathway of crystallization plays a role on the way the same salt can cause damage in some conditions and not in others.



## KEYNOTE LECTURE

### Kinetics of crystallization in pores

George W. Scherer<sup>1</sup> and Rosa M. Espinosa-Marzal<sup>1,2</sup>

<sup>1</sup>Civil and Environmental Engineering/PRISM, Princeton University, Eng. Quad. E-319, Princeton, NJ 08544, USA

<sup>2</sup>Laboratory for Surface Science and Technology, Department of Materials, ETH Zurich, Wolfgang-Pauli-Strasse 10, CH-8093 Zurich, Switzerland

#### ABSTRACT

The conventional Johnson-Mehl-Avrami-Kolmogorov (JMAK) does not correctly describe the growth of crystals in a porous network, because it does not take account of confinement. However, there are extensions of that model that do describe growth confined within pores that are cylindrical, spherical, planar, or polyhedral, and where nucleation occurs on the pore walls and/or in the solution [1,2]. In this paper, we extend these models to describe growth in a network of pores, and compare their performance in describing experiments on growth of sodium sulfate salts in the pores of limestone upon cooling. The analysis takes account of the changing supersaturation in the pores, and the resulting time dependence of the crystal growth rate. The implications of these models for the poromechanical prediction of crystallization pressure are developed, and used to interpret measurements of the dilatation of limestone that results from growth of salt.

First we consider the model obtained by Villa and Rios [Error! Bookmark not defined.] for growth at rate  $G[t]$  from a fixed number of sites per unit area,  $N_S$ , confined within a cylinder of radius  $R$ . Use of this model implies that the stone can be represented as a network of cylindrical pores joined at nodes, as in Figure 1, and that the salt nucleated in one pore cannot branch into other pores in the network.

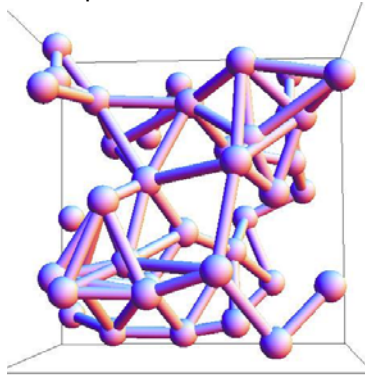


Figure 1: Schematic of pore network in stone

If the nucleation rate is high enough so that there is at least one nucleus between every pair of nodes in the pore network, then this model is ideal. If the nucleation rate is low, then by the time that a significant amount of crystallization has occurred, the length of each crystal is much larger than the pore diameter, so growth is primarily parallel to the axis of the cylindrical pore. In that limit, the volume fraction of crystals is

$$V_C[\theta] \approx 1 - \exp[-4\pi\lambda\theta] \quad , \quad \theta > 2, \quad \lambda \leq 0.003 \quad (1)$$

where  $\lambda = R^2 N_S$  and the reduced time is

$$\theta = \int_0^t \left( \frac{G[t']}{R} \right) dt' = \int_0^t \left( \frac{K(\beta[t'] - 1)}{R} \right) dt' \quad (2)$$

where  $\beta$  is the thermodynamic supersaturation and  $K$  a kinetic parameter. Growth stops when the concentration is reduced to the solubility limit ( $\beta = 1$ ). Unless diffusion from neighboring pores is allowed, no pore will be completely filled with salt, so little or no crystallization pressure will be produced. When such diffusion is allowed, this model provides a good fit to data for crystallization of sodium heptahydrate and mirabilite in limestone, and it predicts that a residual supersaturation will exist that will contribute to crystallization pressure.

A different model is required, if the salt is able to branch into the other pores at intersections in the network [1]. In that case, filling of pores with crystals requires diffusion to occur over a distance comparable to the radius of the crystallized region, so the kinetics are entirely different, and high crystallization pressure is less likely.

#### REFERENCES

- [1] J.W. Cahn, The time cone method for nucleation and growth kinetics on a finite domain, *Mat. Res. Soc. Symp. Proc.*, 398, 425-437, 1996.
- [2] E.Villa, P.R. Rios, "Transformation kinetics for surface and bulk nucleation", *Acta Materialia*, 58, 2752–2768, 2010.
- [3] G.W. Scherer, "Effect of Inclusions on Shrinkage", pp. 503-514 in *Better Ceramics Through Chemistry IV*, eds. B.J.J. Zelinski, C.J. Brinker, D.E. Clark, and D.R. Ulrich (Mat. Res. Soc., Pittsburgh, PA, 1990)

# Characterizing salt transport and crystallization damage in porous limestone with neutron radiography and X-ray micro-tomography

Hannelore Derluyn<sup>1,2</sup>, Dominique Derome<sup>2</sup>, Iwan Jerjen<sup>2</sup>, Jan Dewanckele<sup>3</sup>, Veerle Cnudde<sup>3</sup>, Eberhard Lehmann<sup>4</sup>, Jan Carmeliet<sup>1,2</sup>

<sup>1</sup>ETH Zurich, Chair of Building Physics, Zurich, Switzerland

<sup>2</sup>EMPA, Swiss Federal Laboratories for Materials Science and Technology, Dübendorf, Switzerland

<sup>3</sup>Department of Geology and Soil Science - SGIWUGCT, Ghent University, Ghent, Belgium

<sup>4</sup>Paul Scherrer Institut, PSI, Spallation Neutron Source Division, Villigen, Switzerland

## ABSTRACT

Information on saline transport, pore filling and fracturing due to salt crystallization is essential for the understanding of the coupling between transport and mechanical processes related to salt weathering. This knowledge is required for the selection of the best suited materials and conservation methods for civil constructions and our cultural heritage. Additionally, such datasets are needed to advance numerical modeling of crystallization in porous media.

Our aim is to collect threefold information on liquid transport, salt distributions and fracturing processes on the same sample. Savonnières limestone is chosen as the porous material for our study and samples are subjected to repeated wetting-drying cycles. A hydrophobic treatment is applied on the top side and vapour and liquid tight foil is applied on the lateral sides. The hydrophobic treatment is intended to prevent salt efflorescence at the surface and to induce in-pore crystallization. Repeated uptake and drying of a salt solution should lead to the accumulation of an amount of salt inside the material sufficient for (1) the quantification of salt distributions and (2) for inducing fracturing. Due to the repetitive character of the experiments, non-destructive techniques are needed. As hydrogen highly attenuates neutron radiation, transmission-based neutron imaging is a well suited technique to study liquid transport. The higher spatial resolution achievable with X-ray micro-computed tomography ( $\mu$ CT) allows assessing porosity changes and fracture formation due to salt crystallization. Therefore we opted to combine neutron radiography and X-ray  $\mu$ CT on our samples. Additionally, the adequacy of these two techniques for the study of salt crystallization in porous materials is presented.

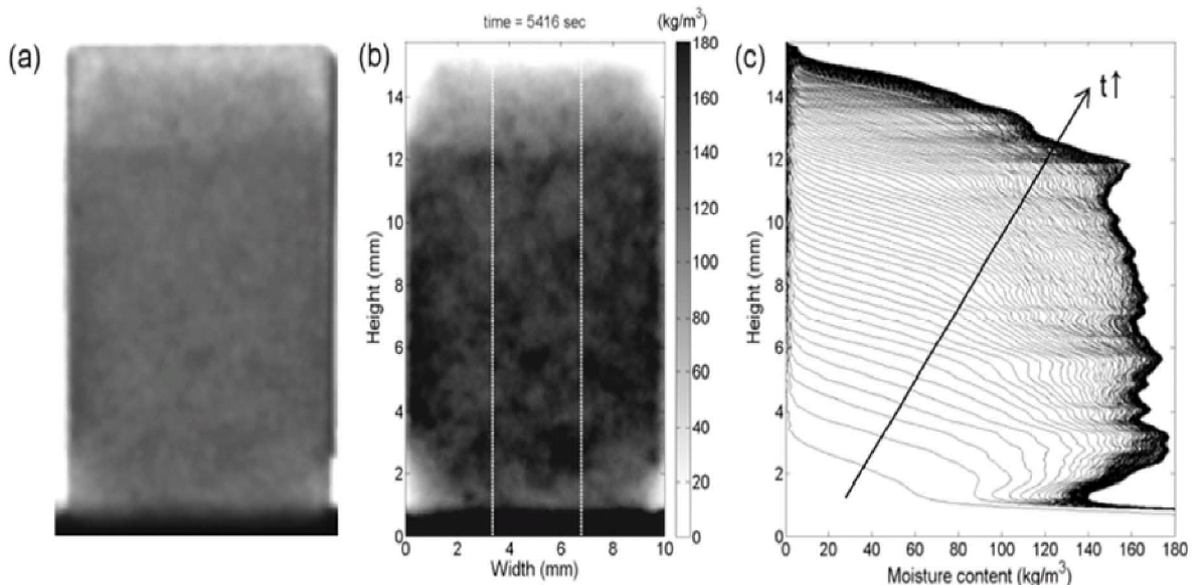


Figure 1: (a) Transmission image and (b) moisture distribution of a Savonnières sample, hydrophobically treated on the top side, after capillary uptake of water. The white lines border the central area over which we average to obtain the moisture profiles. (c) The moisture profiles at 32 s intervals.

We will present the results of two experimental test series conducted on samples of Savonnières limestone. This limestone has 5 pore systems with characteristic sizes ranging between 100 nm and 1 00



pm. The porous structure is depicted in Fig. 2a. All samples were scanned in their initial state in a laboratory X-ray  $\mu$ CT setup. In the first test series, capillary uptake (at about 25°C) of water, 5.8 molal sodium chloride solution and 1.4 molal sodium sulfate solution was visualized with neutron radiography on prismatic samples of 10x10~15 mm<sup>3</sup>. Moisture profiles are derived from the 2D moisture distributions (see Fig. 1) and are further analyzed determining the moisture penetration coefficient and the moisture diffusivity. An important decrease of these two coefficients is observed for the salt solutions compared to water uptake. This decrease can be attributed to the change in surface tension  $\sigma$  and viscosity  $\eta$ . The penetration coefficient scales as  $\sqrt{\sigma/\eta}$  and the diffusivity as  $\sigma/\eta$ . This indicates that the calcitic Savonnieres stone matrix does not read with the water or salt solution.

In the second test series, drying (at 45°C) was visualized with neutron radiography on prismatic samples of 10x10x8 mm<sup>3</sup>. Smaller samples were taken with the aim of characterizing the first and the start of the second drying period during a time span of about 10 hours. Pore blocking by sodium sulfate crystals is observed leading to a slower drying with every subsequent wetting-drying cycle.

Moreover, sodium chloride precipitates, deformation and damage are observed already after the first wetting-drying cycle. Consecutive wetting-drying cycles cause additional deformation and damage. Samples containing precipitated sodium sulfate salt get damaged by the rewetting step, but only when sufficient salt is present in the porous structure, i.e. after several wetting-drying cycles.

Salt profiles are quantified based on neutron and X-ray image analysis of the dried samples. The zone of salt precipitation is located at the upper part of the samples, partly in the hydrophobized zone and partly just below this zone. This is caused by the long first drying period of Savonnieres limestone. The Porosity reduction due to salt precipitation was quantified up to the resolution of the laboratory X-ray pCT datasets (14  $\mu$ m). These datasets also revealed the damaging character of the salts as the fracture morphology could clearly be identified (see Fig. 2c). The tomographic study was further extended by acquiring synchrotron radiation X-ray tomographic datasets of cylindrical Savonnieres samples (3.3 mm diameter, resolution of 3.7  $\mu$ m). The salt distribution before and after drying was visualized and quantified for repeated wetting-drying cycles (see Fig. 2b). This let us conclude that salt crystals precipitate in all pore systems of Savonnieres limestone. The damage most likely occurs in the mechanically weak zones (zones with less cohesion between the calcite grains), as these zones are accessible to saline liquids.

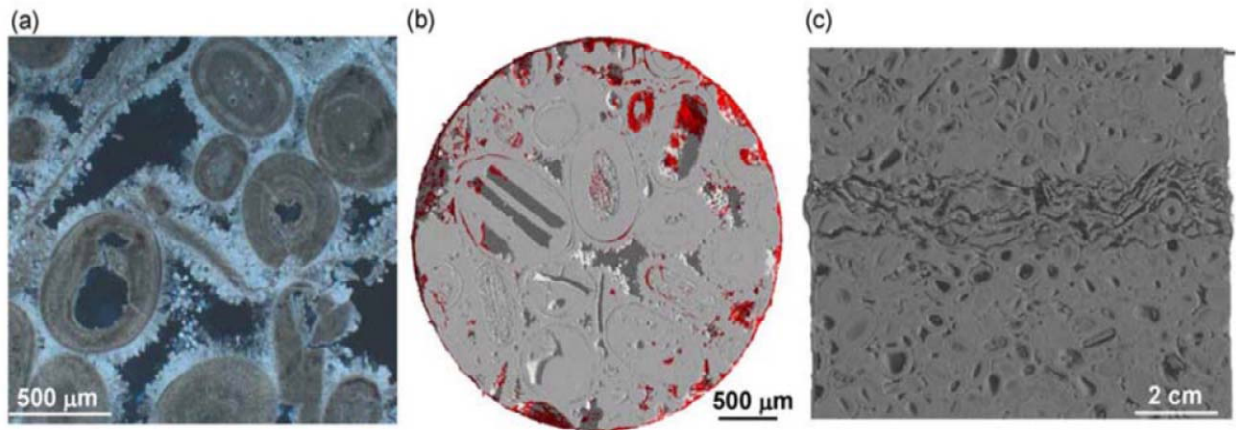


*Figure 2: (a) Thin section of Savonnieres limestone visualized by optical microscopy. (b) Cross-sectional slice obtained from a 3D synchrotron radiation X-ray  $\mu$ CT dataset of a dry Savonnieres sample, with precipitated NaCl crystals in red. (c) Vertical slice of upper part of a dry sample after repeated wetting-drying cycles within 1.4 molal sodium sulfate solution, as obtained from a 3D laboratory X-ray  $\mu$ CT dataset.*

## Numerical modeling of crystallization induced damage processes

Hannelore Derluyn<sup>1,2</sup> Peter Moonen<sup>1,2</sup> Jan Carmeliet<sup>1,2</sup>

<sup>1</sup>ETH Zürich, Chair of Building Physics, Zürich, Switzerland

<sup>2</sup>EMPA, Swiss Federal Laboratories for Materials Science and Technology, Laboratory for Building Science and Technology, Dübendorf, Switzerland

### ABSTRACT

Water and dissolved salt ions penetrate into building materials due to diffusive and convective transport. Upon changes in the environmental conditions (temperature and vapour pressure), salt can crystallize at the surface (efflorescence) or inside the material (subflorescence). Subflorescence is accompanied with the development of crystallisation pressures in the porous material, which may lead to spalling and cracking of the solid material matrix. To this day, the mechanism of crystallisation in confined conditions and the related damage processes, as well as the computational modelling, are subject of scientific debate.

This presentation follows another talk at Crispom III [1]. In [1] we discussed the use of neutron radiography and X-ray micro-tomography for the visualization and quantification of saline transport, salt distributions and fracture morphology in Savonnières limestone. We found that damage due to crystallization most likely occurs in mechanically weak zones of the material, which are accessible by liquids. Based on the experimental results, constitutive relations can be formulated and implemented in a finite element model combining: (1) a coupled heat, moisture and salt transport model; (2) a crystallization model and (3) a model describing the mechanical coupling between salt, moisture and the solid matrix. The coupling of the transport and crystallization model has been described in [2] and was presented during Crispom II [3]. In this presentation we will focus on the coupling with the mechanical behaviour using the theory of poromechanics [4]. The fracturing due to salt crystallization pressures is incorporated using a strong discontinuity framework as described by [5]. The properties to describe ion transport, crystal growth and crystallization pressures for two single salts, sodium sulfate ( $\text{Na}_2\text{SO}_4$ ) and sodium chloride ( $\text{NaCl}$ ), have been included. All properties are both temperature and concentration dependent. Sodium sulfate has different crystal phases that form upon cooling or drying: mirabilite ( $\text{Na}_2\text{SO}_4 \cdot 10\text{H}_2\text{O}$ ), heptahydrate ( $\text{Na}_2\text{SO}_4 \cdot 7\text{H}_2\text{O}$ ) and thenardite ( $\text{Na}_2\text{SO}_4$ ). Sodium chloride has one stable crystal phase above the freezing point: halite ( $\text{NaCl}$ ). Various climatic conditions can be imposed and the response of a structure can be assessed for longer time periods (decades), as also described in [6].

In this presentation the model performance will be validated by repeating the wetting-drying experiments discussed in [1] by numerical simulations. The applicability of the model for cooling induced damage or damage induced by deliquescence cycles will be illustrated as well. We will show how, by varying model parameters, numerical modeling can help in understanding damage due to salt crystallization and how modeling studies can complement experimental results

### REFERENCES

- [1] H. Derluyn, D. Derome, I. Jerjen, J. Dewanckele, V. Cnudde, E. Lehmann, J. Carmeliet, Characterizing salt transport and crystallization damage in porous limestone with neutron radiography and X-ray micro-tomography, Proc. Crispom III, Troia, Portugal, 4-7 September, 2012.
- [2] H. Derluyn, R.M. Espinosa-Marzal, P. Moonen, J. Carmeliet, A coupled transport-crystallization FE model for porous media, Proc. EURO-C 2010 (Computational modeling of concrete structures), Rohrmoos-Schladming, Austria, 15-18 March, 471-479, 2010.
- [3] H. Derluyn, R.M. Espinosa-Marzal, P. Moonen, J. Carmeliet, Experimental and numerical study on sodium sulfate and chloride crystallization in porous limestone, Proc. Crispom II, Brienz, Switzerland, 15-18 June, 17, 2010.
- [4] O. Coussy, Mechanics and Physics of Porous Solids, Wiley, Chichester, 2010.
- [5] P. Moonen, L.J. Sluys, J. Carmeliet, A continuous-discontinuous approach to simulate physical degradation processes in porous media, International Journal of Numerical Methods in Engineering 84(9), 1009-1037, 2010.
- [6] H. Derluyn, D. Derome, J. Carmeliet, E. Stora, R. Barbarulo, Influence of hysteretic moisture behaviour on mass transfer in concrete, submitted to Cement and Concrete Research (under review).



# Gypsum crystal growth under bridge foundations

Eduardo E. Alonso<sup>1</sup> and Anna Ramon<sup>1</sup>

<sup>1</sup>Department of Geotechnical Engineering and Geosciences, UPC, Barcelona. eduardo.alonso@upc.edu, anna.ramon@upc.edu)

## ABSTRACT

Gypsum crystal growth in a deep stratum located below the massive Pont de Candí pile foundations explains the important heave experienced by the central pillars after construction [1]. The 413 long bridge is located in the high speed Madrid-Barcelona railway. Pillars are founded on groups of 3x3 deep bored piles 1.65 m in diameter with an average length of 20 m. Piles are socketed in a stiff Eocene claystone having a significant content of gypsum and anhydrite. The geologic formation has been studied in detail [2] due to the severe swelling experienced by the nearby Lilla tunnel floor.

A heave rate ranging from 5 to 10 mm/month was measured by levelling the bridge structure. Vertical displacements were also measured at ground surface in an area 200 meters wide along the bridge axis. Contours of equal vertical displacements were drawn. They had an elliptical shape whose major axes were parallel to the direction of water flow. Deep continuous extensometers were installed inside boreholes. Swelling strains were recorded at deep positions, below piles' tip (Fig. 1). An active layer, 12-15 m thick, was defined. Time records of vertical displacements exhibited a constant heave rate with no indication of slowing down in the relatively long recording period (2.5 years).

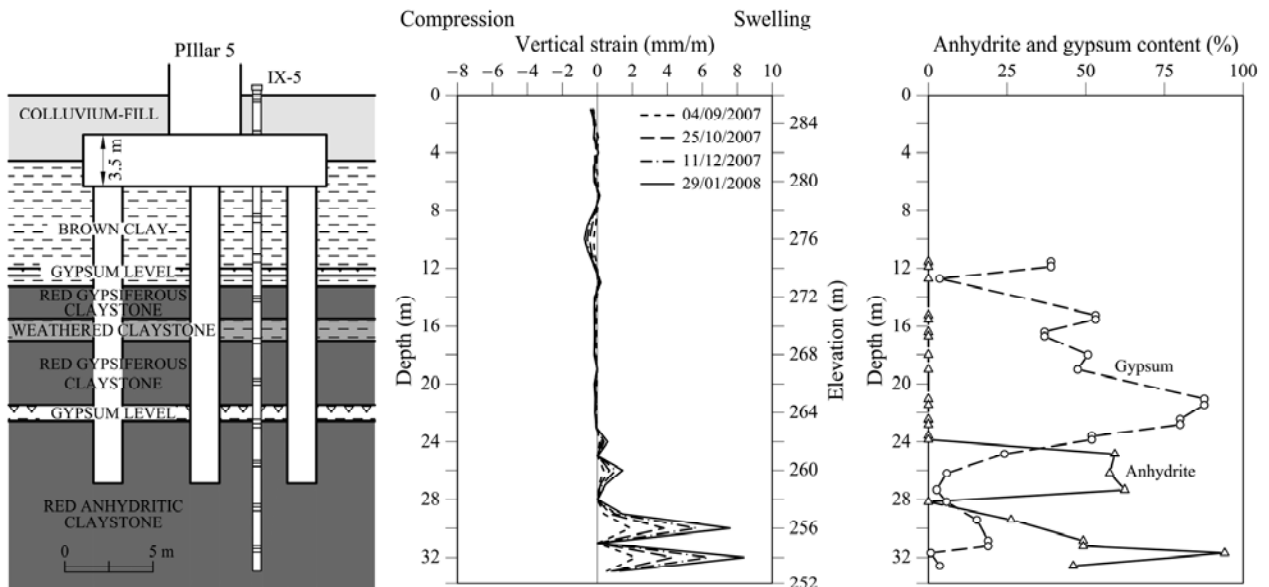


Figure 1: Measurements in extensometer IX-5 (Initial reading: 12/July/2007) and profiles of anhydrite and gypsum content (X-ray diffraction technique)

Figure 1 shows a typical variation of gypsum and anhydrite content with depth. The comparison between the vertical strains and the distribution of anhydrite and gypsum shows that swelling strains were associated with the presence of anhydrite. Gypsum crystals were observed in cores recovered from boreholes at depths corresponding to the active layer. Needles of gypsum crystals, oriented perpendicular to the plane of discontinuities, filled partially open discontinuities. Some of the crystals seemed to be very recent. The open discontinuities partially clogged with gypsum needles allow the flow of water within the active zone. Flake gypsum crystals growth inside the clay matrix was also observed. Since the calcium sulphate concentration of water in equilibrium with anhydrite is higher than the saturation concentration with respect to gypsum, at the temperatures present in Pont de Candí rock mass (Fig. 2), anhydrite will tend to dissolve and gypsum will precipitate.

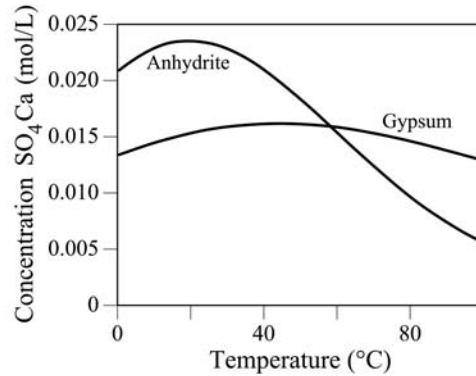


Figure 3: Equilibrium concentration of  $\text{SO}_4\text{Ca}$  water with respect to gypsum and anhydrite

A campaign of hydraulic cross-hole tests revealed a system of hydraulically connected horizontal discontinuities in the active expanding layer. Low values of permeability were found above and below the active zone. The crystallization of gypsum in discontinuities produces a flat-jack effect pushing upwards the soil and rock layers above the active zone, as well as the bridge pillars. It is believed that the set of boreholes and foundation piles performed connected the upper aquifer with the deeper fissured anhydritic claystone, triggering the heave phenomenon.

A model for gypsum crystal growth has been formulated within a general framework for hydro-mechanical analysis for saturated porous media [3]. The dissolution of anhydrite and precipitation of gypsum has been taken into account in the formulations [4]. The model also keeps track of solute evolution. Kinetic equations, adapted from [5], describe the rate of mass precipitated or dissolved in terms of the current concentration of the solute and the concentration for saturated conditions. The precipitation or dissolution of crystals will reduce or increase porosity. Strains are calculated from the precipitated crystal volume and the prevailing effective stress.

A column of the foundation material at the position of central pillar was modeled under plain strain conditions [4]. The active layer, 15 m thick, was included between 2 stable layers. A horizontal flow was forced in the active layer. The model is able to reproduce the heave measured at central pillars of the bridge. A sensitivity analysis performed provides an additional insight into the phenomenon.

## REFERENCES

- [1] E.E. Alonso, & A. Ramon, Heave of a railway bridge induced by gypsum crystal growth. field observations. Submitted for publication. 2012.
- [2] E.E. Alonso, I.R. Berdugo, D. Tarragó, & A. Ramon, Tunnelling in sulphate claystones. Proc. 14th European Conference on Soil Mechanics and Geotechnical Engineering, Madrid, 24-27 September, 1, 103-122. Invited Lecture. 2007.
- [3] DIT-UPC 2002. CODE\_BRIGHT, a 3-D program for thermo-hydro-mechanical analysis in geological media: User's guide, Centro Internacional de Métodos Numéricos en Ingeniería (CIMNE), Barcelona.
- [4] A. Ramon, & E. Alonso, Heave of a railway bridge. Modelling of gypsum crystal growth. Submitted for publication. 2012.
- [5] A.C. Lasaga, Chemical kinetics of water-rock interactions. Journal of Geophysical Research Vol. 89, No: B6, 4009-4025, 1984.

## KEYNOTE LECTURE

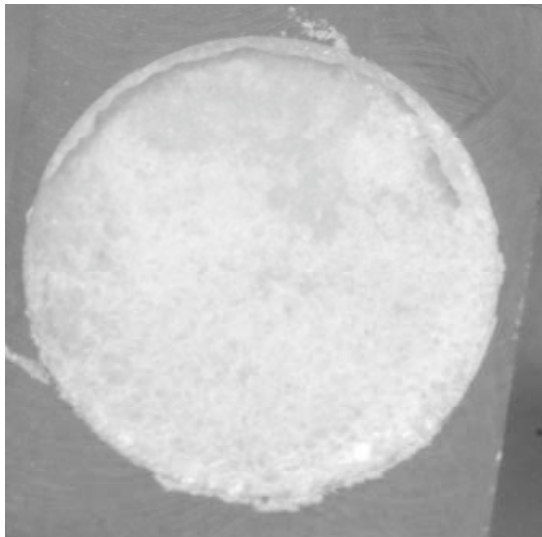
### How to make crusty or patchy efflorescence

Prat Marc<sup>1</sup>

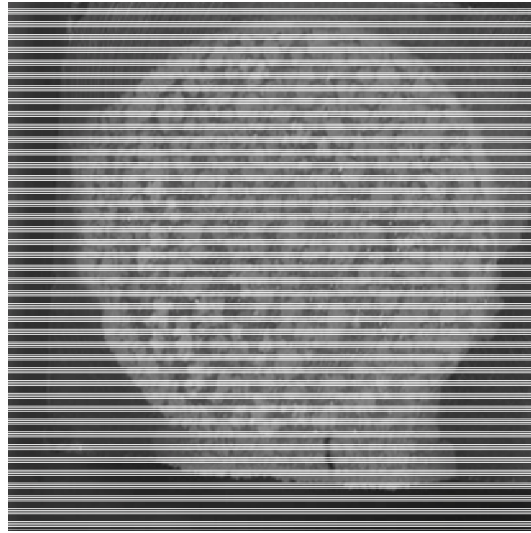
<sup>1</sup>INPT, UPS, IMFT (Institut de Mécanique des Fluides de Toulouse), Université de Toulouse, Allée Camille Soula, F-31400 Toulouse, France and CNRS, IMFT, F-31400 Toulouse, France

#### ABSTRACT

We present an experimental study of drying in the presence of dissolved sodium chloride. The process is characterized by the formation of crystallized salt, referred to as efflorescence, at the evaporative surface of the porous medium. By varying the average size of the beads forming the porous medium, we show that the formation of the crystal layer does not affect significantly the drying process and can even enhance the drying rate when the beads are sufficiently large. By contrast the crystal layer can greatly affect the drying process and even blocks the evaporation process for sufficiently small beads. We therefore show the existence of a transition between the two regimes, namely the blocking regime and the enhanced drying rate regime. It is shown that the two regimes correspond to two different types of efflorescence, referred to as crusty and patchy respectively. Then by varying the initial salt concentration for a given bead size, we show that the interplay between drying and the efflorescence formation leads to a non-monotonous variation of the drying rate with the initial salt concentration when the efflorescence is patchy but not when the efflorescence is crusty.



Crusty efflorescence



Patchy efflorescence

#### REFERENCES

H. Eloukabi, N.Sghaier, M. Prat, S. Ben Nasrallah, Experimental study of the effect of sodium chloride on drying of porous media: the crusty-patchy efflorescence transition, to be submitted.



## **Effect of ferrocyanide ions on the drying behavior of NaCl contaminated porous material**

S.Gupta<sup>1</sup>, Henk Huinink<sup>1</sup>, L.Pel<sup>1</sup>

<sup>1</sup>Eindhoven University of Technology, Department of Applied Physics, Den Dolech 2, 5600MB, Eindhoven, The Netherlands (email:sgupta@tue.nl)

### **ABSTRACT**

While the mechanisms of salt damage in porous materials have received considerable attention in recent years, effective treatment methods for ameliorating this problem still remain limited. Recently, the use of ferrocyanide inhibitors has been proposed as a potential preventive treatment method against NaCl damage [1]. However, until now the suitability of these inhibitors for the treatment of salt damage is still under discussion. One of the reasons behind this is lack of adequate experimental data for understanding the moisture and ion transport mechanisms in the porous materials while drying. In lieu of this, a detailed experimental study has been performed to understand the effect of inhibitors on the drying behavior of salinated porous materials at varying environmental conditions. Nuclear Magnetic resonance Technique (NMR) has been used for carrying out non-destructive and quantitative measurements of both the moisture and salt ions content simultaneously. Drying experiments using 3m NaCl solution containing different concentration of potassium hexacyanoferrate (II) trihydrate inhibitor have been performed at varying relative humidity conditions. In a previous study we have reported the drying behavior of salt saturated materials with and without inhibitor at low relative humidity [2]. In this work, further investigation has been done to understand the drying behavior of the bricks at higher relative humidity conditions. We have used fired-clay brick as a model porous material. The relative humidity was varied between 0%, 55% and 70%.

Initially, drying experiments were performed on salt contaminated bricks without inhibitor. The results show that approx. 45% of salt crystallize as efflorescence at high relative humidity (55% and 70% relative humidity) compared to only 6% efflorescence seen at low relative humidity. Also, drying rate of the salt contaminated brick was higher at high relative humidity in comparison to the one dried at low relative humidity. This is due to the formation of efflorescence at high humidity. The salt efflorescence acts as a porous network that increases the effective surface area for evaporation and pumps more and more dissolved salt ions along with the moisture content towards the drying surface seen as efflorescence. Due to transfer of salt outside the material as efflorescence, there was no blockage of pores near the drying surface to hinder evaporation of water (as is the case of bricks dried at low relative humidity) and thus the drying rate increases at high relative humidity. Next drying experiments were performed in the presence of inhibitor. The maximum effectiveness of inhibitor was seen at low relative humidity (0% relative humidity). At low relative humidity in the presence of inhibitor a significant amount of salt crystallize out as efflorescence and a delay in attaining saturation concentration was seen. However, at high relative humidity (55% and 70% relative humidity) not much difference was seen in the amount of efflorescence formed with and without inhibitor. Also, the saturation concentration was attained almost at the same time inside the material.

These results show that the formation of efflorescence changes the drying kinetics of porous materials. The use of ferrocyanide ions as an inhibitor against NaCl damage will be more beneficial in faster drying regions e.g. the regions of low relative humidity and the regions with high air flow rates. For such regions the use of inhibitor helps to crystallize salt outside the materials as efflorescence and can prevent NaCl damage. However, in the regions with high relative humidity the use of inhibitor may not be very beneficial as no significant difference was seen in the drying behavior of the bricks with and without inhibitor.



## REFERENCES

- [1] B. Lubelli & R.P.J van Hees, Effectiveness of crystallization inhibitors in preventing salt damage in building materials, *Journal of Cultural Heritage*, 8(3), 223-234, 2007.
- [2] S. Gupta, Terheiden. K, Pel. L & Sawdy. A, Influence of ferrocyanide inhibitors on the transport and crystallization processes of sodium chloride in porous building materials, *Journal of Crystal Growth & Design*, 12, 3888–3898, 2012.

## **Effect of inhibitors on sodium sulfate crystallization**

Barbara Lubelli<sup>1</sup>, Timo G. Nijland<sup>1</sup>, Rob P.J. van Hees<sup>1</sup>

<sup>1</sup>Faculty of Architecture, Delft University of Technology, Julianalaan, 134, 2628 BL, Delft, The Netherlands

### **ABSTRACT**

Salt crystallization in porous materials constitutes one of the most frequent causes of decay of buildings in a wide range of environments. Up to now no definitive solution exists to avoid salt crystallization damage, apart from removing either the salt or the moisture. The possibility of making the process of salt crystallization less harmful by means of crystallization inhibitors has only recently been considered. Crystallization inhibitors are ions or molecules able to delay nucleation and to modify the growth rate of the crystals. For some salts, as sodium chloride, the effectiveness of crystallization inhibitors in delaying crystallization and reducing salt crystallization damage under certain well defined conditions has been demonstrated, whereas for other salts, as sodium sulfate, results obtained until are unsatisfactory. In this research a series of systematic investigations on the effectiveness of different types of inhibitor (amino-tris-methylene-phosphonic acid (ATMP) and sodium salt of polyacrylic acid (PA)) for sodium sulfate was carried out. First, the effectiveness of the inhibitors in bulk solution was investigated. Crystallization experiments in bulk solution were performed under different temperature and RH conditions: the weight of the solution was monitored and the occurrence of crystallization checked by optical microscope. Additionally, crystallization experiments in bulk solution were carried out in a XRD chamber with controlled RH (50 and 80% RH) and temperature(20 °C)conditions.

In a second experiment, inhibitors were mixed in during the preparation of a lime-cement mortar. Mortar specimens were made and accelerated crystallization tests were carried out to study the effect of the inhibitors on the development of salt damage.

In this paper the obtained results will be discussed as well as new research lines.



## **Salt transport in porous media: preliminary experimental and theoretical Analysis of salt diffusion**

J.M.P.Q. Delgado<sup>1</sup>, A.S. Guimarães<sup>1</sup>, V.P. de Freitas<sup>1</sup>

<sup>1</sup>LFC – Laboratório de Física das Construções, Departamento de Engenharia Civil, Universidade do Porto, Rua Dr. Roberto Frias, s/n; 4200-465 Porto, Portugal

### **ABSTRACT**

Damage of building materials and building structures has a significant economical and ecological impact worldwide. Salt damage is a multi-factor problem, resulting from the interplay between the nature and structure of the porous object, the physical and chemical behavior of the salt solution, and the environmental conditions. Moisture plays an important role as the transport medium for salt in porous building materials.

Moisture and especially salt transport and crystallization in pores are widely recognized as one of the primary causes of the deterioration of porous building materials and in the conservation of historic buildings. In cold climates, like Portugal, sodium chloride can lead to durability problems when the building structures are exposed to marine environment. Various experimental methods have been developed to measure salt diffusion, some methods are based on Fick's law and use a "diffusion cell" and others on the Nernst-Planck equation and use a "migration cell". The main purpose of the work is to describe and illustrate the use of a new method to measure molecular diffusion coefficients which is applicable to all porous building materials. In the theoretical analyze, we consider a vertical column containing a building material specimen, and filled with liquid to some level above the top of the specimen (liquid "pool"). If a concentrated salt solution is then poured into this liquid "pool", with uniform concentration, the tracer will gradually penetrate down the building material sample. The concentration of tracer in the liquid "pool" decrease gradually in the time, until a uniform concentration of tracer, equilibrium, is reached in the whole liquid. Analysis of the process of salt diffusion may be made in analogy with the process of diffusion from a stirred solution of limited volume. Values of the "effective" molecular diffusion coefficient were obtained for different building materials, at temperatures between 5 °C and 45 °C. The results show that the increase in temperature resulted in an increase in molecular diffusion coefficient.

The experimental results obtained are in good agreement with the theoretical values of molecular diffusion coefficient presented in literature. Empirical correlations are presented for the prediction of "effective" molecular diffusion coefficient over the entire range of temperatures studied.



## **Influence of limestone microstructure on gypsum crystallization**

Dewanckele, J<sup>1</sup>, De Boever, W,<sup>1</sup> De Kock, T<sup>1</sup>, Boone, M A<sup>1</sup>, Boone, M N<sup>3</sup>, Brabant, L<sup>3</sup>, Fronteau, G<sup>2</sup>, Van Hoorebeke, L<sup>3</sup>, Cnudde, V<sup>1</sup>, Jacobs, P<sup>1</sup>

<sup>1</sup>Department of Geology and Soil Science – SGIG/UGCT, Ghent University, Ghent, Belgium

<sup>2</sup>University of Reims Champagne-Ardenne (URCA), GEGENAA, EA3795, Reims, France

<sup>3</sup>Department of physics and Astronomy – UGCT, Ghent University, Ghent, Belgium

### **ABSTRACT**

In this study, we describe the use of high resolution X-ray CT (HRXCT) combined with thin section microscopy and SEM-EDS to investigate weathering patterns inside two different limestone facies due to gypsum crystallization. The combination of both techniques allows to obtain a time lapse visualization of those specific disintegration processes. The objective was to compare the visualized and quantified weathering patterns inside the rock with its microstructure. The study focuses on the micromorphology of two time equivalent (Eocene) natural building stones, the Belgian Lede stone and the French Noyant limestone, and the susceptibility of the rock forming components (bioclasts, cement, matrix, etc.) to gypsum crystallization. Both Lede stone and Noyant limestone contain a significant amount of bioclasts, especially foraminifera. In order to predict weathering phenomena and their process rates, first, the role of the microstructure has to be investigated. Most literature provides general weathering rate process information but is less focussing on specific features of the stone. On the other hand, Fronteau et al. (2010) already illustrated the relationship between building stone microfacies and morphology of the lower layer of the sulphated encrusting on the Euville, Savonnières and Courville limestone and thus underlined the importance of the microstructure of the stone [1].

The microscopic texture of the Lede stone can be described as a laminated packstone and a bioclastic packstone or grainstone without structure. The porosity of the stone is very heterogeneous (4-10 %) due to a varying macroporosity of dissolved fossil fragments. Commonly, the fossil fragments in Lede stone are bivalves, gastropods and foraminifera. The latter belong mostly to the subgroup Miliolina and Rotaliina (*Nummulites*). The stone contains 40-70% of quartz grains and is cemented by a micritic-microsparitic cement. The Noyant stone is an almost pure very porous limestone (up to 45 % porosity) with a micritic matrix and contains, similar to Lede stone, a high percentage of fossil fragments (Miliolina). Furthermore, some dispersed, sub-angular quartz grains are present.

In this study, sulphated encrustations were obtained on both Lede and Noyant stone in laboratory after an induced strong acid test. The reader is referred to [2] for further details. Basically, the samples were put in an acid environment according to the European Standard NBN EN 13919 (2003) for 21 days. At the bottom of the recipient, a mixture of  $500 \pm 10$  ml  $H_2SO_3$  and  $150 \pm 10$  ml de-mineralized  $H_2O$  was added. The cylindrical samples of both Lede and Noyant fine stone were scanned with HRXCT before and after the weathering test. SEM/BSE-EDS was performed on the final failed rock samples.

For the Lede stone, a relatively thick, external gypsum crust is visible on the thin sections and a preferential infilling is obtained in the wall structures of the foraminifera (Miliolina) and shell fragments after the exposure to an acid environment. In general, it is observed that the microsparitic cement around the fossil fragments is more resistant than the wall structure of the Miliolina. When looking to a differential volume of the CT-scan made before and after weathering, the same weathering patterns are visible. Figure 1 shows a reconstructed slice before and after weathering and a differential image. The latter reveals the places where gypsum was crystallized in micro-pores and on the surface (white) and where new pores were formed due to dissolution of calcium carbonate (black).

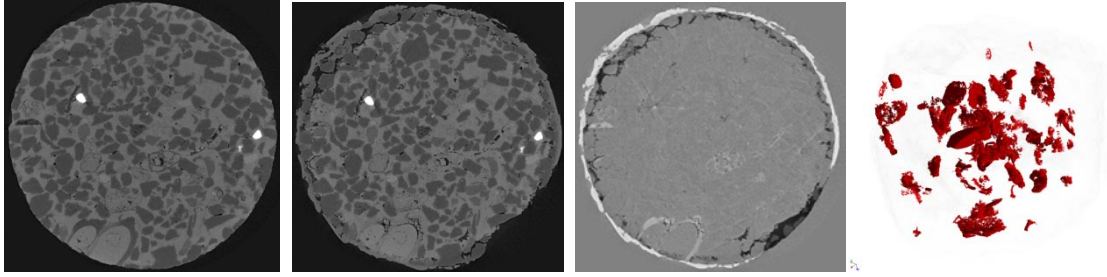


Figure 1: X-ray CT image before acid test (1), after acid test (2), differential image (3) and 3D rendered volume of gypsum crystallization inside the Miliolina fragments (4). On the differential image, the new pores (black) and gypsum (white) are visible. Diameter of the core is 1.6 mm.

The segmented volume reveals the location of gypsum inside the stone in 3D and as can be seen on figure 1, the gypsum concentrates inside the Miliolina and shell fragments (red). Their shape can easily be distinguished thanks to the complete recrystallization of calcium carbonate into gypsum. The highly porous wall structure of the Miliolina favors the crystallization of gypsum. On the other hand, the *Nummulites* show almost no recrystallization because of their hyaline, non-porous walls. A totally different weathering phenomena is observed for the Noyant stone. A thick weathering crust ( $\pm 300 \mu\text{m}$ ) of gypsum and recrystallized calcium carbonate was detected. The highly porous micritic matrix was completely deformed by cracking as can be seen on the X-ray CT slices before and after the test (figure 2). Registration of the volumes was impossible due to this severe deformation. As the BSE-EDS images show, only Miliolina at the surface of the samples were attacked and others are only partially transformed or show no conversion into gypsum.

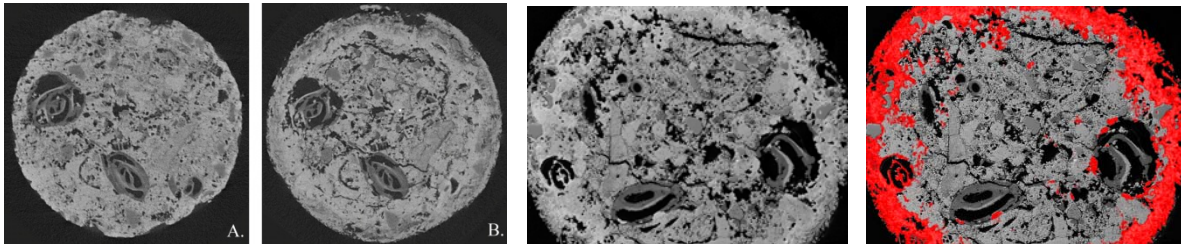


Figure 2: X-ray CT slice before and after weathering (left; A and B) and BSE/EDS image of a weathered Noyant stone (right) the gypsum is shown, in red. Diameter of the core is 1.6 mm.

The highly micro-porous micritic matrix of the Noyant stone made it more sensitive to recrystallizations than the bioclast present within the stone. On the contrary, the bioclasts (Miliolina and shell fragments) in the Lede stone were less resistant to weathering than the cement of the stone, resulting in internal preferential crystallization spots. The knowledge of the influence of the microstructure, including porosity, reactive surface and roughness is of prime importance in the understanding of the crystallization patterns. In addition, this approach illustrates that the characterization and prediction of weathering of natural building stones due to gypsum benefits of the combined use of thin section microscopy, BSE/SEM-EDS and X-ray CT.

## REFERENCES

- [1] G. Fronteau, C. Schneider-Thomachot, E. Chopin, V. Barbin, D. Mouze, A. Pascal, Black-crust growth and interaction with underlying limestone microfacies, Geological Society, London, Special Publications, 333, 25-34. Title of journal article, Journal of Crystallization 13, 121-143, 1923.
- [2] J. Dewanckele, T. De Kock, M.A. Boone, V. Cnudde, L. Brabant, M.N. Boone, G. Fronteau, L. Van Hoorebeke, P. Jacobs, 4D imaging and quantification of pore structure modifications inside natural building stones by means of high resolution X-ray CT

# Effects of NaCl and NaNO<sub>3</sub> on the capillary suction, drying kinetics and vapour permeability of three building stones

Vânia Brito<sup>1</sup>, Teresa Diaz Gonçalves<sup>1</sup>

<sup>1</sup>National Laboratory for Civil Engineering (LNEC), Lisbon, Portugal

## ABSTRACT

Salt decay is closely related to drying of porous materials, not only as a consequence but also because the salts are an influencing factor in drying processes. This influence, however, is not yet totally clear, as are not in general the effects of soluble salts on liquid and vapour transport through complex pore networks such as those of porous building materials.

Here, we analyse the role of two soluble salts, NaCl and NaNO<sub>3</sub>, on the capillary suction and drying kinetics of three natural stones. The physical morphology of the efflorescence layer occurring in each case and the effect of such layer on vapour transport are also analysed.

Sodium chloride and sodium nitrate are among the most common salts in decayed buildings and also, particularly sodium chloride, two of the most used in laboratory experiments. Despite of their distinct composition, their equilibrium relative humidity is similar: 75.47% for NaCl and 75.36% for NaNO<sub>3</sub> at 20°C [1]. Four solutions with different concentration were tested in the case of NaCl and three in the case of NaNO<sub>3</sub>.

The natural stones were the Bentheimer sandstone (B) and two Portuguese limestones that correspond to the Ançã limestone (CA) and a current limestone of lower porosity (CC).

The experiments followed RILEM procedures [2] and consisted on performing sequentially, on the same specimens, the following three types of test: determination of the absorption coefficient with water and the salt solutions, measurement of the evaporation curve, and determination of the coefficient of water vapour conductivity of the uncontaminated and salt contaminated specimens.

As regards the influence on liquid capillary transport, the results show that, for the three stones, the sorptivity of the salt solutions scales precisely as  $(\sigma/\eta)^{1/2}$ , where  $\sigma$  is the surface tension and  $\eta$  the viscosity of the liquid, as predicted theoretically [3]. The greatest sorptivity reduction occurs thus for NaNO<sub>3</sub>: the values for the saturated solution are around 60% of those obtained for pure water, whereas for NaCl they are around 70%.

In relation to the drying kinetics, although for the concentrations closer to saturation the differences are sometimes less clear, a general trend can be observed: the higher the salt concentration the slower the drying. However, some isolated specimens deviate from this general trend, depicting a markedly slower drying kinetics. There were occurrences for the three materials and the two salts, which have an apparently random nature: the drying curves of the affected specimens diverge suddenly, triggered by some unidentifiable event or character.

At the end of drying, a layer of efflorescence was observable on the surface of the specimens. Its morphology was often similar for the two salts but varied significantly with the type of stone. As revealed by optical microscopy:

- CA developed thick crusts of vertically oriented crystals, apparently more compactly packed for the chloride than for the nitrate;
- CC presented shrivelled NaCl salt crusts which possessed holes at most of the hills and occasional fissures; the holes tend to develop at areas where dark clasts are present on the stone surface, which should correspond to a less porous mineral; for NaNO<sub>3</sub>, most surfaces were covered by a porous coat of whisker-like efflorescence.
- B developed nodules of cauliflower-like efflorescence lying on a thin vitreous coat of salt; the two specimens which had much slower drying showed a different efflorescence morphology consisting on a thick and compact vitreous layer.

The vapour permeability of the efflorescence-covered materials, overall, decreases linearly with the concentration of the salt solution used, i.e., with the thickness of the efflorescence layer. The changes, however, are mostly irrelevant in all cases except for CA with sodium chloride. This difference seems to be closely related to the morphological characteristics, and particularly the porosity, of the efflorescence layer. What probably happens is that for CA with sodium chloride the efflorescence layer is compact enough to significantly disturb the transport of vapour. In all the other cases the porosity of the



efflorescence layer is higher, either because the packing of the crystals is less compact or because the salt crust possesses holes and fissures, therefore, there is not much influence on vapour transport. In general, the variations in drying kinetics are consistent with the differences in vapour permeability or efflorescence morphology, inclusively in the cases of the specimens with random deviant behaviour. Summarizing, the work done until the present moment indicates that:

- The changes induced by soluble salts in capillary transport are due to their effect on the surface tension and viscosity of the liquid and are proportional to  $(\sigma/\eta)^{1/2}$ , as predicted theoretically.
- The vapour transport hindering effect of salt deposits is very dependent on the habit and packing of the crystals. This was observed for external salt deposits (efflorescence crusts) but it is logical to expect that a similar effect may happen at the pore level, i.e., for internal deposits (subflorescence).
- Compact crusts of salt may relevantly hinder the passage of vapour. However, porous efflorescence layers with a negligible influence on vapour transport are probably also frequent. The difference between the two types is not easily detected by the naked eye and can be elusive in current site observations.
- Efflorescence morphology depends on factors such as the type of salt and the characteristics of the porous material, as previously concluded also by other researchers. However, it seems to incorporate also random causal factors, which may prove to be ultimately significant, probably derived from small casual inhomogeneities in the environmental conditions or in the complex pore network of the building material.

### **Acknowledgements**

This work was performed under the research project DRYMASS (ref. PTDC/ECM/100553/2008) which is funded by national funds through the Fundação para a Ciência e a Tecnologia (FCT) and LNEC.

### **REFERENCES**

- [1] L. Greenspan, Humidity fixed points of binary saturated aqueous solutions. *Journal of Research of the National Bureau of Standards-A, Physics and Chemistry*, 1: 89-96, 1977.
- [2] RILEM TC 25-PEM, Recommended tests to measure the deterioration of stone and to assess the effectiveness of treatment methods. *Materials and Structures*, 13: 197-199, 209, 205-207, 1980.
- [3] C Hall, WD Hoff, *Water Transport in Brick, Stone and Concrete*. Spon Press, London and New York, 2002, ISBN 0-419-22890-X.

Thursday, September 06, 2012

8 : 3 0 - 9 : 1 0	<u>Michael Steiger</u> and Kirsten Linnow	Keynote lecture 4 - Hydration reactions in confinement: salt hydrates in porous materials for thermochemical heat storage
9 : 1 0 - 9 : 3 5	<u>P. A. J. Donkers</u> , J. F. M. van Rens, L. Pel and O.C.G. Adan	Na <sub>2</sub> SO <sub>4</sub> , the first step to thermo chemical heat storage
9 : 3 5 - 1 0 : 0 0	Inge Rörig-Dalgaard	Determination of the deliquescence point in salt mixtures by utilizing the dynamic vapour sorption method
1 0 : 0 0 - 1 0 : 2 5	<u>Kirsten Linnow</u> and Michael Steiger	Experimental studies of the mechanism and kinetics of hydration reactions
1 0 : 2 5 - 1 0 : 5 5	Coffee break	
1 0 : 5 5 - 1 1 : 3 5	<u>José Delgado Rodrigues</u>	Keynote lecture 5 - Salts in stone conservation. From insidious enemies, to transient friends and inconvenient neighbors
1 1 : 3 5 - 1 2 : 0 0	<u>Berta Mañas Alcaide</u> , Xavier Mas-Barberà and Stephan Kröner	Differences in poulticing behavior depending on materials and application techniques
1 2 : 0 0 - 1 2 : 2 5	<u>Roel Hendrickx</u> , Hilde De Clercq, Sebastiaan Godts and Chiara Giannotti	A moisture transport-based approach to estimate the effect of desalination poultices and salt accumulating renders
1 2 : 2 5 - 1 2 : 5 0	<u>Sebastiaan Godts</u> , Hilde De Clercq, Roald Hayen and Roel Hendrickx	The crystallization of salt mixtures in relation to a climate study to mitigate salt decay in Medieval Murals and Limestone Tracery
1 2 : 5 0 - 1 3 : 5 0	Lunch	
1 4 : 0 0	Gathering at the hotel lobby	
1 4 : 1 5 - 1 5 : 0 0	Walk to Tróia marina (through the beach)	
1 5 : 0 0 - 1 8 : 0 0	Boat tour with dolphin watching	
1 9 : 3 0 - 2 0 : 3 0	Aperitif at the bar	
2 0 : 3 0	Dinner	



## KEYNOTE LECTURE

### Hydration reactions in confinement: salt hydrates in porous materials for thermochemical heat storage

Michael Steiger<sup>1</sup> and Kirsten Linnow<sup>1</sup>

<sup>1</sup>Department of Chemistry, University of Hamburg, Inorganic and Applied Chemistry

#### ABSTRACT

Many salts occur in different hydrated forms and hydration reactions are generally considered as important causes of damage in construction materials or natural rock. Hydration–dehydration equilibria are also of increasing interest due to the use of salt hydrates as thermochemical heat storage materials. Such a thermochemical system is based on the release of the heat of hydration. A salt hydrate storage system is charged by the endothermic thermal dehydration of the higher salt hydrate. Many salts can be dehydrated at temperatures that can well be achieved using solar thermal collectors. In this state, the energy can be stored over long periods of time implying its application for seasonal storage. The exothermic back reaction may be initiated by simply increasing the water vapor partial pressure. The hydration–dehydration equilibrium of  $\text{MgSO}_4 \cdot 7\text{H}_2\text{O}$  and  $\text{MgSO}_4 \cdot \text{H}_2\text{O}$  is one promising example with a very high theoretical energy density for both seasonal and short term energy storage.

The performance of a salt hydrate storage system largely depends on the kinetics of the hydration and the dehydration reactions. Such reactions are solid state reactions, hence, they are slow and often they are under kinetic control. In effect, hydration–dehydration reactions of most salts are characterized by the formation of metastable phases. In order to predict the behavior of a particular salt, a complete phase diagram including stable and metastable phases is required. There are different approaches to optimize the kinetics of hydration reactions including the addition of hygroscopic salts and the use of composite materials of a porous substrate carrying the salt hydrate.

The dispersion of crystals to submicrometer size in porous substrates offers the advantage of a significantly increased crystal surface area available for gas–solid heterogeneous reactions. In addition, using nanoporous materials increases the overall heat effect by increasing the heat of hydration of the embedded salt by the heat of sorption of the porous substrate. However, it is well known that crystal growth during hydration reactions in porous substrates generates substantial stress. Therefore, a complete phase diagram to predict the hydration–dehydration behavior of salts needs to consider the pressure dependence of the phase equilibria. It is also well known that the pressures generated by confined growing crystals in a hydration reaction are substantial and may exceed the tensile strength of many materials. In the case of energy storage, a high tensile strength is an important property of a suitable host material with high cycle stability. In the case of construction materials, very often the tensile strength is not sufficient and the pressure generated in hydration reactions causes severe damage. The origin of this pressure is sometimes subject to controversial discussion and is attributed to both hydration and crystallization pressure.

In this talk, we will discuss the theory and experiments to establish the phase diagrams of salt hydrates and to assess the influence of pressure on the phase equilibria. The pressure dependence also includes the treatment of the thermodynamic background of hydration and crystallization pressure and their relevance for understanding damage in construction materials.



# Na<sub>2</sub>SO<sub>4</sub>, the first step to thermo chemical heat storage

P. A. J. Donkers<sup>1</sup>, J. F. M. van Rens<sup>1</sup>, L. Pel<sup>1</sup> and O.C.G. Adan<sup>1</sup>

<sup>1</sup>Department of Physics, Technical University of Eindhoven, Den Dolech 2, 5612 AZ, Eindhoven, The Netherlands

## ABSTRACT

Systems that buffer energy are needed to match the demand and supply of renewable energy. There are several ways to store energy; one of the most promising systems is based on thermo chemical energy. This system uses the energy release of a chemical reaction. For heat storage application this system is profitable, because this reaction is reversible.

One particular heat storage method with a high potential makes use of the crystallization energy of salts. The reaction is given by:



where A is a salt, some promising salts are MgSO<sub>4</sub>, CaCl and LiCl; B is a solvent, mentioned in literature are H<sub>2</sub>O, NH<sub>3</sub> and CH<sub>3</sub>OH and AB is the salt crystal of A and B. The heat generated by this reaction depends on the salt-solvent combination, but can be in the order of 500 kWh/m<sup>3</sup>. This means that by picking a good combination of salt and solvent a system of 10 m<sup>3</sup> can store your energy consumption of a whole year! A drawback of the system is that by cyclic crystallization-decomposition of the salt systems the efficiency decreases<sup>[1]</sup>.

Here we have used NMR to get more information on the crystals during cyclic reactions. To this end we make use of a 4.7T magnet, as to be able to measure at very low moisture contents. A special insert was designed to control the temperature of the sample and to measure simultaneously the mass of the sample. The relative humidity over the sample can be changed within a range of 0-98% RH. Special attention was given to the Bird-cage design as to be able to measure short relaxation times, i.e., to distinguish on basis of relaxation analysis which is free and hydrated water.

As an example in figure 1a the measured moisture profiles of a dehydration experiment are given for a sample filled with Na<sub>2</sub>SO<sub>4</sub>·10H<sub>2</sub>O crystals. Air is blown over the sample with a relative humidity of 0%. These preliminary results already show that a sharp dehydration front is observed. In figure 1b we have also given the results for various measurements with different crystal sizes. These results show that for large crystals the dehydration is faster in time. In the near future we want to use this information for modeling the reaction processes in these reactors during cycling.

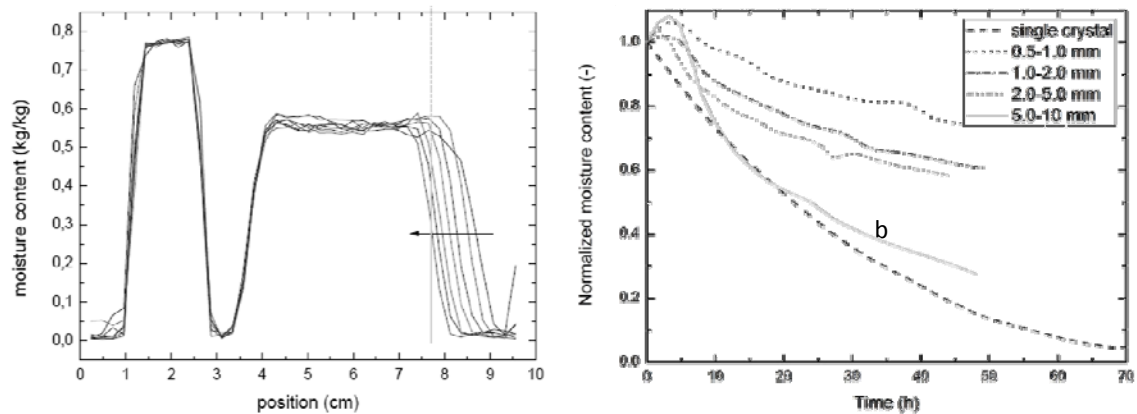


Figure 1a: The moisture content profiles of the dehydration experiments of Na<sub>2</sub>SO<sub>4</sub> with grain size of 0.5-1.0 mm. The time between 2 plotted profiles is 8 hours. Figure 1b: The normalized moisture content plotted against the time for different grain sizes of Na<sub>2</sub>SO<sub>4</sub>.

## REFERENCES

[1] K. E. N'Tsoukpoe et al., Renewable and Sustainable Energy Reviews, 13, 2385-2396,2009.



# Determination of the deliquesce point in salt mixtures by utilizing the dynamic vapour sorption method

Inge Rörig-Dalgaard<sup>1</sup>

<sup>1</sup>Department of Civil Engineering, Technical University of Denmark

## ABSTRACT

### Background and objectives

Salts are generally recognized to be one of the main courses for deterioration of porous materials. The damage and eventual removal of the salt is dependent of whether the salt is crystallized or dissolved. In relation to desalination of church vaults for future preservation of the murals it is of interest to limit the applied liquid during the desalination e.g. to prevent drying cracks and creating conditions for microbial growth [1]. At present climate chambers with a specific temperature and relative humidity are used to prevent salt induced deterioration and also in this relation it is of interest to find the deliquescence point since the relative humidity can be kept on the most effective level without causing damage. The deliquescence point for single salts is well known; however, in case of salt mixtures the combinations are comprehensive. In order to find deliquescence points for specific salt mixtures different simulation programs have been used as e.g. RUNSALT [2], ECOS [3], however several assumptions have to be made and therefore these programs are by several considered as limited reliable. In [4] phase diagram for the  $\text{Na}_2\text{SO}_4\text{-H}_2\text{O}$  system was calculated on basis of thermodynamic data as a function of temperature. In [5] a model approach was made to predict phase equilibria in case of salt mixtures and safe ranges of environmental conditions taking temperature, varying ions, moisture contents and activities into account. The model was based on the semi-empirical model from Pitzer where some parameters were experimental determined. The results were given in RH as a function of temperature. In order to understand the fundamental mechanisms such a model as deduced in [5] is essential. The need for incorporating the transport properties of the porous material and dissolution and crystallization kinetic of the various salts is mentioned to be strongly depended to the transport properties of the various salts in reality [5]. Measurements of the deliquescence point and the kinetics for some specific salt mixtures in materials at a specific temperature would further contribute to the understanding of salt mixtures and this is the content of the present work by utilizing dynamic vapor sorption method (DVS).

### The Dynamic vapor sorption method

The deliquescence point can empirically be found by producing water vapor sorption isotherms which previously were found by time and labor intensive desiccators and saturated salt solutions. A further development of the original water vapor sorption isotherm method is the dynamic vapor sorption method (DVS). The DVS method is a gravimetric technique measuring the velocity and the extent to which a solvent is absorbed by a sample. In a DVS experiment this is accomplished by exposing a sample to a series of step changes in relative humidity and monitoring the mass change as a function of time. The sample mass must be allowed to reach gravimetric equilibrium at each step change in humidity before progressing to the next humidity level. Then, the equilibrium mass values at each relative humidity step are used to generate the isotherm. The DVS method has previously been used for identifying a stable crystalline salt in order to allow clinical development activities. During this work a hysteresis effect was measured when exposed to high humidity's which they propose was caused by a change from an anhydrous salt to a more hydrated salt [6].

### Expected results

The DVS will be used to determine the sorption isotherm for NaCl (for comparison with reference values),  $\text{Na}_2\text{SO}_4\text{-H}_2\text{O}$  (for comparison with [4]) and salt mixtures taken from three different positions from the vault of Rørby Church, Denmark (to be used during future desalination). On basis of the results which are to be measured in august 2012, it will be discussed whether satisfactory results can be obtained with the DVS method for determination of the deliquescence point in relation to salt mixtures at a specific temperature.

It has to be discussed whether it is of interest to determine a precise deliquescence point of a salt mixture in practice or whether the deviation between the three taken samples in Rørby church makes such a precise determination meaningless.

Also in case of establishing a climate chamber to prevent further salt induced deterioration a RH could be chosen to the climate chamber on basis of determination of the deliquescence point in a limited temperature



intervals. Since temperatures are most often recorded in advance to desalination the deliquescence point at one specific temperature would give valuable information.

In a previous work the known value for the deliquescence point of the single salt NaCl was confirmed by very primitive measurements in a microclimate and it was shown that in case of dissolved ions (and possibly a limited contribution from the compress plaster) a high desalination efficiency was obtained by use of a new electrokinetic method [7-9].

### **Acknowledgements**

The A.P. Møller and wife Chastine Mc-Kinney Møllers foundation for common purposes is gratefully acknowledged for financial support given in the end of May 2012.

### **REFERENCES**

- [1] K. Petersen, Mikroorganismen beschleunigen den Zerfall mittelalterlicher Wandgemälde. In Krumbein W.E. Schäden an Wandmalereien und ihre Ursachen. Ein forschungsprojekt des BMFT Arbeitshefte zur Denkmalpflege 8. 115-121, 1990.
- [2] P.K. Larsen, The salt decay of medieval bricks at a vault in Brarup church, Denmark. *Environ. Geol* 52:375-383, 2007.
- [3] Alison & Heritage. Evaluating the influence of mixture composition on the kinetics of salt damage in wall paintings using time lapse video imaging with direct data annotation. *Environ. Geol* 52:303-315, 2007.
- [4] M. Steiger, S. Asmussen. Crystallization of sodium sulfate phases in porous materials: The phase diagram  $\text{Na}_2\text{SO}_4\text{-H}_2\text{O}$  and the geration of stress. *Journal of Geochimica et Cosmochimica Acta* 72, 4291-4306, 2008.
- [5] M. Steiger, Salts in Porous Materials: Thermodynamics of Phase Transitions, Modeling and Preventive Conservation, *Bauinstandsetzen und Baudenkmalpflege* 11 (6), 419-432, 2005.
- [6] A.C. Hodson, P.G. Ferrie, A.B. Dennis, Identification of a hydrate using the complementary techniques of dynamic vapour sorption (DVS), DSC, TGA and hot stage microscopy, *European Journal of Pharmaceutical Science* 4, 181, 1996.
- [7] I Rörig-Dalgaard. Desalination for preservation of murals by electromigration and regulated climate. *Structural Studies, Repairs and Maintenance of Heritage Architecture XI*, Tallinn, Estonia 71-82 (2009)
- [8] I. Rörig-Dalgaard. Preservation of murals with electrokinetic – with focus on desalination of single bricks. PhD thesis. Technical University of Denmark, 2009.
- [9] I. Rörig-Dalgaard, L. M. Ottosen, K.K. Hansen, Diffision and electromigration in clay bricks influenced by differences in the pore system resulting from firing. *Journal of Construction and Building Materials* 27, 390-397, 2012.

## Experimental studies of the mechanism and kinetics of hydration reactions

Linnow Kirsten<sup>1</sup>, Steiger Michael<sup>1</sup>

<sup>1</sup>Department of Chemistry, University of Hamburg, Inorganic and Applied Chemistry Martin-Luther-King-Platz 6, 20146 Hamburg, Germany

### ABSTRACT

The mechanism and kinetics of hydration reactions are not only important to understand the pressure exerted in confined space but also for the application of a salt hydrate as thermochemical heat storage material. Sodium sulfate and magnesium sulfate monohydrate were chosen in this study because they are both promising as thermochemical heat storage materials due to their high theoretical energy density of  $2.2 \text{ GJ}\cdot\text{m}^{-3}$  and  $2.4 \text{ GJ}\cdot\text{m}^{-3}$ , respectively. Moreover, it is well known that both salts cause severe damage of building materials. Hence, they are often used in durability tests of building materials, such as the ASTM aggregate sound test.

Hydration reactions under several climatic conditions were observed by using Raman microscopy. It turns out that during the hydration at higher humidities droplets of solutions saturated with respect to the lower hydrate are formed which are supersaturated with respect to the higher hydrated phase and subsequently crystallization takes place. As an example the hydration of thenardite at 92% RH and  $23^\circ\text{C}$  is shown in Fig. 1. After one hour exposure time (Fig. 1a) small thenardite crystals were dissolved (arrow) while larger crystals remained as thenardite and the formation of mirabilite was not yet observed. Two hours later the large crystals (arrows in Fig. 1b) were hydrated to mirabilite whereas medium sized crystals dissolved. In the interior of the large droplet (Fig. 1b) thenardite is clearly visible and was identified by Raman spectroscopy. Shortly after the droplet got in contact with the mirabilite particle spontaneous crystallization of mirabilite occurred, thus providing clear evidence for crystal growth from a highly supersaturated solution. After 6 hours some droplets were still present and all crystals shown in Fig. 1c consist of mirabilite.

At low humidities hydration reactions are significantly slower and neither visible solution nor the Raman spectrum of a sulfate solution was found. In addition water vapor sorption experiments were carried out and hydration rates were determined. The experimental observations are discussed on the basis of the well known  $\text{Na}_2\text{SO}_4\text{-H}_2\text{O}$  and  $\text{MgSO}_4\text{-H}_2\text{O}$  phase diagrams. It turns out that the hydration rate increases with increasing humidity. However, above the deliquescence humidity of the lower hydrate a through solution mechanism takes place further accelerating the water uptake.

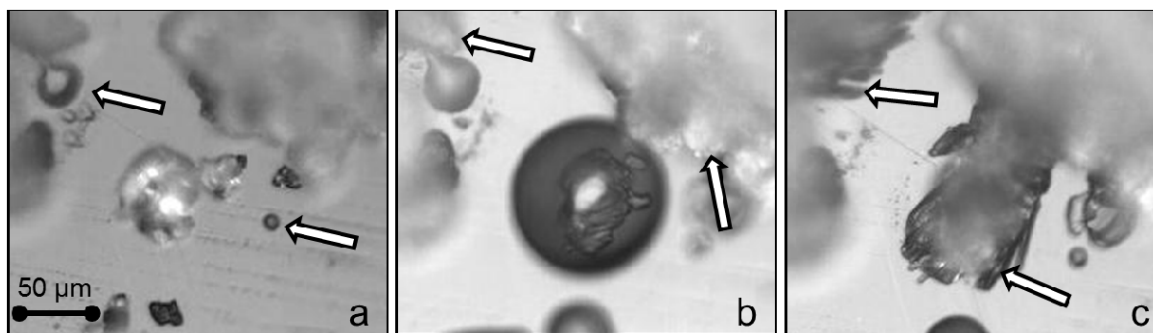


Figure 1: Hydration progress of thenardite at 92% RH and  $23^\circ\text{C}$  after exposure times of (a) 1h 47min, (b) 3h 16min and (c) 6h 6min.



## KEYNOTE LECTURE

### Salts in stone conservation: From insidious enemies, to transient friends and inconvenient neighbours

J. Delgado Rodrigues<sup>1</sup>

<sup>1</sup>Geologist, Principal Research Officer (ret.) National Laboratory of Civil Engineering, Lisbon, Portugal

#### ABSTRACT

Salts are well known deterioration agents [1] and are widespread in our constructions. Sulphates, chlorides, nitrates and carbonates represent the most frequent anions, but others less frequent such as phosphates and oxalates can be found. They combine with cations to form a very large number of mineral species, the real entities that we find in our walls. They can be seen popping up at the surface, or staying concealed below it, or just moving up and below, as the weather conditions determine. There are typical places to find them in good amounts [2], best seasons to harvest, established methods for tracking them, but they can be found anywhere, and nowhere is absolutely safe from them. They may be circumstantially associated to many other entities, but only water can be considered as a constant companion to them. And they move around, in our constructions. Sometimes the occurrence patterns inform where they come from, the composition may be an indication of their birthplace, but it is hardly feasible to guarantee which paths they have followed and how they have interacted during their journey. They may be strong fighters and highly destructive warriors, or be simple aesthetic disturbing presences, but they are never totally innocuous and irrelevant. A disturbing agent that can be found everywhere, uses camouflage strategies, may have multiple origins, characters and movements is, in fact, a very **insidious enemy** that demands to be carefully considered and counteracted.

And yet, salts are one of the most praised and recurrent ingredients of researchers and scientists [3]. From Brard [4] and Thomson (1862) [5] (quoted from Honeyborn (1965)[6], to modern researchers, salts have been a work material and their role an intriguing problem, but apparently a very frequent cherished source for curricula nourishment. Salts are instrumental to help testing materials (RILEM [7], ASTM [8]) and to decide whose to be accepted or to be rejected. They may serve as a stressing agent to newly treated specimens to force treatments to demonstrate how good or how bad they are for the stone [9]. And they may even help us to prepare our specimens to more accurately mimic aged materials to obtain samples adequate to serve as working materials in our experiments [10]. It is not simple to understand what they cause and what the results mean, but this is our fault, and in this aspect these **transient friends** are not to be blamed for.

In the daily practice in stone conservation, we have almost always to assume that “they” are there. They are in that large band parallel to the ground that runs along most of the ground level. They are also high in the wall near those uncared windows, below those broken tiles of the roof. And in that degraded vault over the transept, and in those recently repaired joints. They are threatening the remains of the original mural painting, and are waiting to bursting out below those ugly black crusts. It is not question to avoid them. They arrived there before us. And it is not question to eliminate them completely either. We need to learn how to “live” with them. We may consider eliminating part of them and keeping their amount at a safer level. We may command where we want them to stay by managing properly an overlying plaster cover [11]. And we may consider eliminating them superficially to allow us to treat the decayed stone in a safer way [12,13].

We know for sure that water is an inseparable companion and a critical logistic factor for salts. They may look unpleasant, but without water they are almost harmless. So, knowing how difficult is to defeat them, move your efforts to take water away from them. Repair those leaking points, avoid conditions for condensation, install a damp proof courses, and any other tricks to keep them with dry “feet” as far as possible. They may offer nice fluffy crystals that may give an erroneous feeling of peaceful actors, but in fact they are not companies to be recommended and have to be considered as permanent **inconvenient neighbours**.

Starting from illustrations of damage situations induced by salt crystallisation, the presentation will discuss a few examples on laboratory use of salts for testing purposes, ending with a few examples of practical applications of conservation actions is salt laden objects.

#### REFERENCES

- [1]Evans, I.S. 1970 – “Salt crystallization and rock weathering: A review”. *Revue de Géomorphologie Dynamique*, 19:153–177.
- [2]Arnold A. 1982 – “Rising damp and saline minerals”. *Proc. 4<sup>th</sup> In. Ccongress on the Deterioration and Preservation of Stone Objects, Louisville (Ky.)*. Edited by K.L. Gauri and J.A. Gwinn, University of Louisville, pp.11-28.
- [3]Charola, A.E. – 2000 – “Salts in the deterioration of porous materials: an overview”. *Journal of the American Institute for Conservation*, Vol. 39, No. 3.
- [4] De Thury , H. 1828 – “Sur la procédé proposée par M. Brard pour reconnaître immédiatement les pierres que ne peuvent pas résister à la gelée, et que l'on désigne ordinairement par les noms de pierres gélives ou pierres gélisses“ . *Annales de Chimie et de Physique* 38:160–192.
- [5] Thomson, J. – Report of the 32<sup>nd</sup> Meeting of the British Ass. For the Advancement of Science, Oct. 1862, London, John Murray 1863.
- [6] Honeyborn, D.B. 1965 – “Weathering processes affecting inorganic building materials”. *Building Research Station, Internal Note IN 141/65*. Garston, Nov. 1965.
- [7] RILEM, 1980 – “Tentative Recommendations, Commission 25PEM, Test V.1- Cristallisation test by total immersion and Test V.2 – Cristallisation test by partial immersion”. *Matériaux et Constructions*, Vol. 13, No 75, pp. 175-253.
- [8] ASTM C 88–90, 1997 – “Standard test method for soundness of aggregate by use of sodium sulfate or magnesium sulphate”. *Annual Book of ASTM Standard 4.2:37–42*
- Correns, C.W. 1949 – “Growth and dissolution of crystals under linear pressure”. *Discuss. Faraday Soc.* 5:267–271.
- [9] Costa, D. and Delgado Rodrigues, J. 2008 – “Consolidation treatment of salt laden materials. Methodology for their laboratory study”. *11th Int. Congress on Deterioration and Conservation of Stone*. Edited by Jadwiga W. Lukaszewicz and Piotr Niemcewicz. Nicolaus Copernicus University Press, Torun, pp. 827-836.
- [10] Delgado Rodrigues J.; Ferreira Pinto, A. P. and Paulos Nunes, C. 2007 - “Preparation of aged samples for testing stone treatments”. *Atti del Convegno Scienze e Beni Culturali, Bressanone*
- [11] Gonçalves, T.D., Pel , L. and Delgado Rodrigues, J. 2007 – “Drying of salt contaminated masonry: MRI laboratory monitoring”. *Environ. Geol.* 52:293–302
- [12]Delgado Rodrigues, J. and Costa, D. 2008 - “The conservation of granite in Évora Cathedral. From laboratory to practice”. *Proc. Int. Seminar on Stone Consolidation in Cultural Heritage. Research and Practice*, Edited by J. Delgado Rodrigues & J.M. Mimoso, LNEC, Lisbon, pp. 101-110.
- [13]Delgado Rodrigues, J.; Paulos Nunes, C. L. and Costa, D. 2008 - “Preparatory studies for the consolidation of granite in Évora cathedral. Desalination by poulticing”. *Proc. Int. Seminar on Stone Consolidation in Cultural Heritage. Research and Practice*, Edited by J. Delgado Rodrigues & J.M. Mimoso, LNEC, Lisbon, pp. 159-167

## Differences in poulticing behavior depending on materials and application techniques

Berta Mañas Alcaide<sup>1</sup>, Xavier Mas-Barberà<sup>2</sup>, Stephan Kröner<sup>2</sup>

<sup>1</sup>Instituto Valenciano de Conservación y Restauración de Bienes Culturales, Valencia (Spain).

<sup>2</sup>Institut Universitari de Restauració del Patrimoni, Universitat Politècnica de València, Valencia (Spain).

### ABSTRACT

The presence of soluble salts and water, among other circumstances, in porous building materials, is considered one of the most harmful causes of stone decay on cultural heritage [1, 2]. This decay is produced by different mechanisms that have been widely studied during last decades [1, 3 and 4].

When soluble salts and water presence produce a decay of support and/or polychrome, it is necessary to apply a treatment that mitigates or paralyzes the decay. Treatments used for this purpose are: methods for insolubilizing salts, modification of room humidity and temperature, and partial or total desalination of the support. Desalination treatments are numerous, and can be grouped in two types depending on their applicability: those which can be applied on small and/or detached works of art, and those applicable on any kind of work of art.

Drying poultice is a common technique used by restorers for salt extraction to reduce soluble salts levels in porous materials that can be applied on any kind of work of art. This method is relatively easy: the poultice is made of one or more hydrophilic materials mixed with water and other substances, which is placed over the porous material for a certain time before being removed. Many authors have referenced that desalination by poulticing has two phases: a) the first one of support humectation where water gets into the porous system of the support, solving soluble salts, and b) the second phase of support and poultice drying where soluble salt extraction takes place [5-7].

The physical principles that take place on desalination treatments by poulticing are diffusion during the first phase of humectation and, diffusion and mainly advection during the second phase of salt extraction [5, 6, and 8]. Depending on salt transport process, other conditions are necessary to perform an effective salt extraction.

Based on the latest investigations about physical principles of the salt and moisture transport, this research studies the different behaviors depending on the porosity and pore size distribution of support and poultice, application techniques and poultices materials.

This study compares the results of the extracted salts (amount and maximum extraction depth) with three different kinds of poultices, on two types of natural stone with a great difference in porosity and pore size distribution. Other variables commonly performed on salt reduction treatments by dry poulticing have been fixed in order to reduce alternatives. These variables are the type of soluble salt added (NaCl), the thickness of the poultice (0.5 cm), the time of contact (48 hours) and the number of applications (3).

Six test specimens have been analyzed: three of Tosca Rocafort (travertine) and three of Bateig Novelda (biocalcarene). All the test specimens were previously desalinated by several deep immersions in deionized water. A saturated solution of 360g of NaCl per liter of water was prepared and stone test specimens were immersed during 10 days. Three types of poultices were applied: a thin porous poultice (sepiolite), a mixed porous poultice (sepiolite and glass) and thick-thin porous consecutive poultices (cellulose powder-sepiolite).

A considerable amount of samples from support and poultices have been analyzed. Samples on support were taken at five depths (0-0.5 cm, 0.5-1.5 cm, 1.5-3 cm, 3-4.5 y 4.5-6 cm), before saturation with NaCl, after salt saturation and after each of the three poultices applications. Poultices applied on the six test specimens after each of the three applications were also measured.

The quantitative content in soluble salts was determined by ionic conductivity following the procedure described at the Italian Norma UNI 11087-novembre 2003 [9].

The main objective of this research is to compare the behavior of these three different poultices on different stone materials. Differences in behavior may be explained because of the relation between the support and the poultice porosity. The experimental part of this research is still going on and sampling measures have not been finished yet. Results of this sampling will be ready by the end of May 2012. As long as main results are established and studied, conclusions will be ready by the end of June 2012.

## **Acknowledgements**

Financial support is gratefully acknowledged from the National Spanish "I+D+I MEC" Project HAR2011-29538.

## **REFERENCES**

- [1] A.E. Charola, and Herodotus. Salts in the deterioration of porous materials: an overview, *Journal of American Institute Conservation* volume 39, Number 3, Article 2, 2000.
- [2] C. Bläuer-Böhm. Quantitative salt analysis in conservation of buildings, *Restoration of Buildings and Monuments* 11, 409-18, 2005.
- [3] S. Lewin. The susceptibility of calcareous stones to salt decay, *First International Symposium on the Conservation of Monuments in the Mediterranean Basin*, 59–53, 1990.
- [4] R. Snethlage and E. Wendler. Moisture cycles and sandstone degradation, *Saving our architectural heritage: The conservation of historic stone structures*, 7–24, 1997.
- [5] L. Pel, A. Sawdy and V. Voronina. Physical principles and efficiency of salt extraction by poulticing, *Journal of Cultural Heritage* 11, 59-67, 2010.
- [6] A. Sawdy, B. Lubelli, V. Voronina, L. Pel. Optimizing the extraction of soluble salts from porous materials by poultices, *Studies in Conservation* 5, 26-40, 2010.
- [7] V. Vergès-Belmin, and H. Siedel. Desalination of masonries and monumental sculptures by poulticing: a review, *Restoration of Buildings and Monuments (Bauinstandsetzen und Baudenkmalpflege)* 11 (6), 391-408, 2005.
- [8] M. Auras. Poultices and mortars for salt contaminated masonry and stone objects, *Salt Weathering on Buildings and Stone Sculptures, Proceedings from the International Conference 22-24 October 2008, National Museum Copenhagen, Denmark*, 2008.
- [9] UNI 11087. Beni Culturali, Materiali lapidei naturali ed artificiali, *Determinazione del contenuto di Sali solubili*, Ente Nazionale Italiano di Unificazione, 2003.

## **A moisture transport-based approach to estimate the effect of desalination poultices and salt accumulating renders**

Roel Hendrickx<sup>1</sup>, Hilde De Clercq<sup>1</sup>, Sebastiaan Godts<sup>1</sup>, Chiara Giannotti<sup>1</sup>

<sup>1</sup>Royal Institute for Cultural Heritage (KIK-IRPA), Brussels, Belgium ([www.kikirpa.be](http://www.kikirpa.be))

### **ABSTRACT**

This contribution presents the on-going investigations at KIK-IRPA to estimate the effects of desalination poultices and salt-accumulating renders (or plasters) on salt contaminated porous substrates. The working principle of both types of materials is based on the absorption of liquid water into the substrate (ceramic brick) and the subsequent dissolution of salt crystals present, followed by the reverse transport towards the new layer(s) during drying. The physical principles were investigated in [1], [2] and [3]. However, in current practice the effectiveness is still generally assessed by either in-situ trials [4] or replica-experiments in the lab.

The two key parameters for poulticing are: the depth over which salts are removed, the quantity and the required time of application. Another important question is whether the substrate should be pre-wetted and how much. A larger timescale applies for salt accumulating renders (typically several years) for which the goals are slightly different. Ion transport towards the render may be a rather long-term wicking-like process where the moisture and salt source is typically the soil behind or below the wall. The efficiency of the application depends on the position of the drying front and the evaporation rate at this front.

The investigation carried out at KIK-IRPA is based on the theory of moisture transport and consists of three parts: (1) the experimental determination (on-site and in the lab) of relevant moisture transport parameters of substrates in practical cases, (2) the measurement (in the lab) of relevant moisture transport parameters of a number of commercial salt accumulating renders and (3) the numerical simulation of heat, moisture and salt transport in the combined system substrate-poultice or substrate-render.

In total 20 types of render and 2 types of poultices were investigated. The number of renders reduces to some 7 multilayer systems. Test specimens of these systems were produced for salt crystallisation tests. The selected test procedure is an interrupted wicking experiment. The material properties and the sequence of the layers were modelled in the simulation software.

The software used is Delphin 5, which is developed for heat- air and moisture (HAM) transport simulations, but which also contains a salt module which includes diffusion and advection, evaporation and condensation, hydration and dehydration and deliquescence of salts [5]. It uses the Pitzer model for ion and water activities. Osmotic pressure is not taken into account.

### **REFERENCES**

- [1] L. Pel, A Sawdy, V Voronina, Physical principles and efficiency of salt extraction by poulticing, *Journal of Cultural Heritage* 11, 1, 59-67, 2010.
- [2] J. Petkovic, H.P. Huinink, L. Pel, K. Kopinga, RPJ van Hees, Moisture and salt transport in three-layer plaster/substrate systems, *Construction and Building Materials* 24, 118-127, 2010.
- [3] V. Voronina, Salt extraction by poulticing: an NMR study, PhD thesis, Eindhoven University of Technology, 2011.
- [4] B. Lubelli, RPJ van Hees, H. De Clercq, Fine tuning of desalination poultices: try-outs in practice, Salt weathering on buildings and stone sculptures, Limassol, 19-22 October, 381-396, 2011.
- [5] A. Nicolai, Modeling and numerical simulation of salt transport and phase transition in unsaturated porous building materials, PhD thesis, Syracuse University, 2007.





## The crystallization of salt mixtures in relation to a climate study to mitigate salt decay in Medieval Murals and Limestone Tracery

Sebastiaan Godts<sup>1</sup>, Hilde De Clercq<sup>1</sup>, Roald Hayen<sup>1</sup>, Roel Hendrickx<sup>1</sup>

<sup>1</sup>Royal Institute for Cultural Heritage (KIK-IRPA), Monument Laboratory, Jubelpark 1, 1000 Brussels, Belgium.

### ABSTRACT

As salts are commonly found in monuments, and particularly in industrial environments such as Liege (Belgium), the salt content found in the murals and limestone tracery of the 16<sup>th</sup> century main entrance porch from the Saint Jacobschurch in Liege has been investigated and evaluated in relation to the indoor climate conditions. The research includes the determination of the actual and hygroscopic moisture contents and the quantitative ion content of lifted samples, the prediction of their phase equilibriums and a climate monitoring for a period of 12 months.

While the deliquescence points and the conditions for damage of single salts are well documented, the deterioration processes in case of salt mixtures become considerably more intricate. For building materials contaminated with a complex mixture of ions, an understanding of the thermodynamics of their phase transitions is required to assess the critical environmental conditions and the potential risks of salt damage. The computer program ECOS/RUNSALT is capable of predicting the crystallization behavior of salt mixtures based on a thermodynamic approach [1][2]. From the data obtained by the quantitative ion analyses the computer model enables the user to determine ranges of temperature and relative humidity (RH) in which phase transitions are kept to a minimum. The ECOS/RUNSALT outputs can then be compared to the climatic conditions monitored in the main porch of the church to evaluate the potential risk of salt damage.

In the murals and limestone tracery gypsum was identified together with a mixture of sodium nitrate, sodium chloride and calcium nitrate. The crystallization of these salts (excluding gypsum) will occur at RH between 25 and 65%. The climate study reveals that conditions of approximately 30% RH are measured numerous times and during several hours in afternoons and early evenings in the summer, such that the crystallization of hygroscopic salts such as calcium nitrate – crystallizing only under very dry conditions – cannot be ignored. During periods of extreme drought, often not considered, hygroscopic salts can become an important factor in the decay of historic building materials.

The results of the scientific process and possible conservation methods are presented and contribute to formulate a mitigation strategy to prevent further salt decay of the murals and tracery. The results show that the required conditions for preserving the murals and the tracery in the porch are a RH of at least 65% and a temperature of 20°C. In these conditions the salts are constantly dissolved in ambient moisture and no salt transitions occur. Knowing the appropriate thermohygrometric ranges, the question remains whether these climatic conditions are feasible. Today, the indoor climate conditions of the church porch are almost equal to the external climate as a result of damaged leaded glass windows and the lack of thermal insulation under the saddle roof or beneath the stone floor. Furthermore, the porch is regularly left open during religious ceremonies. Apart from basic repairs such as preventing water infiltration, a building physical approach of the complete porch is required to formulate a proper implementation of thermal insulation requirements and recommendations concerning the future use of the porch. These measures will result in a more controlled climate and a mitigation of salt damage. Another approach includes the extraction of salts using poultice materials tailored to the properties of the salt contaminated surface, such as the pore size distribution [3][4][5]. This method could be applied on the limestone tracery. However, such an approach is not applicable to the murals, which contain an organic binder hindering the moisture transport.

### REFERENCES

- [1] C. A. Price, (Ed.). An expert chemical model for determining the environmental conditions needed to prevent salt damage in porous materials. European Commission Research Report No 11, (Protection and Conservation of European Cultural Heritage). London: Archetype Publications, 2000.
- [2] D. Bionda, and P. Storemyr, Modeling the behavior of salt mixtures in walls: a case study from Tenaille von Fersen, Suomenlinna, Finland. In: T. Von Konow, ed. *The study of salt deterioration mechanisms. Decay of brick walls influenced by interior climate changes*. Helsinki: Suomenlinnan hoitokunta, pp. 95-101, 2002.

- [3] A. Bourgès, and V. Vergès-Belmin, Comparison and optimization of five desalination systems on the inner walls of Saint Philibert Church in Dijon, France. In: *Salt Weathering on building and Stone Sculptures, SWBSS Proceedings from the first International Conference, 22-24 October*. Copenhagen: The National Museum of Denmark, pp. 29-40, 2008.
- [4] B. Lubelli, , and R.P.J. Van Hees Desalination of masonry structures: Fine tuning of pore size distribution of poultices to substrate properties. *Journal of Cultural Heritage*, 11 (1): 10-18, 2009.
- [5] A. Sawdy, A. Heritage, L. Pel, A review of salt transport in porous media, assessment methods and salt reduction treatments. In: *Salt Weathering on building and Stone Sculptures, SWBSS Proceedings from the First International Conference, 22-24 October 2008*. Copenhagen: The National museum of Denmark, pp.1-28, 2008.

Friday, September 07, 2012

8 : 3 0 - 9 : 1 0	Encarnación Ruiz Agudo	Keynote lecture 6 - Physical and chemical mechanisms of salt weathering: combined strategies
9 : 1 0 - 9 : 3 5	<u>Leo Pel</u> and Tamerlan A. Saidov	Sodium sulfate crystallization in porous building materials due to drying
9 : 3 5 - 1 0 : 0 0	<u>Florian Osselin</u> , Antonin Fabbri, Teddy Fen-Chong, Arnault Lassin, Jean-Michel Pereira and Patrick Dangla	Poromechanics of the crystallization of salt during carbon dioxide injection in a deep saline aquifer
1 0 : 0 0 - 1 0 : 2 5	<u>Anna Ramon</u> and Eduardo E. Alonso	Thaumasite and ettringite massive crystal growth in two railway embankments
1 0 : 2 5 - 1 0 : 5 5	Coffee break	
1 0 : 5 5 - 1 1 : 3 5	Nima Shokri	Keynote lecture 7 - Pore scale investigation of the mechanisms governing evaporation from porous media
1 1 : 3 5 - 1 2 : 0 0	<u>Teresa Diaz Gonçalves</u> , Vânia Brito, Leo Pel, José Delgado Rodrigues	Magnitude of the stage I drying rate of porous building materials with different porosity
1 2 : 0 0 - 1 2 : 2 5	<u>W. de Boever</u> , W.V. Cnudde, J. Dewanckele, M. Boone, T. de Kock, M.N. Boone, E. Van Ranst, G. Silversmit, L. Vincze, H. Derluyn, P. Modregger, M. Stampanoni, K. de Buysser and G. de Schutter	Characterisation of sandstone (Kandla Grey) weathering behaviour by frost and salt action
1 2 : 2 5 - 1 2 : 5 0	<u>Rita Nogueira</u> , Ana Paula Ferreira Pinto and Augusto Gomes	Artificial weathering of lime mortars Desalination control by the drilling resistance measurement system
1 2 : 5 0 - 1 3 : 5 0	Lunch	
1 4 : 2 0	Bus transfer to Lisbon - boarding (the arrival times we estimated were: Airport – 16:50; LNEC – 17:15)	



## KEYNOTE LECTURE

### Physical and chemical mechanisms of salt weathering: combined strategies for preventing damage to porous materials

Encarnación Ruiz-Agudo<sup>1</sup>

<sup>1</sup>Dept. Mineralogía y Petrología, Universidad de Granada, Fuentenueva s/n, 18002 Granada, Spain

#### ABSTRACT

Crystallization within the void spaces of rocks and man-made materials is considered a mayor physical weathering process, and it is relevant to nearly every field of science, from industrial concerns related to pipe clogging in heating, cooling and oil recovery systems, to pore blockage in CO<sub>2</sub> sequestration, cement setting, crystal growth in gels, biomineralization, and conservation of cultural heritage and modern constructions affected by frost and salt damage. Conversely, the possible role of salts in the chemical weathering of minerals has been generally neglected, and previous studies have failed to disclose any relation between chemical and physical weathering phenomena induced by salts. Here we present evidence obtained by a combination of experimental techniques such as Atomic Force Microscopy (AFM), X-Ray Diffraction (XRD), Thermogravimetric Analysis (TGA), Differential Scanning Calorimetry (DSC) and Environmental Scanning Electron Microscopy (ESEM), on the chemical (dissolution) and physical (crystallization pressure) weathering induced by common and damaging soluble salts on a mayor rock-forming mineral such as calcite, and we propose novel strategies that may help preventing salt damage of porous materials by tackling both chemical and physical aspects of salt damage based on the formation of an organic (i.e. organophosphonate) nanofilm.

The results of our research show that, at high phosphonate concentration (> 5 mM), the reaction of calcite surfaces with phosphonates follows a pathway of dissolution of the substrate followed by precipitation of a calcium phosphonate phase. The presence of this overgrowth reduces calcite dissolution rate, thus representing a new treatment aimed at reducing solution-induced weathering of rock-forming minerals. As well, our results demonstrate that these additives act as crystallization promoters of inorganic salts on calcitic substrates, an effect that results in a (measured) decrease in the critical supersaturation reached by these salts when crystallizing in confined geometries, i.e., a pore, thus resulting in a reduction in crystallization pressure and damage to porous substrates such as building stones.

These results have implications in fields where in-pore crystallization of salts results in damage or plugging of the porous network, e.g., cultural heritage conservation and in the oil industry, where phosphonates are used as crystallization inhibitors.



## **Sodium sulfate crystallization in porous building materials due to drying**

Leo Pel, Tamerlan A. Saidov, Department of Applied Physics, Eindhoven University of Technology,  
PO Box 513, 5600 MB Eindhoven, the Netherlands

### **ABSTRACT**

Sodium sulfate is known as one of the most destructive salt leading to the deterioration of porous materials such as, monuments, sculptures and civil engineering structures. While sodium sulfate crystals are growing in a porous material a crystallization pressure will built up. The three main crystalline phases which can be formed are: thenardite ( $\text{Na}_2\text{SO}_4$ , anhydrous salt), mirabilite ( $\text{Na}_2\text{SO}_4 \cdot 10\text{H}_2\text{O}$ ) and the thermodynamically metastable heptahydrate ( $\text{Na}_2\text{SO}_4 \cdot 7\text{H}_2\text{O}$ ). In order to predict and prevent crystallization damage it is necessary to know the salt phase that is responsible for damage as well as its nucleation and growth behavior in a porous material. In this study we have used Nuclear Magnetic Resonance (NMR) to non-destructively measure the concentration in materials during drying. We have combined the non-destructive measurement of the concentration of the pore solution in a material by using Nuclear Magnetic Resonance (NMR) with optical measurement of the dilation of the material during crystallization, giving the possibility to study the expansion due to crystallization. It was observed that for all studied materials thermodynamically metastable heptahydrate rather than the stable mirabilite is being formed.





# Poromechanics of the crystallization of salt during carbon dioxide injection in a deep saline aquifer

Florian Osselin<sup>1,3</sup>, Antonin Fabbri<sup>2</sup>, Teddy Fen-Chong<sup>1</sup>, Arnault Lassin<sup>3</sup>, Jean-Michel Pereira<sup>1</sup>, Patrick Dangla<sup>1</sup>

<sup>1</sup> Laboratoire Navier (IFSTTAR, CNRS, ENPC), 2 Allée Kepler - 77420 Champs-Sur-Marne, France

<sup>2</sup> ENTPE, DGCB, 3 Rue Maurice Audin 69120 Vaulx-en-Velin, France

<sup>3</sup> BRGM, 3 Avenue Claude Guillemin, Orléans-la-Source, France

## ABSTRACT

In the context of increasing environmental concern, Carbon Capture transport and geological Storage (CCS) appear to be an interesting solution to cope with global warming and increasing carbon content in the atmosphere. However, development of the deep saline aquifer storage requires additional research and development particularly in physics of porous media and coupled processes. Indeed, injection of supercritical carbon dioxide in a deep saline aquifer disturbs dramatically the equilibrium of the medium leading to highly coupled THMC (Thermo-Hydro-Mechanical-Chemio) behavior. For instance, numerical simulations have shown the strong effect of the precipitation induced by carbon dioxide injection on the porosity and permeability. Indeed, by adding solid matter in the porous medium, precipitation decreases porosity, which has a huge impact on permeability by clogging the percolating paths. A few percent decrease of porosity can often lead to a drop of several orders of magnitude in permeability [1].

On the other hand, it is known since Correns (see [2] for a commented translation of the original paper), that crystallization of salt in a porous medium is the cause of the creation of strong stresses on the pore wall, able to fracture and damage the porous medium. This mechanical effect named crystallization pressure, which is commonly not considered in CCS studies, may lead to counteract the diminution of injectivity by creating a connected micro-fracture network. This also arises several security issues because the damage on the host rock may open leaking paths that can be detrimental to the adjacent environment.

The aim of our work is to determine the balance between clogging and damage in order to predict the evolution of porosity and permeability during carbon dioxide injection at the material scale. The study presented here is based on both experimental and theoretical work. At first an updated expression of the so-called Correns law [4] has been developed taking into account temperature and pressure variations, and then a microscopic model has been obtained in order to calculate the creation and evolution of crystallization pressure in a representative elementary volume using the poromechanical framework developed at Laboratoire Navier (cf. Figure 1).

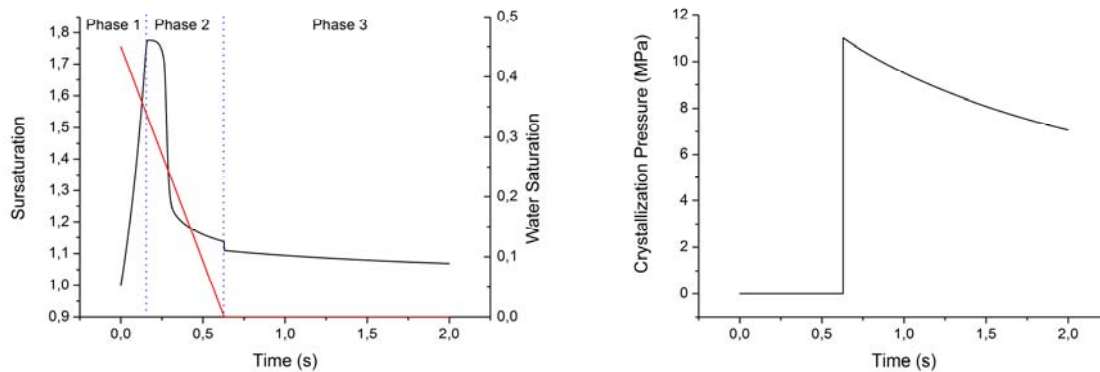


Figure 1: Evolution of sursaturation (left) and crystallization pressure (right) in a pore subjected to flow through drying

This theoretical work is conducted in parallel with an experimentation of reactive percolation allowing the injection of supercritical carbon dioxide in a plug of rock saturated with brine, and under geotechnical conditions (temperature and triaxial stresses). The aim of this experiment is to give an insight of the evolution of porosity and permeability during the carbon dioxide injection, conjointly to results on the crystallization pattern and porous matrix evolution in order to determine the relative importance of both clogging and damage.

## REFERENCES

- [1] I. Gaus, P. Audigane, L. André, J. Lions, N. Jacquemet, P. Durst, L. Czernichowski-Lauriol & M. Azaroual, Geochemical and Solute transport Modelling for CO<sub>2</sub> storage, what to expect from it ? *International Journal of Greenhouse Gas Control*, 2, 605-625, 2008.
- [2] R. Flatt, M. Steiger & G. Scherer, A Commented translation of the paper by C.W. Correns and W. Steinborn on crystallization pressure *Environmental Geology*, 52, 187-203, 2006.
- [3] O. Coussy Deformation and stress from in-pore drying-induced crystallization of salt *Journal of the Mechanics and Physics of Solids*, 54:1517-1547, 2006.
- [4] M. Steiger, Crystal Growth in Porous Materials -II : Influence of crystal size on the crystallization pressure, *Journal of Crystal Growth*, 28, 470-481, 2005.

# Thaumasite and ettringite massive crystal growth in two railway embankments

Anna Ramon<sup>1</sup> and Eduardo E. Alonso<sup>1</sup>

<sup>1</sup>Department of Geotechnical Engineering and Geosciences, UPC, Barcelona. (anna.ramon@upc.edu, eduardo.alonso@upc.edu)

## ABSTRACT

Thaumasite and ettringite crystal growth is at the origin of an intense expansion that affected two embankments, 18 meters high, located in the Madrid-Barcelona high speed railway. The embankments were made of compacted sulphated Tertiary claystone. The embankments material belongs to the same geologic formation where Lilla tunnel [1] and Pont de Candí bridge [2], [3], have experienced severe heave problems due to gypsum crystal growth.

Pallaessos embankments give access to a bridge 196 meters long. A transition wedge was built next to abutment structures in both embankments in order to provide a progressive change of stiffness when trains approach the rigid bridge structure. Cement treated soil was used for the construction of both wedges.

Heave of the surface of embankments, near the abutments, was detected at an early time after the end of the embankments construction during the track leveling monitoring carried out periodically by the railway administration. Afterwards a grid of jet grouting columns was executed on both embankments to stabilize the embankment material. However, heave rate did not stop after the jet grouting treatment. Continuous extensometers installed in boreholes through the embankments showed that strains were developing in the upper 8-10 metres of the embankments (fig. 1).

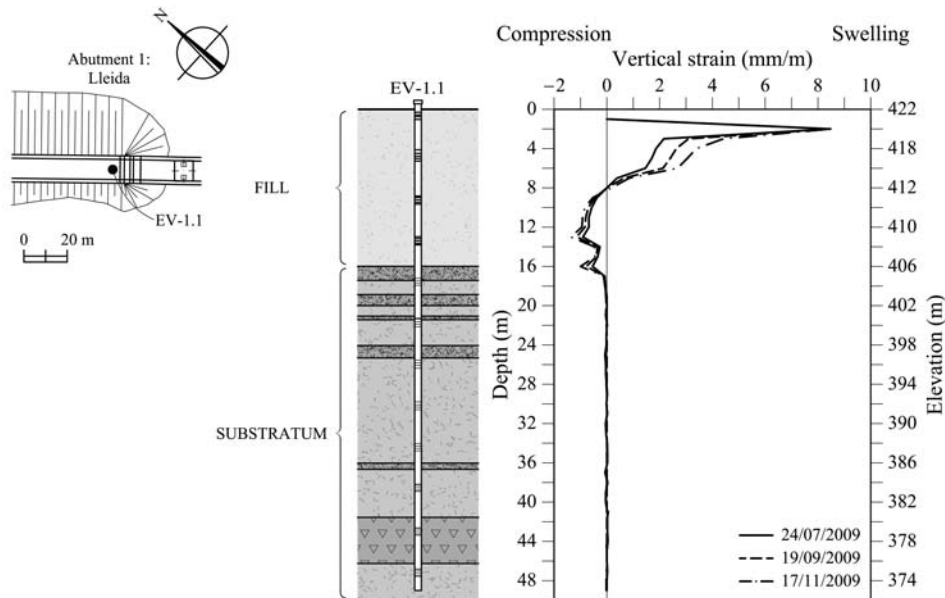
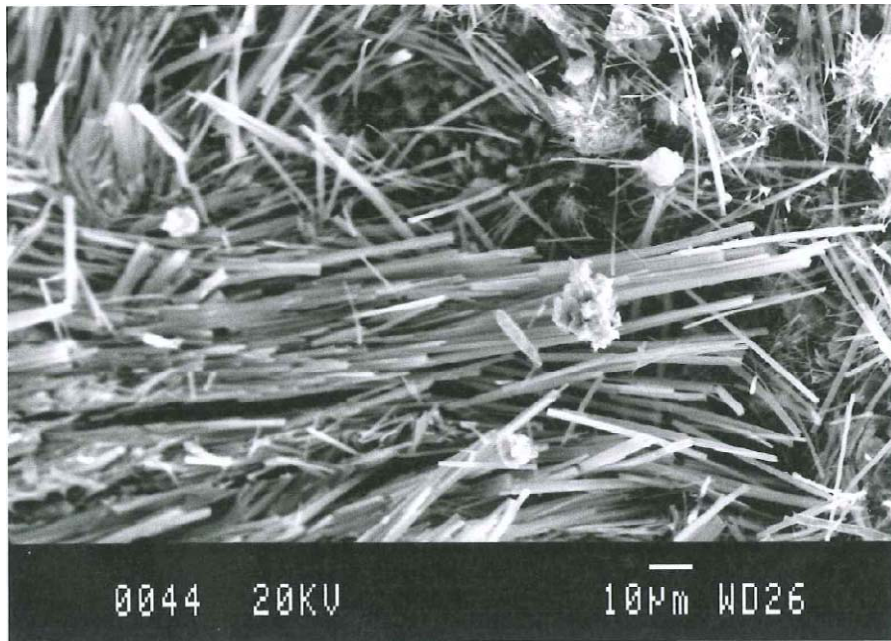


Figure 1: Vertical strains measured by sliding micrometer EV-1.1

Inclinometers installed in boreholes indicated that swelling deformations occur not only in the vertical direction, but also in the horizontal direction. Monitoring of topographic marks installed on the surface of the embankments confirmed that a volumetric swelling was deforming the embankments. The distribution of displacements along the embankment axis agrees with the intensity of the jet-grouting treatment.

Samples of embankment material recovered from boreholes were studied by means of X-ray diffraction (XRD) and scanning electron microscope with an energy dispersive spectrometer (SEM-EDS). Ettringite and thaumasite crystals were found in all the samples analyzed (Fig. 2). Ettringite crystals require an environment with a high pH value and the presence of calcium, sulphates, aluminum and water for its growth. Silicon and carbonates are also needed for the formation of thaumasite. The hydration of cement components, present in the transition wedges and in the jet-grouting treatment, rises the pH value. The

resulting alkaline environment dissolve clay minerals and releases aluminium and silicate ions. High pH values also favor the dissolution of sulphate minerals (gypsum). Then the combination of sulphates from the soil, alumina released from clay minerals, calcium from cement components and gypsum, and the availability of water from rainfall leads to the formation of ettringite. The dissolution of calcite in carbonic acid releases the carbonates which are necessary for the formation of thaumasite from ettringite crystals previously developed. The formation of thaumasite and ettringite is essentially unlimited because of the availability of the necessary components for its formation in the embankments. It was concluded that deformations in the embankments will proceed for a long time if no remedial measures are carried out. A finite element model of embankment swelling was developed to calculate the swelling loads against the bridge abutments and also to estimate the state of stress on the embankments. It was found that a dangerous state of passive stresses had been developed on the upper 8-10 m of the embankment. The costly remedial measures carried out will also be outlined in the presentation.



*Figure 2: Ettringite needles and thaumasite flat crystals found in a tested sample*

## REFERENCES

- [1] E.E. Alonso, I. R. Berdugo, D. Tarragó and A. Ramon, Tunnelling in sulphate claystones. Proc. 14th European Conference on Soil Mechanics and Geotechnical Engineering, Madrid, 24-27 September, 1, 103-122. Invited Lecture, 2007.
- [2] E.E. Alonso, A. Ramon, Heave of a railway bridge induced by gypsum crystal growth. field observations. Submitted for publication, 2012.
- [3] A. Ramon & E. Alonso, Heave of a railway bridge. Modelling of gypsum crystal growth. Submitted for publication, 2012.

## KEYNOTE LECTURE

### Pore scale investigation of the mechanisms governing evaporation from porous media

Nima Shokri<sup>1</sup>

<sup>1</sup>Department of Earth and Environment, Boston University, Boston, MA, USA

#### ABSTRACT

Drying of porous media is strongly influenced by the interplay between transport properties of the medium and external boundary conditions. Initial stages of evaporation are supported by capillary-induced liquid flow connecting a receding drying front (i.e. the interface between saturated and unsaturated zone) to evaporation surface, the so-called stage-1 evaporation. At a certain drying front depth, gravity overcomes capillary and viscous forces and a transition from liquid flow-supported stage-1 to diffusion-supported stage-2 evaporation occurs [1]. Characteristic lengths deduced from transport properties of porous media are proposed to predict the end of stage-1 evaporation under different boundary conditions. Effects of pore size distribution [1], wettability [2-5] and structure [6] of porous media are considered in the proposed characteristic lengths. The model predictions are checked and evaluated by a complete series of micro- and macro-scale evaporation experiments using cutting-edge techniques such as synchrotron x-ray tomography [7] and neutron radiography [8].

Along with the analysis of stage-1 evaporation under different boundary conditions, stage-2 evaporation was investigated in detail. We show that end of stage-1 evaporation is followed by jump of the liquid meniscus from the surface to a level below whose thickness could be estimated by a characteristic length of connected clusters at the secondary drying front (i.e. the interface between unsaturated and dry zone) obeying a power law with the system's Bond number. The subsequent drying is governed by the capillary liquid flow from the wet zone to the secondary drying front, vaporization at that level and vapor diffusion through the overlying dry layer [9].

Besides, new insights regarding dynamics of drying front displacement [4, 8], its three dimensional structure [10] and preferential flows affected by texture, wettability and structural heterogeneity of drying porous media [2, 5-6] are discussed. Our results also offer new tools to manipulate the drying of porous media in desired ways to control the evaporative water losses and also solute transport and deposition patterns in drying porous media [2, 5, 7, 11].

#### REFERENCES

- [1] P.S. Lehmann, S. Assouline, and D. Or, Characteristic lengths affecting evaporative drying of porous media, *Phys. Rev. E*, 77,056309, 2008.
- [2] N. Shokri, P. Lehmann and D. Or, Effects of hydrophobic layers on evaporation from porous media, *Geophys. Res. Lett.*, 35, L19407, doi:10.1029/2008GL035230, 2008.
- [3] N. Shokri, P. Lehmann, and D. Or, Characteristics of evaporation from partially-wettable porous media, *Water Resour. Res.*, 45, W02415, doi:10.1029/2008WR007185, 2009.
- [4] N. Shokri, M. Sahimi, and D. Or, Morphology, Propagation Dynamics and Scaling Characteristics of Drying Fronts in Porous Media, *Geophys. Res. Lett.*, 39, L09401, doi:10.1029/2012GL051506, 2012.
- [5] N. Shokri, D. Or, Drying patterns of porous media containing wettability contrasts, *Chem. Eng. J.* (in review), 2012.
- [6] N. Shokri, P. Lehmann and D. Or, Evaporation from layered porous media, *J. Geophys. Res.*, 115, B06204, doi:10.1029/2009JB006743, 2010.
- [7] N. Shokri, P. Lehmann, and D. Or, Liquid phase continuity and solute concentration dynamics during evaporation from porous media- pore scale processes near vaporization surface, *Phys. Rev. E*, 81, 046308, 2010.
- [8] Shokri, N., P. Lehmann, P. Vontobel, and D. Or (2008), Drying front and water content dynamics during evaporation from sand delineated by neutron radiography, *Water Resour. Res.*, 44, W06418, doi:10.1029/2007WR006385
- [9] N. Shokri, and D. Or, What determines drying rates at the onset of diffusion controlled stage-2 evaporation from porous media?, *Water Resour. Res.*, 47, W09513, doi:10.1029/2010WR010284, 2011.
- [10] N. Shokri, and M. Sahimi, The structure of drying fronts in three-dimensional porous media, *Phys. Rev. E* (in review), 2012.

[11] M. Norouzi Rad, M. and N. Shokri, Nonlinear effects of salt concentrations on evaporation from porous media, *Geophys. Res. Lett.*, 39, L04403, doi:10.1029/2011GL050763, 2012.

# Magnitude of the stage I drying rate of porous building materials with different porosity

Teresa Diaz Gonçalves<sup>1</sup>, Vânia Brito<sup>1</sup>, Leo Pel<sup>2</sup>, José Delgado Rodrigues<sup>1</sup>

<sup>1</sup>National Laboratory for Civil Engineering (LNEC), Lisbon, Portugal

<sup>2</sup>Technical University of Eindhoven (TUE), The Netherlands

## ABSTRACT

In building conservation, many problems are related to the presence of water in porous materials such as stone, mortars and ceramics. Indeed, moisture can be seen as the catalyst for many deterioration mechanisms. It gives rise to harmful chemical reactions, such as sulphate attack, enables biodeterioration and prompts salt decay, one of the most harmful deterioration mechanisms of porous building materials. A better understanding of drying processes can provide an important basis to find efficient ways of controlling the presence and, therefore, mitigating the damaging effects of moisture. This is particularly important in the case of salt decay because it typically occurs during drying when water and ions are transported towards the surface as the water evaporates. Therefore, a better knowledge of drying is also necessary for the understanding of the decay mechanism itself.

In this study we have looked at the evaporation from various porous materials with different porosity and surface roughness.

Generally, a two-stage model (Fig. 1) is considered appropriate to describe drying of porous materials. The two stages are the constant drying rate period (CDRP), which takes place at the higher moisture contents, and the falling drying rate period (FDRP), at the lower moisture contents. In the CDRP, the drying front is very close to the outer surface. Liquid moisture transport dominates and the evaporation rate is highest. In general, it is in this period that most of the moisture content in a material drying from saturation is eliminated. In this period, if salts are present, they will be transported to the surface where they crystallize as efflorescence.

It is often assumed that the CDRP drying rate is similar to that of a free water surface, due to the presence of a liquid film covering the whole surface of the material during this period. This idea has been contradicted by experimental results of different researchers [1-3], who reported that the CDRP evaporation rate of porous building materials was not necessarily equal, and may even be significantly higher than that from a free water surface subjected to similar environmental conditions.

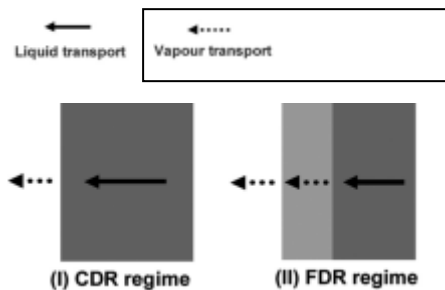


Figure1: Drying of a porous building material

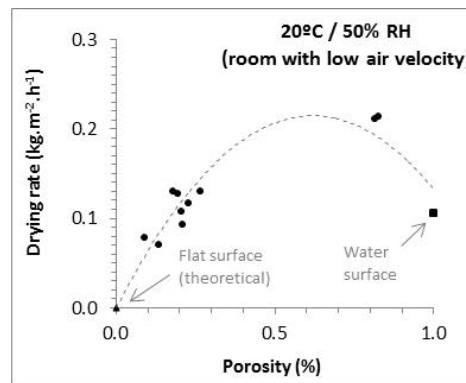


Figure2: Variation of the CDRP evaporation rate with the capillary porosity of the materials

In this study we analyze the CDRP drying rate for eight porous building materials. Both natural stones and artificial materials were tested: the Bentheimer sandstone, four limestone varieties (Ançã, Lecce, Malta's Globigerina, and a Portuguese low porosity limestone), red ceramic brick, slaked lime/sand mortar (1:3 in volume) and three kinds of calcium silicate material. The capillary porosity of the stones, mortar and bricks is in the interval 9-27%, whereas two of the calcium silicate materials (with 82% and 83% porosity, respectively) cover the higher range of values.

Several experiments were performed following RILEM procedure for measurement of the "evaporation curve" [4], at 20°C and various RH.



The results of one of these experiments can be seen in Fig. 2, which shows the CDRP drying rate as a function of capillary porosity. Here, a free water surface is regarded as a material with 100% porosity ( $P=1$ ). Point (0,0) is attributed to a theoretical material with 0% porosity ( $P=0$ ).

These results show that the CDRP drying rate varies among the different materials. In some cases it is lower than that of the free water surface, which is inconsistent with the presence of a liquid film covering the whole surface of the material during this period. In other cases, it is higher than that, as was also found in other studies [1-3].

It can be concluded that the drying rate is a function of the capillary porosity. If we consider only materials with porosity up to 27%, i.e., the common building materials (natural stones, bricks and mortar), the relationship is almost linear, as reported in a previous article [3]. However, when we consider also the materials with higher porosity (above 80%) and the free surface of water (100% porosity), a linear relationship is no longer able to describe this relation. In this case, a better approximation can be made by parabolic function.

We hypothesize that changes in drying rate are due to the variation of the effective surface of evaporation. Roughening with sand or polishing were not successful in creating significant differences in the drying rate of a same material [3]. However, surface texture measurements performed with an optical method revealed that the surface area of the materials increases exponentially as the measurement scale decreases, tending to infinity as the scale approaches zero. This behavior indicates that the measured surfaces have fractal properties, which is in accordance with previous studies. Hence, surface irregularity due to internal features (i.e., porosity) could be relevant to explain the observed differences in the CDRP drying rate. This hypothesis will be discussed based on the obtained results.

#### **Acknowledgements**

This work was performed under the research project DRYMASS (ref. PTDC/ECM/100553/2008) which is supported by national funds through the Fundação para a Ciência e a Tecnologia (FCT) and LNEC.

#### **REFERENCES**

- [1] C. Hammecker, Importance des transferts d'eau dans la dégradation des pierres en oeuvre. Thèse de doctorat, Université Louis Pasteur, Strasbourg, France, 1993.
- [2] B. Rousset-Tournier, D. Jeannette, C. Destrigneville, Stone drying: an approach of the effective evaporating surface area, Proc. 9th Int. Congress on Deterioration and Conservation of Stone, Venice, June 19–24, 629-635, 2000.
- [3] T. Diaz Gonçalves, V. Brito, L. Pel, Water vapor emission from rigid mesoporous materials during the constant drying rate period. *Drying Technology* 30, 462–474, 2012.
- [4] RILEM TC 25-PEM, Recommended tests to measure the deterioration of stone and to assess the effectiveness of treatment methods, *Materials and Structures* 13, 175-253, 1980.

## Characterisation of sandstone (Kandla Grey) weathering behaviour by frost and salt action

De Boever, W.<sup>1</sup>, Cnudde, V.<sup>1</sup>, Dewanckele, J.<sup>1</sup>, Boone, M.<sup>1</sup>, De Kock, T.<sup>1</sup>, Boone, M.N.<sup>2</sup>, Van Ranst, E.<sup>1</sup>, Silversmit, G.<sup>3</sup>, Vincze, L.<sup>3</sup>, Derluyn, H.<sup>4</sup>, Modregger, P.<sup>5,6</sup>, Stampanoni, M.<sup>5,7</sup>, De Buysser, K.<sup>8</sup>, De Schutter, G.<sup>9</sup>

<sup>1</sup>Dept.ofGeologyandSoilScience,GhentUniversity,GhentBelgium

<sup>2</sup>Dept.ofSubatomicandRadiationPhysics,GhentUniversity,Ghent,Belgium

<sup>3</sup>Dept.ofAnalyticalChemistry,GhentUniversity,Ghent,Belgium

<sup>4</sup>ChairofBuildingPhysics,ETHZürich,Switzerland

<sup>5</sup>SwissLightSource,PSI,Villigen,Switzerland

<sup>6</sup>UniversityofLausanne,SchoolofBiologyandMedicine,Lausanne,Switzerland

<sup>7</sup>InstituteforBiomedicalEngineering,UZH/ETHZürich,Switzerland

<sup>8</sup>Dept.ofInorganicandPhysicalChemistry,GhentUniversity,Ghent,Belgium

<sup>9</sup>Magnel Laboratory for Concrete Research, Ghent University, Ghent, Belgium

### ABSTRACT

Imported natural building stones are becoming increasingly important in Western Europe, often as a replacement of traditional, locally extracted building materials. Unlike these traditional stones, which have been used for several centuries, the weathering behaviour of newly imported materials in the current climatic conditions is often unknown. Not only are the stones exposed to a lot of water, they also have to be resistant to mechanical stresses created by the crystallisation of de-icing salts in the pore network. These de-icing salts are frequently used in Western European winters, and their use goes together with constant fluctuation between freezing and thawing conditions. De-icing salts can have harmful effects on natural building materials in many ways: by creating a hydration pressure or crystallisation pressure; by having a different thermal expansion than the rock in which they are present; by generating thermal shock (Siegesmund *et al.*, 2002) or by frost salt scaling (Valenza and Scherer, 2006).

Changes in the internal structure of the pore network are difficult to monitor when different weathering mechanisms are active. This means that, in order to understand the influence of de-icing salts, it is of great importance that the materials' inner structure is characterised under changing environmental conditions, with and without the presence of de-icing salts. In this study we focussed on the Indian Kandla Grey sandstone, which is frequently imported in Belgium over the last years. Kandla Grey is a subarkose sandstone, consisting mainly out of quartz and feldspars. The stone contains both macroscopically visible, dark laminations (rutile enriched, figure 1a) and microscopically visible laminations of muscovite (figure 1b).

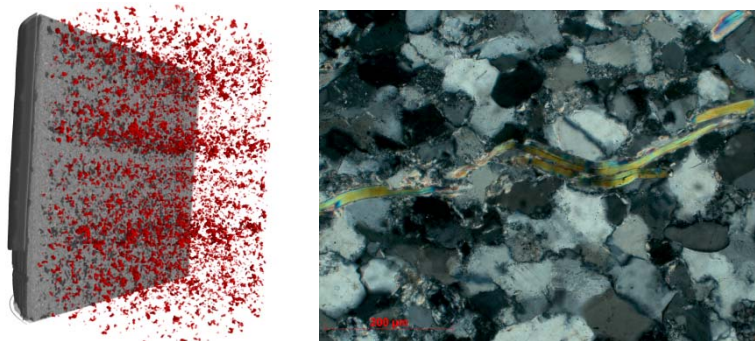


Figure 1: a) Distribution of the dense minerals (rutile) in a 15 mm Kandla Grey core. b) optical microscopy image of Kandla Grey (crossed polars), showing quartz and a mica lamination.

Kandla Grey was first characterised in several ways, according to the European Standards regarding natural stone testing. These tests included capillary water absorption, water absorption under vacuum (to calculate open porosity and apparent density), drying rate and determination of the water vapour permeability. In addition to this, X-ray diffraction (XRD) and X-ray fluorescence (XRF) were used to determine the chemical composition of Kandla Grey. Furthermore, the pore structure was investigated using optical fluorescent microscopy, scanning electron microscopy (SEM) and high resolution X-ray

computed tomography (HRXCT, both in laboratory as at the synchrotron facility). The effect on de-icing salts on the thermal expansion coefficient of Kandla Grey was measured using thermo mechanical analysis (TMA). Finally, the weathering behaviour (salt- and frost-induced) was monitored, providing a link between this behaviour and the characteristics of the stone.

Kandla Grey has an open porosity of just 3.02 ( $\pm$  0.62) vol.% and an apparent volumic mass of 2683 ( $\pm$  7.67) kg/m<sup>3</sup>. Pores are not visible by using traditional optical microscopy, indicating that porosity in Kandla Grey consists almost completely out of micropores (smaller than 1  $\mu$ m). SEM demonstrated that the regions around the mica layers are the most porous of the stone. Although water absorption by capillarity showed that the capillary water coefficient C was the same for absorption parallel to the laminations as for absorption perpendicular to the laminations, migration and crystallisation of a saline solution in the material demonstrate that preferential transport along some of the laminations did occur. The total amount of absorbed liquid during the capillarity test is similar when using distilled water or a solution containing 7.5 mass-% de-icing salt solution. When drying the saturated samples of Kandla Grey under constant temperature and relative humidity, the drying rate was lower for those samples saturated with the saline solution compared to those saturated with distilled water. TMA clearly revealed the effects that crystallised salts have on the thermal expansion of a material. When comparing the thermal expansion coefficients of Kandla Grey with and without the presence of salts, values of respectively 12  $\mu$ m.m<sup>-1</sup>.°C<sup>-1</sup> and 17  $\mu$ m.m<sup>-1</sup>.°C<sup>-1</sup> were found. This indicates that de-icing salts cause additional stresses within the material. When exposing Kandla Grey to the frost resistance test (EN 12371), one out of six samples developed a fracture along its entire length, indicating that Kandla Grey failed to withstand the test. In the European test to determine salt weathering resistance (EN 12370), only spalling of the surfaces of the samples occurred.

Water transport is clearly influenced by the internal structure of Kandla Grey: preferential liquid uptake and water vapour transport occurs along the macroscopically invisible mica laminations. The preferential moisture transport inside these layers causes them to be zones of weakness in the material. Water in these laminations creates a vulnerability towards frost-thaw weathering. Frost weathering phenomena are accelerated by the presence of salts in the pore space, since they cause a drop in the drying rate of the material. Furthermore, these salts have another thermal expansion coefficient than the surrounding material, creating additional stresses due to differential thermal expansion. When using Kandla Grey as a building material for outside use, the intrusion of liquid and saline solutions should be kept to a minimum, since this study demonstrates that the properties of the laminations in the stone influence the frost-weathering behaviour. Based on the experiments that have been carried out in this research, it can be concluded that Kandla Grey has zones that are sensitive to frost and salt weathering in the Western European climate.

## REFERENCES

- [1] S. Siegesmund, T. Weiss, et al., Salt weathering: a selective review. Natural Stone, Weathering Phenomena, Conservation Strategies and Case Studies. G. Society. London, Special Publications: 51-64, 2002..
- [2] J.J. Valenza, and G. W. Scherer, "Mechanism for salt scaling." Journal of the American Ceramic Society **89**(4): 1161-1179, 2006.

## Artificial weathering of lime mortars desalination control by the drilling resistance measurement system

Rita Nogueira<sup>1</sup>, Ana Paula Ferreira Pinto<sup>1</sup>, Augusto Gomes<sup>1</sup>

<sup>1</sup>UTL-Instituto Superior Técnico - ICIST, Lisbon, Portugal

### ABSTRACT

Artificial salt crystallization tests are frequently used as a research tool estimator of the porous materials durability and susceptibility because salt weathering is one of the most important deterioration mechanisms that building materials undergo in a wide range of environments [1, 2]. Pressures created by salt crystallization in pores weaken the material until the overcome of its mechanical strength and material damage [3].

Salt crystallization tests promote artificial deterioration by salt crystallization-dissolution processes that occur in materials interior. For the assessment of deterioration caused by salt crystallization tests, it may be necessary to undertake a desalination process on tested materials.

Desalination may be performed by poultices impregnated with deionized water, or, in the case of low dimension samples, by immersion in deionized water. Desalination evolution may be controlled by monitoring the increasing amount of salts dissolved in the water over time. Since we are in the presence of diluted salt solutions there is a linear dependence between ion concentration and specific conductivity. Therefore, conductivity measurement provides information on the total content of ionic species and, for that reason, on soluble salts. However, this test does not give information about the total amount of salts that remain inside the material and how they are distributed on the sample. The present work shows the possibility of using the drilling resistance measurement system (DRMS) for identifying the salt distribution within the tested samples, monitoring desalination process and assessing mechanical alteration on lime mortars due to salt crystallization.

The drilling resistance test enables the evaluation of resistance in depth and has been used to characterize materials like stones and mortars. Considering that the deteriorated material will not have a higher mechanical resistance than it had before the ageing process, the measurement of higher values of drilling resistance on the aged samples can only be explained by the presence of salt inside the material.

To accomplish the proposed aim, two air lime mortars formulations (CA1 and CA2), with a 1:4 binder-aggregate ratio, by volume, and different water-binder ratio (1.05 and 1.10, respectively), were studied and submitted to artificial salt crystallization ageing tests, employing a sodium chloride solution (15%w/w), after a curing period of 3 months [Figure 1].

The salt crystallization procedure adopted was based on the test performed by Selwitz [4] and Agostinho *et al.* [5] and 3 cycles were performed on standard samples (40x40x160mm), previously dried at 60°C until constant mass. A cycle comprises four phases of a one week period each, the first for the saline solution absorption and the others for the salt displacement and crystallization inside samples. The samples were placed, vertically, inside individual glass dishes with the same amount of saline solution or water according to cycle phase. Paraffin wax was used to prevent evaporation, sealing the system.

Desalination was accomplished by samples immersion, firstly on water supplied by utilities and later on distilled water. The samples of each mortar formulation were desalinated using different containers. Conductivity of the water where the samples were immersed was measured and replaced by the same water volume every week. After a desalination period of 3 months, the conductivity stabilized and the desalination process was ended [Figure 2].

The deterioration of both tested mortars was evaluated by visual observation, determination of mass variation, water absorption by capillarity, porosity, density, ultrasound velocity and drilling resistance.

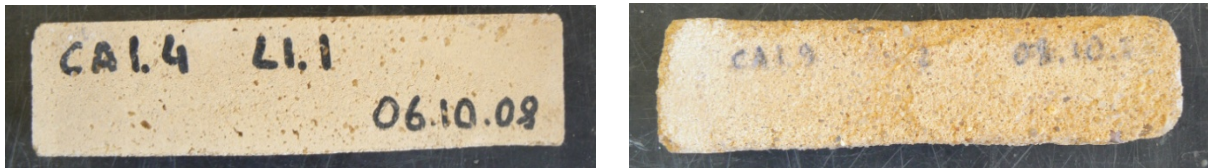


Figure 1: CA1 mortar samples before ageing (left) and after ageing (right).

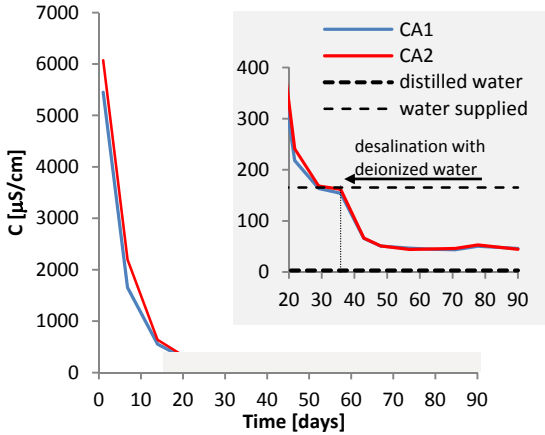


Figure 2: Evolution of the conductivity during desalination.

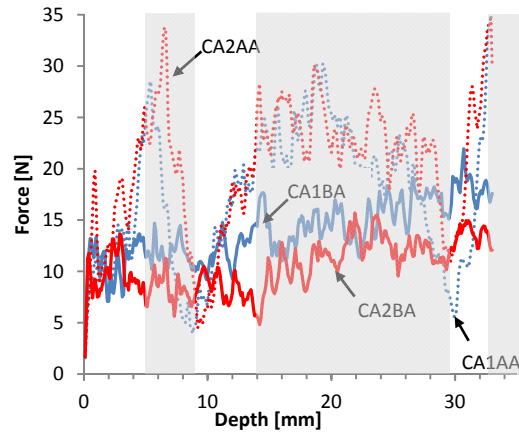


Figure 3: Drilling resistance of the tested mortars before (BA) and after ageing (AA).

After ageing and desalination, both tested mortars registered mass loss [Figure 1] and an increase of water absorption through capillarity. On the contrary, the mechanical characterization performed points to an increment of the mechanical properties of the aged mortars, which can only be explained by the presence of salts inside the tested samples.

The mortars drilling resistance, before and after ageing is presented in Figure 3, and each drilling profile corresponds to an average of 9 drilling tests. The drilling profiles of the tested mortars before ageing show a certain regular drilling resistance in-depth and a higher mechanical resistance for CA1, confirming compressive strength results. The drilling tests performed on weathered samples show an irregular in-depth resistance behavior, which confirms the salt presence inside the samples and gives information about their distribution. Figure 3 enables the identification of salt presence in the following depth ranges: 4-8mm, 13-28mm and >32mm.

As conclusion, the drilling resistance was able to identify salt presence on the desalinated samples and the salt distribution inside the samples, differentiating high resistance results where salts are concentrated and lower resistance results where mortar deterioration was more pronounced. The results point DRMS as a useful tool for monitoring desalination processes, mechanical alteration and salt distribution on lime mortar due to salt crystallization.

## REFERENCES

- [1] F. Henriques, A.E. Charola, Development of lime mortars with improved resistance to sodium chloride crystallization, Proc. 9th Int. Congress on Deterioration and Conservation of Stone, Venice, 19-24 June, 335-342, 2000.
- [2] C. Rodriguez-Navarro, E. Doehne, E. Sebastian, How does sodium sulfate crystallize? Implications for the decay and testing of building materials, Cement and Concrete Res. **30**, 1527-1534, 2000,.
- [3] G.W. Scherer, Stress from crystallization of salt, Cement and Concrete Res. **34**, 1613-1624, 2004,.
- [4] C. Selwitz, E. Doehne, The evaluation of crystallization modifiers for controlling salt damage to limestone, Journal of Cultural Heritage, **3**, 205-216, 2002.
- [5] C. Agostinho, A.P. Ferreira Pinto, A. Gomes, Advantages of using lime putty on the formulation of compatible replace mortars, Proc. 1st Historical Mortars Conference, Lisbon, 24-26 September, 2008.

## POSTER PRESENTATIONS

### **Salt degradation in stone of historical Buildings: The importance of water absorption coefficient**

J.M.P.Q. Delgado<sup>1</sup>, A.S. Guimarães<sup>1</sup>, V.P. de Freitas<sup>1</sup>

<sup>1</sup>LFC – Laboratório de Física das Construções, Departamento de Engenharia Civil, Universidade do Porto, Rua Dr. Roberto Frias, s/n; 4200-465 Porto, Portugal

#### **ABSTRACT**

The crystallization of soluble salts is a major mechanism of degradation of some building materials, including stone. This mechanism of deterioration is based on the pressure exerted by the formation of salt structures in porous materials, with increased volume and is dependent on the type of salts involved and the size and arrangement of pores. When the pressure exceeds the internal strength of the material, and particularly when the salt formations undergo cycles of crystallization and dissolution in response to fluctuating levels of humidity, the deterioration of materials typically becomes apparent.

It is therefore essential to understand the phenomenon of crystallization and dissolution of salts, i.e., to know the conditions of crystallization of each salt, depending on relative humidity and air temperature.

For this purpose we developed an experimental work, using four samples of stone (one limestone and three granites), which consists, initially, to study the variation of the water absorption coefficient with and without soluble salts (NaCl,  $Mg(NO_3)_2 \cdot 6H_2O$  and  $K_2SO_4$ ). An analyze of the water absorption coefficients values obtained with the classification used with Germany code; it was possible to classify the samples as to their permeability. Thus, the limestone, old granite-1 and old granite-2 samples are classified as “Preventive against water”, while new granite sample is classified as “Water repellent”.



## Extraction of sulphates by electromigration in two different granites

Jorge Feijoo Conde<sup>1</sup>, Teresa Rivas Brea<sup>1</sup>, Nóvoa X.R.<sup>2</sup>, Iván de Rosario Amado<sup>1</sup>, Javier. Taboada<sup>1</sup>

<sup>1</sup>Dept. of Natural Resources, University of Vigo. Campus Lagoas , 36310 Vigo-Spain. jfeijoo@uvigo.es; ivanderosario@gmail.com ; trivas@uvigo.es; jtaboada@uvigo.es

<sup>2</sup>ENCOMAT group, EEI, University of Vigo. 36310 Vigo-Spain. rnovoaa@uvigo.es

### ABSTRACT

Desalination by electromigration is a salt extraction method whose application in cement and concrete (in the case of chlorides) is well developed [1, 2, 3]. In the case of other building materials, there are only references on the application of this method for brick desalination [4]; In the case of other building materials (as ornamental rocks), electromigration as a desalination method has not been addressed sufficiently. The authors of this work have recently applied this method for the first time with the aim of extract the chloride from contaminated granitic rocks [5], obtaining a very satisfactory efficiency. This paper deals with the study of the effectiveness of electromigration in the extraction, also in granites, of sulfate ion; the sulfate salts (gypsum, thenardite and mirabilite) are involved in the development of severe deterioration forms in rocks used in construction (see [6] and [7] and references therein), being responsible, in granites, of the formation of surficial detachments [8].

The method of desalination by electromigration has been applied in two granites from the NW of Iberian Peninsula widely used in construction of the architectural heritage. Both granites, with different texture and pore size distribution, were contaminated with 14% Na<sub>2</sub>SO<sub>4</sub> solution.

The desalation effectiveness has been evaluated taking into account 1) the analysis of ion content in anode and cathode during and after the trial and 2) the analysis of ion content in the rock at different distances from the electrodes at the end of the trial. The possible harmful effects on the rock were also evaluated, controlling during the test the pH on the rock surfaces in contact with the electrodes and measuring the color changes on the rocks after the test.

At the end of test, the sulphate content was significantly reduced, indicating that the method is effective even for polyvalent ions such as sulfate. pH changes in anode and cathode that occur during migration have been minimized achieving the maintenance of pH at values near neutrality by means the use of a buffered electrolyte and the placement of poultices with neutralizing capacity between the electrodes and the rock surfaces. The color changes detected after the test seem not to be related to the principle of the method. An influence on the desalation effectiveness of the pore structure of the rocks was also observed, which reaffirms the need of previous characterization and knowledge of the properties of rock materials prior to be undergone a conservation treatment.

### REFERENCES

- [1]M. Castellote, C. Andrade, C. Alonso, Electrochemical removal of chlorides: modelling of the extraction, resulting profiles and determination of the efficient time of treatment. *Cement and Concrete Research* 30, 615-621, 2000.
- [2] B.Elsener, U. Angst, Mechanism of electrochemical chloride removal. *Corrosion Science* 49, 4504–4522, 2007.
- [3]J.C. Orellan, G. Escadeillas, G. Arliguie, Electrochemical chloride extraction: efficiency and side effects. *Cement and Concrete Research* 34, 227–234, 2004.
- [4] L.M. Ottosen, I. Rørig-Dalgaard, Electrokinetic removal of Ca(NO<sub>3</sub>)<sub>2</sub> from bricks to avoid salt induced decay. *Electrochimica Acta*, 52[10], 3454-3463, 2007.
- [5]J.Feijoo, X.R. Nóvoa, T. Rivas, M.J. Mosquera, J. Taboada, C. Montojo, F. Carrera. in press, 2012.
- [6]M. Angeli, J.P. Bigas, D.Benavente, B. Menéndez, R. Hebert, C.David, Salt crystallization in pores: quantification and estimation of damage. *Environ Geol*, 52:205–213, 2007.
- [7] A.E. Charola, Salts in the deterioration of porous materials: an overview. *Journal of America Institute if Conservation* 39, 327-343, 2000.
- [8] B. Silva, T. Rivas, B. Prieto, Soluble salts in granitic monuments: origin and decay effects. en *Applied Study of Cultural Heritage and Clays*. J.L.Pérez (Ed.). pp 113-130, 2003.





## Gypsum efflorescence on clay brick masonry

Jacek Chwast<sup>1</sup>, Jan Elsen<sup>1</sup>

<sup>1</sup>Section Geology, Department of Earth and Environmental Sciences, Katholieke Universiteit Leuven, Celestijnenlaan 200E, PO Box 2408, 3001 Heverlee, Belgium

### ABSTRACT

Efflorescence is a common problem affecting the surface of a building made of brickwork or concrete. It appears mostly as a thin deposit of salts. Most types of efflorescence appear just after construction and are easily cleaned by natural weathering. However, recently in Belgium there is a growing number of complaints about efflorescence appearing on clay facing brickwork after a couple of years of construction (see Figure 1). In contrast to the other kinds of efflorescence, these deposits consist of hardly soluble salts, what makes it very hard to remove. Similar cases of persistent efflorescence, mainly composed of gypsum, were reported in the Netherlands [1] and the UK [2]. There is in general a lack of understanding about the source, the genesis and the mechanism of formation for this type of efflorescence.

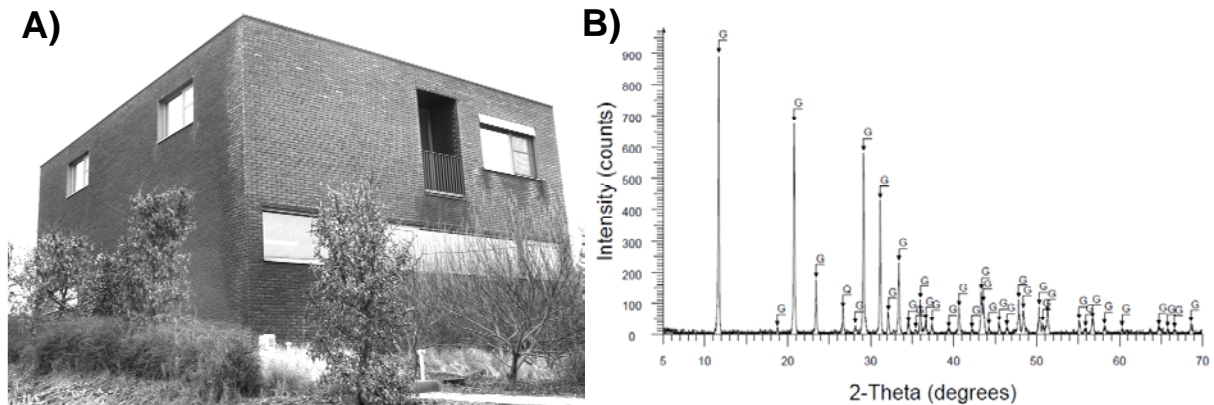


Figure 1 A) An example of a house affected with persistent efflorescence. B) An XRD analysis of the deposit collected from the house showing clearly that efflorescence is composed of gypsum (G).

A specific source of soluble sulphates is necessary for the development of gypsum efflorescence. This kind of efflorescence occurs typically after a couple of years, suggesting that the availability of this sulphate source is delayed by some processes that progress after the wall construction.

Although sulphates may originate from many sources as for example mortar, brick, rain and soil, it seems that in case of the gypsum efflorescence the source of sulphates is mortar. The origin of sulphates in mortars could be the addition of gypsum to control the setting of cement. During the hydration of cement, sulphates are recrystallised into ettringite and monosulphate phases. A hypothesis was proposed indicating the source of gypsum may be the carbonation of cementitious phases, which were developed during mortar setting [1]. Several published papers reported that ettringite decomposes due to carbonation to i.e. gypsum and vaterite [3–5].

The aim of this project is to reveal the mechanism of the development of the persistent efflorescence and to use this expertise in order to design a mortar with a low GL-efflorescence risk. During a field survey, the first part of this research, we investigated a number of buildings showing persistent efflorescence. The aim of this first step is to identify salts forming the deposit, characterize the appearance of efflorescence and gather relevant data such as the type of brick type used for construction and the age of a building. These data are put into a database, which is later analysed to determine which salts form persistent efflorescence, factors which hinder or facilitate efflorescence development and to choose materials for further studies.

In the next step we will collect samples of bricks and mortars from selected locations. These samples will be analyzed to identify minerals which may be a potential source of efflorescence. Their distribution may already give an indication of the mechanism of efflorescence development. If the case study confirms that the carbonation of mortar may trigger the soluble sulphates source, we will investigate this mechanism in laboratory conditions. It will be realised by subjecting cement paste samples to accelerated carbonation conditions and monitoring the development of soluble sulphates and mineral composition. The knowledge

of the mechanism will be the basis for designing an accelerated test method to develop persistent efflorescence on masonry wallettes. This method will be applied to study the impact of brick properties and to design a mortar formulation with no or low risk of persistent efflorescence.

The samples of deposits were collected by gentle scraping the surface affected with efflorescence. The mineralogical composition of the collected samples was determined by powder X-ray diffraction with a Philips PW1830 diffractometer using CuK $\alpha$  radiation (45kV, 30mA). Standard 2 $\theta$  scan range was taken as 5-70° with a step size of 0.02° 2 $\theta$  and a counting time of 1s.

During the field survey we have analyzed 19 cases of persistent efflorescence, for 10 of these buildings the age of construction was known and varying between 1997 – 2010. All the investigated houses were made with hand-moulded bricks. The deposit may have different forms: varying from foggy efflorescence, where single grains of salts forming deposit may be distinguished, to a thicker layer of deposit tightly covering the surface of masonry or even locally occurring crust. In most cases efflorescence affects the brick to a greater extent than the mortar. Nevertheless it is evident that efflorescence develops on mortar as well, but usually a slight or moderate discoloration is apparent. In all cases the most affected facades of a building are these facing west, south and south-west direction. This may be explained by the fact that walls facing these directions are the most exposed to the action of rain and wind. The efflorescence is pronounced on upper parts of the façade and on the edges of a building facing south, west or south-west direction. The appearance of efflorescence changes over time, it may depend on the age of the building, time of the year and the dampness of masonry. Nevertheless, it doesn't wash with natural weathering, it permanently affects the appearance of a building.

The XRD analysis revealed that in most cases efflorescence is composed of gypsum. In some cases no gypsum was identified and besides quartz only low amounts of calcite were identified. When gypsum was identified in the sample it was evident that it originates from the efflorescence. In case of calcite its origin in the collected sample scraped from the surface of a brick cannot be unambiguously determined. Calcite is used as a component of sanding mix for some types of bricks, it may be naturally present or added to clay and may develop on the surface as efflorescence. For 3 cases showing gypsum efflorescence we identified brick types and acquired their relevant characteristics. These bricks are characterized by very low soluble sulphates content (below 0.02 %), thus it is unlikely that they are the source of the component of gypsum efflorescence.

## REFERENCES

- [1]H. Brocken, T.G. Nijland, White efflorescence on brick masonry and concrete masonry blocks, with special emphasis on sulfate efflorescence on concrete blocks, *Construction and Building Materials* 18, 315–323, 2004,.
- [2]G.K. Bowler, N.B. Winter, New form of salt staining on external masonry, *British Ceramic Transactions* 95, 82–86, 1996.
- [3]T. Grounds, H.G. Midgley, D.V. Novell, Carbonation of ettringite by atmospheric carbon dioxide, *Thermochimica Acta* 135, 347–352, 1988.
- [4]T. Nishikawa, K. Suzuki, S. Ito, K. Sato, T. Takebe, Decomposition of synthesized ettringite by carbonation, *Cement and Concrete Research* 22, 6–14, 1992.
- [5]Q. Zhou, F.P. Glasser, Kinetics and mechanism of the carbonation of ettringite, *Advances in Cement Research* 12, 131–136, 2000.

## Crystallization behavior of $\text{NaNO}_3\text{--Na}_2\text{SO}_4$ salt mixtures in sandstone and comparison to single salt behavior

Nadine Lindström<sup>1</sup>, Nicole Heitmann<sup>1</sup>, Kirsten Linnow<sup>1</sup>, Michael Steiger<sup>1</sup>

<sup>1</sup>Department of Chemistry, University of Hamburg, Inorganic and Applied Chemistry  
Martin-Luther-King-Platz 6, 20146 Hamburg, Germany

### ABSTRACT

Crystals growing in confined spaces can generate stress and are a major cause of damage in porous materials. While the behavior of several single salts commonly found in building materials is well characterized, only few studies have been carried out on the behavior of salt mixtures. Besides the single salts formed by all possible binary cation–anion combinations, a number of double salts can crystallize from salt mixtures. Not much is known about crystallization behavior and damage potential of double salts. This contribution presents results of an experimental study with the double salt darapskite ( $\text{Na}_3\text{NO}_3\text{SO}_4\cdot\text{H}_2\text{O}$ ) which is an incongruently soluble double salt. Such salts show a complex crystallization behavior and may have a great damage potential, because a solution supersaturated with one of the single salt compounds is formed during the dissolution of the double salt. Therefore, crystallization and damage may occur at high relative humidity or during wetting. Experiments were carried out with sandstone samples ( $15 \times 15 \times 20 \text{ mm}^3$ ) with sealed surfaces on four sides. The samples were impregnated with mixed  $\text{NaNO}_3\text{--Na}_2\text{SO}_4$  solutions. For comparison, samples were also treated with three single salts ( $\text{NaNO}_3$ ,  $\text{Na}_2\text{SO}_4$ ,  $\text{MgSO}_4$ ). After treatment with the salt solutions the samples were exposed to wetting/drying cycles. Damage occurred already after few cycles and was detected by visual inspection, weight changes of the samples and by optical microscopy. It is confirmed that those salts that form supersaturated solutions during wetting of the samples, i.e. sodium sulfate, magnesium sulfate and darapskite have a higher damage potential than sodium nitrate. The phase changes during the wetting–drying cycles were studied by Raman microscopy and are compared to the phase diagrams of the respective salts.



# Capillary suction and drying of natural hydraulic lime and of air lime based mortars

Paulina Faria<sup>1</sup>, Vitor Silva<sup>1</sup>

<sup>1</sup>Dep. Civil Eng., FCT, NOVA University of Lisbon

## ABSTRACT

Air lime and natural hydraulic lime are different binders for mortars to be applied on ancient construction protection. The type of lime, the use of pozzolans, as metakaolin, and the influence of curing conditions are studied in order to evaluate mortar capillary water absorption and drying, when compared to other mortar characteristics.

## Introduction

Lime-based mortars were widely used in the past namely as masonry mortars, rendering or plastering mortars. Until the XIX century mortars were based on air lime (calcium hydroxide). Sometimes pozzolans were added to air lime mortars in order to obtain hydraulic behaviour. In fact, in some applications with low contact with carbon dioxide or abundant contact with water, hydraulic behaviour was needed; otherwise air lime mortars would be unable or would take too long to carbonate. Only by the XIX century natural hydraulic limes appeared. These types of limes, made with calcium carbonate rock but with some amount of clay, still had calcium hydroxide but mainly hydrated compounds.

Many ancient buildings and other structures, as the case of masonry bridges, are still in use worldwide. They are made of lime mortars, with or without pozzolans. Many of those constructions need urgent repair, with mortars that assure their protection [1].

In order to achieve knowledge to lime-based mortars characteristics, pure air lime and recently classified natural hydraulic lime mortars or mortars with these types of lime with different amounts of metakaolin were exposed to different curing conditions characterized and presented in this work.

## Experimental

Mortars were fabricated with binder:sand volumetric proportion of 1:3. The binders were a CL90 air lime LUSICAL H100, a NHL3,5 natural hydraulic lime SECIL and a NHL5 natural hydraulic lime SECIL. These two last binders are new products, recently formulated and classified by the recent version of EN 459-1:2010 [2]. The pozzolan was a metakaolin Argical M 1200 S from IMERYS (Mk). When metakaolin was used, the weight percentage of lime was replaced by the same weight of metakaolin. The percentage of lime substitution by metakaolin in the formulated mortars tried to be related with the hydroxide calcium available in the lime. The sand was a mixture of three calibrated washed siliceous sands (Table I). The mixture of the three sands was previously optimized to achieve a good grading curve.

After demoulding, mortar samples were exposed to laboratorial humid (90% RH) and standard (65% RH) curing and to natural maritime exposure (at Cabo Raso LNEC station).

Mortar samples have been tested at the age of 28 days (and some have been presented elsewhere [3]) and are currently being tested at 90 days for mechanical resistance (dynamic modulus of elasticity, flexural and compressive resistance, resistance to sulphate attack) and for physical characteristic (open porosity, water capillary absorption and drying). These last characteristics will be particularly analyzed in this work.

At 28 days, among other situations:

- the curing conditions were more important for NHL5 and for air lime mortars than for NHL3.5 mortars, and the variation was lower for physical characteristics;
- the substitution of lime for metakaolin improves the capillary coefficient of hydraulic lime mortars and worsen the one of air lime mortars; generally it had no influence on asymptotic value of capillary absorption;
- mortars with NHL3.5 present drying conditions comparable to air lime mortars but the lime substitution for metakaolin slightly difficult the drying of NHL3.5 in all curing conditions.

At the 90 days of age results are still under analysis and will be presented in the conference.

Mortar	Volumetric prop.	Weight Proportion	W/B	Consist. [mm]
CL	1:3	1:12	2,5	158
CL_30Mk	1:3	1:12	2,5	154
CL_50Mk	1:3	1:12	2,6	154
NHL3.5	1:3	1:5	1,1	153
NHL3.5_10Mk	1:3	1:5	1,1	149
NHL3.5_20Mk	1:3	1:5	1,1	143
NHL5	1:3	1:5	1,1	161
NHL5_5Mk	1:3	1:5	1,1	156
NHL5_10Mk	1:3	1:5	1,1	149

*Table 1: Designation (type of lime and w% lime substitution for metakaolin), volumetric and weight proportions, water binder ratio and mortar flow table consistency*

### Conclusions

Comparison can be made showing the influence of the type of lime, the presence of the metakaolin partially substituting the lime and the curing conditions. Characteristics are compared to the expected evolution with ageing [4] and to bibliographic range values [5] that point out the adequacy of the different mortars to different types of application on the repair of ancient buildings and structures, as repointing and rendering mortars. The importance of these parameters on mortar characteristics is highlighted.

### Acknowledgments

The authors wish to acknowledge Fundação para a Ciência e a Tecnologia for the financial support under projects METACAL (PTDC/ECM/100431/2008) and LIMECONTECH (PTDC/ECM/100234/2008), to companies LUSICAL, SECIL and IMERYS for the supply of air lime, natural hydraulic lime and metakaolin and to MSc students João Grilo, João Carneiro, Tiago Branco, Duarte Mergulhão e Rui Antunes who worked in the experimental campaigns.

### REFERENCES

- [1] C. Groot, Developments on repointing of salt-laden historic masonry in the Netherlands, Proc. Int. Conf. on Rehabilitation of Ancient Masonry Structures, Lisbon, 4 May, 5-15, 2012.
- [2] CEN, Building lime. Part 1: Definitions, specifications and conformity criteria. EN 459-1: 2010.
- [3] P. Faria, V. Silva, J. Grilo, J. Carneiro, T. Branco, D.Mergulhão, R. Antunes, Compatible natural hydraulic mortars for historic masonries (in portuguese), Proc. Int. Conf. on Rehabilitation of Ancient Masonry Structures, Lisbon, 4 May, 29-38, 2012.
- [4] A. El-Turki, R. Ball, S. Holmes, W. Allen, G. Allen, Environmental cycling and laboratorial testing to evaluate the significance of moisture control for lime mortars, Construction and Building Materials 24, 1392-1397, 2010.
- [5] R. Veiga, A. Fragata, A. Velosa, A. Magalhães, G. Margalha, Lime-based mortars: viability for use as substitution renders in historic buildings. Int. J. Architectural Heritage 4 (2), 177-195, 2010.

## Capillary water absorption of unstabilized and stabilized earth materials: anomalous time scaling behaviour

Maria Idália Gomes<sup>1</sup>, Teresa Diaz Gonçalves<sup>2</sup>, Paulina Faria<sup>3</sup>

<sup>1</sup> Lisbon Engineering Superior Institute (ISEL), Lisbon, Portugal

<sup>2</sup> National Laboratory for Civil Engineering (LNEC), Lisbon, Portugal

<sup>3</sup> Nova University of Lisbon (UNL), Campus da Caparica, Portugal

### ABSTRACT

Building materials based on natural earth bear important environmental advantages and, so, are becoming widely used all over the world. However, their behaviour as construction materials for walls (rammed earth, adobe) or in mortars (plasters and renders, repair or bedding mortars) is still poorly understood and usually addressed at a purely technological level.

To improve their mechanical resistance and reduce clay swelling, earth-based materials are often stabilized with small amounts of lime or cement.

Here, we present a set of one-directional capillary water absorption experiments [1] performed with four types of earth. Indeed, water is involved in most decay processes and, as evidenced by practice, can be particularly harmful for earth-based materials. To understand the hydric behaviour is, therefore, essential for this type of material.

One of the earth materials is a commercial earth. The other three were collected from the walls of unstabilized rammed earth buildings located in Alentejo region, in south Portugal. The four materials are fully characterized elsewhere [2, 3]. The commercial earth was tested after stabilization with dry hydrated air lime, natural hydraulic lime, Portland cement or natural cement, as well as unstabilized.

The results showed that the unstabilized materials have anomalous capillary suction behavior, evidenced by nonlinear (exponential)  $t^{1/2}$  dependence during the first minutes. The irregularity is especially significant for the commercial earth, but disappears with the addition of even the smallest amounts of binder (5% weight).

The anomaly is probably due to the volume increase of the clay particles as they contact with water, reducing the pore size and, thus, increasing the amount of capillary pores. The use of stabilizers eliminates clay swelling, thereby enabling linear  $t^{1/2}$  dependence in the capillary suction tests.

Despite the regularization of the suction behavior, the stabilizers can hardly be considered to have improved the hydric performance of the earth materials. In fact, they increased the capillary suction and the maximum amount of water absorbed, i.e., the capillary porosity of the material. These effects were more relevant for the air lime and, above all, for Portland cement, but they were also obvious for the higher contents of hydraulic lime and of natural cement. Alike results were obtained for the case of cement stabilization in a previous study [4]. The present results show that other hydraulic binders and also air lime can have similar effect, suggesting that all of them can significantly increase the quantity of capillary pore space in the earth material.

### Acknowledgements

The work was carried out at LNEC. MI Gomes is supported by a doctoral grant from the Fundação para a Ciência e a Tecnologia (FCT). We thank Georg Hilbert for, within the ROCARE EU project, providing the roman cement. Thanks also to Sorgila, Lusalca, Secil and Aubiose companies for providing the remaining materials.

### REFERENCES

[1]RILEM TC 25-PEM, Recommended tests to measure the deterioration of stone and to assess the effectiveness of treatment methods, Materials and Structures 13, 253, 1980.

[2]M.I. Gomes, T. Diaz Gonçalves and P. Faria, Earth-based repair mortars: experimental analysis with different binders and natural fibers, Proc. Int. Conf. on Rammed Earth Conservation – RESTAPIA 2012, 21-23, 2012.

[3]M.I. Gomes, T. Diaz Gonçalves and P. Faria, Unstabilised rammed earth: characterization of the material collected from old constructions in south Portugal and comparison to normative requirements, International Journal of Architectural Heritage, accepted author version posted online on 23 Apr 2012, DOI:10.1080/15583058.2012.683133.



[4]M. Hall and D. Allinson, Influence of cementitious binder content on moisture transport in stabilised earth materials analysed using 1-dimensional sharp wet front theory, *Building and Environment* 44, 688-693, 2009.

## **Influence of ferrocyanide ions on NaCl crystallization in the mixture of salts**

S.Gupta<sup>1</sup>, L.Pel<sup>1</sup>, Michael Steiger<sup>2</sup>

<sup>1</sup>Eindhoven University of Technology, Department of Applied Physics, Den Dolech 2, 5600 MB Eindhoven, The Netherlands (sgupta@tue.nl, l.pel@tue.nl)

<sup>2</sup>Department of Chemistry, University of Hamburg, Inorganic and Applied Chemistry

### **ABSTRACT**

While the mechanisms of salt damage in porous materials have received considerable attention in recent years, effective treatment methods for ameliorating this common problem still remain limited. Recently, the use of ferrocyanide inhibitors has been proposed as a potential preventive treatment method against NaCl damage [1]. Although NaCl is one of the most widely distributed salt, in practice NaCl is accompanied by the presence of other salts in the building materials. The presence of salt mixtures presents a totally different behavior. Thus, before using the inhibitors in practice a better understanding of the kinetics of salt crystallization process in their presence is required. This behavior is still not completely understood, because it is not easy to measure the concentration of ions during dynamic measurements. However, with the help of a specially designed Nuclear Magnetic Resonance set-up [2], we were able to measure both hydrogen and sodium ions simultaneously during dynamic experiments and can thus provide information about the salt concentration. A series of micro-droplet drying experiments were performed with NaCl and mixture of NaCl and KCl solution with and without crystallization inhibitor inside NMR. The main focus was on the effect of the potassium hexa-cyanoferrate (II) tri-hydrate  $K_4 [Fe (CN)_6 ] 3H_2O$  as an inhibitor on the crystallization of NaCl in the presence of other salt. The NMR measurements are coupled with time-lapse microscopy. This gives the possibility to visualize the drying of the droplet while simultaneously obtaining information about NaCl concentration in the droplets. The information of the crystal size and the crystal growth was gathered from the images captured using time lapse microscopy. Such a powerful experimental set-up helps to attain all the information regarding the concentration of the ions and kinetics of NaCl crystallization together.

The results show, for NaCl solution in the presence of inhibitor a delay in crystallization and higher supersaturation was seen prior to the onset of crystallization. However, no significant supersaturation was seen for NaCl in the presence of KCl. Although in both the cases a significant decrease in crystal size and change in crystal morphology is observed. The crystals formed in the presence of inhibitor were more like a fluffy powder and were not strongly adhered to the substrate. Such type of crystal morphology helps to crystallize salt as non-destructive efflorescence. Thus, the use of ferrocyanide as an inhibitor may provide possible solution to the damage problem.

### **REFERENCES**

- [1] C. R. Navarro, L. L. Fernanadez, E. Doehne, E. Sebastian, Journal of Cryst. Growth, 243, 503-516, 2002.
- [2] L. Pel, Moisture Transport in porous building materials. Ph.D. thesis, Eindhoven University of Technology, The Netherlands, 1995.



## Contacts of the participants

Alcaide B.M.	Instituto Valenciano de Conservación y Restauración de Bienes Culturales, Valencia (Spain)	bmalcaide@ivcr.es
Alonso E.E.	Department of Geotechnical Engineering and Geosciences, UPC, Barcelona	eduardo.alonso@upc.edu
Amado de I.R.	Dept. of Natural Resources, University of Vigo. Campus Lagoas Spain.	ivanderosario@gmail.com
Boever W.D.	Dept.ofGeologyandSoilScience,GhentUniversity,GhentBelgium	wesley.deboever@ugent.be
Bonn N.S.	Van der Waals-Zeeman Institute, IOP, University of Amsterdam	n.shahidzadeh@uva.nl
Brito V.	National Laboratory for Civil Engineering (LNEC), Lisbon, Portugal	vbrito@lnec.pt
Carmeliet J.	ETH Zurich	jan.carmeliet@empa.ch
Caruso F.	Institut für Baustoffe (IfB), ETH Zürich	fcaruso@ethz.ch
Chwast J.	Katholieke Universiteit Leuven,Heverlee, Belgium	jacek.chwast@ees.kuleuven.be
Clercq H.D.	Royal Institute for Cultural Heritage (KIK-IRPA), Brussels, Belgium	hilde.declercq@kikirpa.be
Conde J.F.	Dept. of Natural Resources, University of Vigo. Campus Lagoas Spain.	jfejoo@uvigo.es
Dalgaard I.R.	Department of Civil Engineering, Technical University of Denmark	ird@byg.dtu.dk
Delgado, J.D.	National Laboratory for Civil Engineering (LNEC), Lisbon, Portugal	delgado@lnec.pt
Delgado J.M.P.Q.	LFC – Laboratório de Física das Construções, Portugal	jdelgado@fe.up.pt
Derluyn H.	ETHZürich,Switzerland	derluyn@arch.ethz.ch
Derome D.	EMPA, Swiss Federal Laboratories for Materials Science and Technology	dominique.derome@empa.ch
Desarnaud J.	Van der Waals-Zeeman Institute, IOP, University of Amsterdam	j.e.desarnaud@uva.nl
Dewanckele J.	Department of Geology and Soil Science - SGIWUGCT, Ghent University	dewanckele@ugent.be
Donkers P. A. J.	Technical University of Eindhoven, The Netherlands	p.a.j.donkers@tue.nl
Faria P.	FCT, NOVA University of Lisbon	paulina.faria@fct.unl.pt
Flatt R.J.	Institut für Baustoffe (IfB), ETH Zürich	flattr@ethz.ch
Godts S.	Royal Institute for Cultural Heritage (KIK-IRPA), Brussels, Belgium.	sebastiaan.godts@kikirpa.be
Gonçalves T.D.	National Laboratory for Civil Engineering (LNEC), Lisbon, Portugal	teresag@lnec.pt
Gupta S.	Eindhoven University of Technology	sgupta@tue.nl
Hamilton A.	University of Edinburgh,UK	andrea.hamilton@ed.ac.uk
Hauková P.	Institute of Theoretical and Applied Mechanics, Czech Academy of Science, Czech Republic	haukova@itam.cas.cz
Hendrickx R.	Royal Institute for Cultural Heritage (KIK-IRPA), Brussels, Belgium	roel.hendrickx@kikirpa.be
Křivánková D.	Institute of Theoretical and Applied Mechanics, Czech Academy of Science, Czech Republic	krivankova@itam.cas.cz
Kröner S.	Institut Universitari de Restauració del Patrimoni, Universitat Politècnica de València, Valencia (Spain).	ustephan@upvnet.upv.es
Lindström. N	University of Hamburg, Inorganic and Applied Chemistry, Hamburg, Germany	nadine.lindstroem@chemie.uni-hamburg.de
Linnow K.	Department of Chemistry, University of Hamburg, Inorganic and Applied Chemistry	kirsten.linnow@chemie.uni-hamburg.de

Lubelli B.	Delft University of Technology, The Netherlands	barbara.lubelli@tno.nl
Prat M.	Institut de Mécanique des Fluides de Toulouse, Université de Toulouse, France	marc.prat@imft.fr
Mas-Barberà X.	Institut Universitari de Restauració del Patrimoni, Universitat Politècnica de València, Valencia (Spain).	jamabar@upvnet.upv.es
Mtani I.	Dortmund University, Germany	mtanibell@hotmail.com
Niedoba K.	Institute of Theoretical and Applied Mechanics, Czech Academy of Science Czech Republic	krzysztof.niedoba@gmail.com
Nogueira R.	UTL-Instituto Superior Técnico - ICIST, Lisbon, Portugal	ritanog@civil.ist.utl.pt
Osselin F.	Laboratoire Navier (IFSTTAR, CNRS, ENPC), France	florian.osselin@ifsttar.fr
Pel L.	Technical University of Eindhoven, The Netherlands	l.pel@tue.nl
Ramon A.	Department of Geotechnical Engineering and Geosciences, UPC, Barcelona	anna.ramon@upc.edu
Ruiz-Agudo E.	Dept. Mineralogía y Petrología, Universidad de Granada, Granada, Spain	encaruiz@ugr.es
Sánchez Dolado J.	Tecnalia, Spain	jorge.dolado@tecnalia.com
Scherer G.W.	Princeton University, USA	scherer@Princeton.edu
Shokri N.	Department of Earth and Environment, Boston University, Boston, MA, USA	nshokri@bu.edu
Steiger M.	Department of Chemistry, University of Hamburg, Inorganic and Applied Chemistry	michael.steiger@chemie.uni- hamburg.de

## Report workshop CRYSPOM III, Crystallization in porous media

Tróia, Portugal 4-7 September 2012

Workshop Chair: Leo Pel (TU/e) and Teresa Diaz Gonçalves (LNEC)

<http://www.phys.tue.nl/nfcmr/cryspom>

This workshop was a success as almost everybody in research on crystallization damage, who is presently involved and also known from articles, attended the workshop. Moreover there was good mix of people with more fundamental research and people who are more practical. Since everybody was staying in the same hotel with common lunch and dinner, this encouraged the discussions among the participants. From all the participants there were very positive reactions on the workshop.

Concerning the present state of knowledge and research on salt damage a few observations can be made after this workshop:

- By the group of Alonso of the department of Geotechnical Engineering and Geosciences Barcelona a 'new' and for most participants unknown crystallization damage was shown on railway bridges. These examples showed that in these cases the growth of gypsum crystals was able to lift up a complete railway bridge, i.e., a heave rate ranging from 5 to 10 mm/month. These were clearly examples of extreme crystallization damage and could give a new direction to research.
- There were a few presentations on poulticing in order to desalinate object. The general process is by now understood and can clearly be described. Something which is missing is the effects of salt mixes. Moreover there is a need for more simple practical methods in order to determine which poultice is needed on a certain object.
- Concerning damage due to  $\text{Na}_2\text{SO}_4$  after the two previous ones there is now clear consent that metastable heptahydrate has to be taken into account in damage mechanisms. Indeed there were various researchers who showed that this crystal is being formed in porous media. It is also becoming more clear that for damage one has to perform cycles and that just single crystallization event is not enough
- Concerning damage by  $\text{NaCl}$  various researchers have shown that we are getting a better grip on which type of salt damage, i.e, fluffy or crust, is formed under which boundary conditions. This could help in defining the climate to prevent certain types of damage
- Various researchers have shown the effects on inhibitors on salt crystallization, both with positive and negative effect. Clearly more research is needed on the effect on the substrate on inhibitors and the use of inhibitors in case of salt mixes

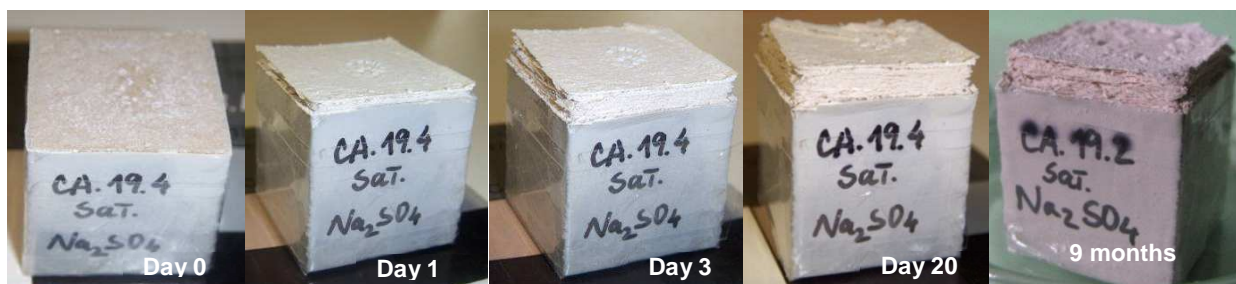


**Fig. 1** – Exfoliation of the Ançã limestone impregnated with saturated  $\text{Na}_2\text{SO}_4$  solution

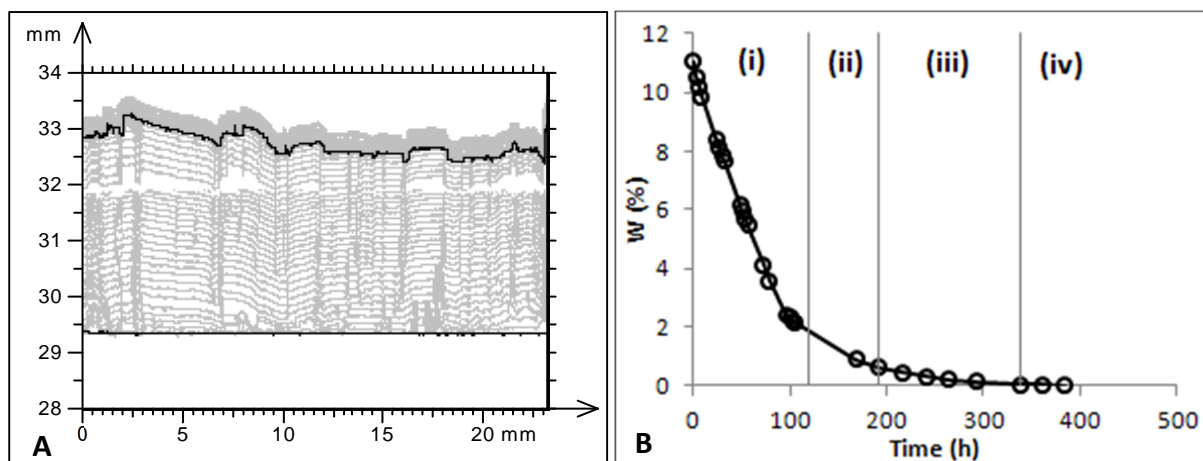


**Fig. 2** – **A**) Profiles of the decayed surface obtained every three hours during drying by optical profilometry. The black lines correspond to the first and last profiles; **B**) Drying curve: (i) detachment of stone layers at an approximately constant rate; (ii) detachment of stone layers at a falling rate; (iii) detachment stopped; (iv) subsidence of the detached stone layers.

## **Possibilities and limitations of optical 3D profilometry in the study of porous building materials of the architectural heritage**

T. Diaz Gonçalves, V. Brito

National Laboratory for Civil Engineering (LNEC), Materials Department  
Av. do Brasil 101, 1700-066 Lisbon, Portugal

### **ABSTRACT**

The texture of porous building materials used in the architectural heritage, such as stone, mortars or ceramic brick, influences their appearance, the adherence they provide to paints, mortars and glues, as well as many of the alteration processes they tend to suffer and eventually undergo. These effects justify the importance of surface texture measurement in conservation science.

Current surface metrology techniques are based on a measuring instrument, with contact or non-contact sensors, connected to a computer equipped with specific software. Non-contact methods, a latter technology, can quickly deliver high resolution profiles, up to the micrometre or even nanometre scale, and allow the (non-destructive) study of friable and brittle surfaces. Measuring instruments can today provide not only the traditional 2D profiles but also 3D surface measurements. The operating software allows performing and repeating these measurements at predefined intervals, and the data analysis software provides a wide range of standard texture parameters.

The current and on-going technological advances in this field suggest a world of possibilities in their application to the weathering-prone porous materials of our cultural heritage. However, surface metrology methods were originally developed to characterize different type of materials such as metal and polymers. Therefore, their application to porous building materials is not always straightforward.

This article is aimed at clarifying some key possibilities and limitations of surface profilometry, and optical methods in particular, to characterize porous building materials and their decay processes. The discussion is based on: (i) measurements of the surface area of eleven building materials; (ii) monitoring of the surface changes arising in three of these materials due to sodium sulphate crystallization.

Surface area defines the dimension of the functional interface of the material. It is therefore an important parameter in different contexts, namely to study the interaction of the materials with their environment or the consumption of coatings and treatments, among others.

Salt crystallization is one of the most frequent, destructive and still less understood decay processes that porous building materials may undergo in historic constructions. Therefore, it is important to have reliable methods that may help clarify its effects on selected materials.



The studied materials encompass six natural stones (a sandstone, a calcarenite and four types of limestones) and five artificial materials (ceramic brick, air-lime/sand mortar and three types of calcium silicate materials).

The surface texture measurements were performed with a Talysurf CLI 1000 instrument, from Taylor Hobson, equipped with a white light gauge.

The work showed that:

(i) The surface of porous building materials depicts morphological complexity which may require the use of concepts beyond those of traditional Euclidian geometry. This complexity may be translated by a fractal dimension which first increases and then decreases with the porosity.

(ii) Optical methods can be an effective way of monitoring surface decay processes of porous building materials such as those deriving from the crystallization of soluble salts.

It also showed that optical methods may be inappropriate to materials incorporating quartz grains.

**Preference: ORAL presentation**

**Preference: Oral presentation**

## **Decay patterns of natural stones during drying due to sodium sulphate crystallization: monitoring by a 3D optical technique**

V. Brito; T. Diaz Gonçalves

National Laboratory for Civil Engineering (LNEC), Lisbon, Portugal ([teresag@lnec.pt](mailto:teresag@lnec.pt))

### **Abstract**

Salt decay is one of the major decay mechanisms of porous building materials in historic constructions, namely of natural stones which were often used for structural or decorative purposes. Among those currently found in this context, sodium sulphate is one of the most frequent, harmful and complex salts. In this article, we analyse the distinct decay patterns to which this salt gives rise during drying of three natural stones of architectural relevance: the Bentheimer sandstone, the Ançã limestone and a second Portuguese limestone with lower porosity. Sound understanding of their decay patterns and of the underlying decay processes is a preliminary requirement for the implementation of appropriate mitigation techniques.

Drying experiments were performed with four sodium sulphate solutions of different concentration. The stones were first contaminated with the salt solution and then let dry in an environment with controlled temperature and relative humidity. The drying process was monitored by periodical weighting. Stone decay was simultaneously monitored using a 3D surface profiling system, equipped with an optical gauge, which allowed its detailed non-destructive evaluation.

The sorptivity of the three stones was also measured, for characterization purposes, at the different salt concentrations. It always scaled as the square root of the ratio between surface tension and viscosity.

The intensity of the damage that arose during drying was observed to depend on the concentration of the salt solution. However, the decay patterns of the three types of stone were totally different: efflorescence in one case, multi-layer delamination in another case and uni-layer delamination in the third case.

The efflorescence showed morphological variations apparently associated to slight differences in the colour of the stone.

The multi-layer delamination (exfoliation) was very pronounced and started in the first day of drying. It took place during a single drying event and, therefore, it did not result, as often suggested, from the successive effect of several wet-dry cycles. The rate at which the layers detached and lifted from the stone surface was constant during the first period of the drying experiment. During this period practically constant drying rate was also observed.

The uni-layer delamination occurred much later in the drying process, typically after three to six days, depending on the salt concentration. It consisted in the bulging and further rupture of a thin stone layer beneath which powdered stone material and salt crystals were observed.

It was concluded that the type of decay was strongly conditioned by the sorptivity of the stones. The optical surface profiling technique showed to be helpful to characterize the salt decay patterns.

Acknowledgements: This work was performed under the research project DRYMASS (ref. PTDC/ECM/100553/2008) which is supported by national funds through the Fundação para a Ciência e a Tecnologia (FCT) and LNEC.

## **Artisanal lime paints and their influence on moisture transport during drying**

**Teresa Diaz Gonçalves\*, Vânia Brito**

\*LNEC, Lisbon, Portugal, teresag@lnec.pt

**Preferential presentation: Oral**

### **Abstract**

Lime paintings were originally used in historical buildings all across Europe and the rest of the globe. This type of finishing is obtained by applying on the surfaces an aqueous suspension of hydrated lime which may also include pigments and additives. Lime paints were commonly applied over lime plasters or directly on stone elements.

In the last century, synthetic paints gradually replaced traditional lime paints which required frequent renewal. However, it was eventually verified that the new formulations gave rise to poorly permeable layers, which hindered drying and exacerbated dampness and salt crystallization problems in old buildings. Today, technicians try to use more permeable paints, specific for old buildings, such as silicate paints. However, for reasons of durability and ease of application, these typically still include a significant proportion of synthetic components. And in practice, they usually do not seem to achieve the performance levels, in terms of permeability, of the artisanal lime paints.

The presence of moisture is in fact a recurring condition in historical buildings. Therefore, it is common sense that this is the default condition to consider when prescribing materials for conservation or restoration interventions.

To try to understand the performance of lime paints on substrates with non-negligible moisture content, we studied the influence of one lime paint without additives in the drying of different materials: a lime mortar and four limestones with different porosity. The water/lime ratio of the lime paint was established from preliminary tests which showed how the porosity of the hardened paste varied with its initial water content. Drying tests were then performed on the painted materials following RILEM procedure. The results showed that the lime paint not only does not hinder drying, but can even accelerate it in some materials. In this article we discuss the possible causes and implications of this phenomenon.

# Transport in Porous Media

## Drying kinetics of porous stones in the presence of NaCl and NaNO<sub>3</sub>. An assessment of the factors affecting liquid and vapour transport

--Manuscript Draft--

<b>Manuscript Number:</b>	
<b>Full Title:</b>	Drying kinetics of porous stones in the presence of NaCl and NaNO <sub>3</sub> . An assessment of the factors affecting liquid and vapour transport
<b>Article Type:</b>	Original Research Paper
<b>Keywords:</b>	Drying; capillary suction; water vapour conductivity; soluble salts; porous building materials
<b>Corresponding Author:</b>	Vânia Brito, M.D National Laboratory for Civil Engineering Lisboa, PORTUGAL
<b>Corresponding Author Secondary Information:</b>	
<b>Corresponding Author's Institution:</b>	National Laboratory for Civil Engineering
<b>Corresponding Author's Secondary Institution:</b>	
<b>First Author:</b>	Vânia Brito, M.D
<b>First Author Secondary Information:</b>	
<b>Order of Authors:</b>	Vânia Brito, M.D Teresa Diaz Gonçalves, PhD
<b>Order of Authors Secondary Information:</b>	
<b>Abstract:</b>	<p>We examine the role of two soluble salts, sodium chloride and sodium nitrate, on the capillary suction, vapour conductivity and drying kinetics of three natural stones. It is experimentally confirmed that sorptivity scales as <math>(\sigma/\eta)^{1/2}</math>, which means that it decreases as the salt concentration increases due to the effect salts have on the surface tension (<math>\sigma</math>) and viscosity (<math>\eta</math>) of the liquid.</p> <p>The obstruction to vapour transport depends on the efflorescence morphology. Porous efflorescence or salt crusts with holes and fissures do not have any effect, which was the case in four out of five experimental conditions. Relevant obstructive effect was observed only for the remaining condition, where a dense efflorescence layer was formed.</p> <p>A general tendency was observed to have a slower drying process as the concentration of the salt solution increased. The mentioned sorptivity reduction is a major cause. Obstruction to vapour transport is, when it exists, an added cause. Lowering of the water activity due to the amount of solute was dismissed as a cause because the solutions saturated at the evaporation front very early in the drying process, hence, the relative humidity above the specimens was similar to the equilibrium relative humidity of the salt regardless of the solution concentration. Efflorescence morphology depends mostly on the type of stone and nature of the salt. However, it incorporates also a component of unpredictability, possibly deriving from small casual inhomogeneities in the pore networks of the stones, which needs to be considered in future studies.</p>

Drying kinetics of porous stones in the presence of NaCl and NaNO<sub>3</sub>. An assessment of the factors affecting liquid and vapour transport

Vânia Brito\*, Teresa Diaz Gonçalves

*National Laboratory for Civil Engineering (LNEC), Materials Department, Av. do Brasil 101, 1700-066 Lisbon, Portugal*

\* Corresponding author – email: vbrito@lnec.pt, tel: + 351 218443241, fax: + 351 218443023

## Abstract

We examine the role of two soluble salts, sodium chloride and sodium nitrate, on the capillary suction, vapour conductivity and drying kinetics of three natural stones.

It is experimentally confirmed that sorptivity scales as  $(\sigma/\eta)^{1/2}$ , which means that it decreases as the salt concentration increases due to the effect salts have on the surface tension ( $\sigma$ ) and viscosity ( $\eta$ ) of the liquid.

The obstruction to vapour transport depends on the efflorescence morphology. Porous efflorescence or salt crusts with holes and fissures do not have any effect, which was the case in four out of five experimental conditions. Relevant obstructive effect was observed only for the remaining condition, where a dense efflorescence layer was formed.

A general tendency was observed to have a slower drying process as the concentration of the salt solution increased. The mentioned sorptivity reduction is a major cause. Obstruction to vapour transport is, when it exists, an added cause. Lowering of the water activity due to the amount of solute was dismissed as a cause because the solutions saturated at the evaporation front very early in the drying process, hence, the relative humidity above the specimens was similar to the equilibrium relative humidity of the salt regardless of the solution concentration.

Efflorescence morphology depends mostly on the type of stone and nature of the salt. However, it incorporates also a component of unpredictability, possibly deriving from small casual inhomogeneities in the pore networks of the stones, which needs to be considered in future studies.

*Keywords: Drying; capillary suction; water vapour conductivity; soluble salts; porous building materials*

# 1 Introduction

Salt decay is a recurrent problem in many types of construction, especially in historical buildings. It causes aesthetic degradation and the loss of historical remains, reduces the health conditions and, in the long run, can put at risk the structural safety of the construction. All this results from the simultaneous presence of soluble salts and water in a porous material subjected to certain environmental conditions. The salts may come from the building materials themselves (stone, ceramics, mortars) or they may have external origin. Upon contact with water, they form solutions that migrate through the pore network to the material. Degradation occurs when the salt crystallizes, which can happen on the surface, as efflorescence, or within the pores, as subflorescence which introduces internal stresses in the material. Although temperature variations can have an effect in the case of salts whose solubility is sensitive to this parameter, salt decay occurs generally as a result of evaporative drying processes by which the concentration of the salt solutions increases until it becomes supersaturated and eventually crystallizes.

Evaporative drying of porous materials can be described as a two-stage process (Fig. 1) where at each moment, the position of the drying front results from a balance between the incoming liquid flow and the outgoing vapour flow which tend to equalize. During stage I, the moisture content is high, the drying rate constant and the drying front is located at the material surface. When salts are present, efflorescence occurs, which may account for aesthetical or health problems in buildings. Stage II happens when, due to a lower moisture content in the material, the liquid flow to the surface is insufficient to compensate the evaporative demand. The drying front recedes inside the material and the drying rate decreases progressively. Salts crystallize inside the pores as subflorescence which can damage the material.

Salt decay is closely related to drying of porous materials, not only as a consequence, but also because soluble salts act as an influencing factor in these processes. However, the influence that soluble salts may have on drying and, in general, on liquid and vapour transport, is not yet well understood and there are several open contradictions.

Ruíz-Agudo et al. (2007) argue that salts can significantly reduce the rate of capillary flow due to their effect on density, viscosity and surface tension.

Rodriguez-Navarro and Doehne (1999) also sustain that capillary flow can be relevantly slower for some salt solutions, depending on the type of salt and solution concentration which was proved experimentally by Rucker et al. (2000). Therefore, during evaporative processes, concentrated salt solutions have more difficulty in reaching the drying surface than pure water or less concentrated solutions, showing a higher tendency to form harmful subflorescence.

Differently, Hall and Hoff (2002) argue that soluble salts do not alter significantly liquid transport across porous materials but that, in contrast, they can induce relevant vapour pressure changes. They maintain that, because soluble salts depress the vapour pressure of the liquid, a slower evaporation rate and, hence, an advancement of the evaporation front towards the outer surface arises during drying. This suggests that the higher tendency of some salt solutions to form subflorescence may arise from a faster evaporation rate rather than from a slower liquid transport. However, many authors suggest that this lower evaporation rate is not fully explained by the lowering soluble salts induce in the vapour pressure of the liquid (Pel et al. 2003; Petković et al. 2007; Gonçalves et al. 2007). And thus, they hypothesized that blocking of the pores by salt crystals is likely to play a major role.

Differently, Sghaier and Prat (2009) report that sodium chloride efflorescence may even contribute to accelerate drying, which is attributed to a capillary pumping effect taking place in porous sodium chloride efflorescence during the early moments of drying of glass beads packings.

Further knowledge on the influence of soluble salts on drying is therefore necessary, not only for the development of methods capable of effectively promoting the drying of salt loaded walls, but also for a better understanding and control of salt decay processes themselves.

Here, we analyze the role of two soluble salts, sodium chloride and sodium nitrate, on the capillary suction and drying kinetics of three natural stones. The vapour pressure above the salt contaminated materials, as well as the physical morphology of the efflorescence layer and its effect on vapour transport are also analyzed. We assess the variations in drying kinetics induced by either salt and discuss the possible causes for the differences that arise as the concentration of the salt solution increases. The data obtained in the tests is complemented with information regarding the characteristics of the efflorescence layer formed during

drying, on which observation optical microscopy is used when necessary. We try to explain the general observed trend of having a slower drying as the salt concentration increases. The four main hypothetical causes of such behavior are discussed.

The influence of soluble salts on liquid transport is evaluated by determining the sorptivity ( $S$ ) of the three materials for different salt solutions. It has the advantage, over empirical coefficients  $A$  (water absorption coefficient) and  $B$  (water penetration coefficient), that can be accurately defined in term of flow theory (Hall and Hoff 2002). From here, it derives that if we measure the sorptivity of a given material using a number of different test liquids,  $S$  should scale as  $(\sigma/\eta)^{1/2}$  where  $\sigma$  is the surface tension and  $\eta$  the viscosity. Earlier experiments based on the imbibition of different organic liquids and water into brick (Gummerson et al. 1980), as well as into other fired clay materials (Beltrán et al. 1988) gave positive indications of the validity of this scaling relation. The present experimental results serve also, therefore, to validate the theory for the case of salt solutions.

## 2 Materials

### 2.1 Salt solutions

Sodium chloride ( $\text{NaCl}$ ) and sodium nitrate ( $\text{NaNO}_3$ ) are among the most common salts in decayed buildings. Above  $0^\circ\text{C}$ , both salts only have one crystalline form, anhydrous halite for  $\text{NaCl}$  and anhydrous nitronatrite for  $\text{NaNO}_3$ . The solubility of  $\text{NaCl}$  practically doesn't vary with temperature, while in the case of  $\text{NaNO}_3$  suffers a significant increase (the solubility diagrams of the two salts can be found for example in the SaltWiki website (Schwarz and Steiger 2011). However, their equilibrium relative humidity ( $\text{RHeq}$ ) at  $20^\circ\text{C}$ , the temperature at which our experiments were performed, is similar: 75.47% for  $\text{NaCl}$  and 75.36% for  $\text{NaNO}_3$  (Greenspan 1977).

The  $\text{RHeq}$  of a salt is the  $\text{RH}$  of the air at which it deliquesces, forming a saturated solution. We may also talk of the  $\text{RHeq}$  of a salt solution which is the  $\text{RH}$  of the air in equilibrium with that salt solution, i.e., the  $\text{RH}$  that develops above a free



surface of the solution. This means that the  $R_{Heq}$  of a salt is equal to the  $R_{Heq}$  of the corresponding saturated salt solution.

This research was carried out with a total of seven salt solutions with different concentration, four solutions of NaCl and three solutions of NaNO<sub>3</sub>. Table 1, depicts the concentration,  $R_{Heq}$ , density, surface tension and viscosity of these salt solutions.

## 2.2 Porous materials

The work was carried out on three natural stones: the Ançã limestone (CA), another Portuguese limestone with much lower porosity which we will call “grey limestone” (CC) and the Bentheimer sandstone (B). These three materials are thoroughly characterized elsewhere (Gonçalves et al. 2012).

CA and CC were used throughout the whole work. The Bentheimer sandstone was not tested with sodium nitrate, except for one capillary absorption test performed with saturated NaNO<sub>3</sub> solution.

Test specimens consisting of small cubes with around 24 mm edge were used. After cutting the cubes, their four lateral faces were sealed with an epoxy resin. Afterwards, the top and bottom faces were gently sandpapered with fine-grained sandpaper: P80 sandpaper was used first to remove any dirt or resin residues; then, the surface was smoothed with P600 sandpaper. In the end, the specimens were cleaned in a Branson 1200 ultra-sound cleaner to ensure that no vestiges of stone powder were left in the pores.

## 3 Methods

The research is based on a set of tests which were carried out sequentially on the same samples: capillary absorption, evaporative drying and vapour conductivity. The RH above the porous materials was also measured at a certain point of drying for specimens of the CA and CC limestones contaminated with NaCl solutions. These four experimental procedures are individually described in the next sections.

### 3.1 Capillary absorption test

The capillary absorption test was performed with the objective of accessing the influence of the salts on liquid transport across the porous material.

The test was carried out according to RILEM (1980) procedure Test No. II.6 “Water absorption coefficient (capillarity)” on the laterally sealed small cubic specimens with 24 mm edge. The Bentheimer sandstone, however, had very quick capillary absorption. The cubic specimens saturated too quickly which did not allow measuring a complete absorption curve. So, for the Bentheimer, the test had to be carried out on longer specimens, with the same flat area (24x24 mm) but with a height of around 120 mm.

For each experimental condition at least four specimens were used. However, for the Bentheimer, the capillary absorption was measured only for pure water and the saturated salt solutions and using just 3 specimens for each condition. In all cases, the mass increase of the specimens was monitored until that mass stabilized or up to the 24 hours.

The results of this test are expressed by the sorptivity ( $S$ ) which is a measure of the capacity of a material to absorb and transmit water by capillarity.  $S$  can be determined from one-directional suction experiment, as explained in detail for example by Reda Taha et al. (2001).  $S$  corresponds to the slope of the absorption curve obtained when the cumulative volume of liquid absorbed per unit volume  $i$  (m) is plotted against the square root of time.  $i$  is obtained by Eq. 3.1:

$$i = \frac{\Delta M}{A \cdot \rho} \quad (3.1)$$

Where  $\Delta M$  (kg) is the cumulative mass of absorbed liquid,  $A$  (m<sup>2</sup>) the area of the suction surface and  $\rho$  (kg/m<sup>3</sup>) the density of the liquid.

$S$  depends on both the material and the test liquid, as shown by Eq. 3.2 (Hall and Hoff 2002):

$$S = \left(\frac{\sigma}{\eta}\right)^{\frac{1}{2}} \mathcal{S} \quad (3.2)$$

$\sigma$  and  $\eta$  are the surface tension and viscosity of the liquid, respectively.  $S$  is the sorptivity and  $\mathcal{S}$  the intrinsic sorptivity, a material property that, therefore, is independent of the properties of the liquid. Eq. 3.2 shows also that  $S$  should scale

as  $(\sigma/\eta)^{1/2}$ , if we measure the sorptivity of a given material using a number of different test liquids.

### 3.2 Drying test

In order to access the influence soluble salts may have on the drying process, evaporation tests were performed according to RILEM (1980) procedure Test No. II.5 “Evaporation curve”. The experimental procedure is quite simple. It consists in soaking the specimens, whose four lateral faces had been previously sealed, and then letting them dry while their mass is recorded to determine the loss of water over time. The bottom face of the specimens is also sealed immediately after the soaking phase in order to induce unidirectional drying through the top surface. The drying test was carried out on the small cubic specimens, described in section 2.2, in a conditioned room at 20°C and 50% RH. It started immediately after the capillary absorption test by which the materials were soaked with the solutions and was therefore performed on the same specimens. Only in the case of the Bentheimer, we could not use the same specimens because those subjected to the capillary absorption tests were longer (see section 3.1).

The results of the drying test are expressed by an evaporation curve that translates the variation of the moisture content over time. The drying rate is given, at any instant, by the slope of that curve. The results of the drying test may also be expressed by a single quantitative parameter called the drying index (*DI*) (Commissione NORMAL 1991) which is obtained through Eq. 3.3:

$$DI = \frac{\int_{t_0}^{t_i} f(w) \times dt}{w_0 \times t_i} \quad (3.3)$$

$f(w)$  reflects the variation over time of the water content  $w$  (%),  $w_0$  (%) is the water content at the beginning of drying and  $t_i$  (h) the total duration of the test.

### 3.3 RH above the salt contaminated specimens

The RH above materials soaked with the salt solutions was measured using a water activity analyzer (Hygrolab 3) by Rotronic. Its principle of measurement is illustrated in Fig. 2. The specimens are placed in the sealed container while the temperature and humidity of the air above the specimen are measured through a

capacitive sensor. The specimen slowly exchanges moisture with the air inside the sealed container until equilibrium is reached. These equilibrium values are the ones considered here.

The measurements were performed at a certain moment (24 h) after the beginning of the drying test described in section 3.2. They were carried out on one specimen of each kind, which afterwards was not returned to the drying test and, therefore, is not considered in the results of that test. The measurements were made only in the case of sodium chloride contaminated specimens of CA and CC limestones.

### **3.4 Water vapour conductivity test**

The vapour conductivity test was performed after the drying test and was aimed at understanding the influence that salt crystals deposited during the drying process had on vapour transport across the porous materials.

We followed RILEM (1980) procedure Test No. II.2 “Coefficient of water vapour conductivity”, but the environmental conditions used were those recommended by EN ISO 12572 (CEN 2001) for the dry cup method. In this test, specimens of the porous materials are placed on the top of a cup containing a desiccant. The driving gradient for vapour transport across the material is created by subjecting the cup-specimen assemblies to a controlled environment with higher RH than that induced by the desiccant in the cup. In our case, the RH was around 0% in the interior and 50% in the exterior of the cup. Both RH values are well below the  $RH_{eq}$  (Table 1) of the crystalline phases present in the samples (halite for NaCl, and nitronatrite for  $NaNO_3$ ). So, there was no risk of deliquescence taking place during the vapour conductivity test.

Before the test, the specimens were dried in a ventilated oven at 40°C until constant mass. Then, they were mounted on acrylic cups containing anhydrous calcium chloride (RH of around 0% at 23°C). The specimen–cup interface was sealed with silicone mastic and covered with plastic tape. Finally, the cup-specimen assemblies were placed in a climatic chamber at 23°C and 50% RH. They were periodically weighed until their mass varied linearly with time, which corresponds to the achievement of a steady state regime (the amount of vapor flowing through the specimens per unit time is constant).

The results of this test are expressed in terms of the equivalent air layer thickness ( $Sd$ ) which expresses the thickness of an air layer with the same resistance to vapour diffusion as the tested specimens (Eq. 3.4):

$$Sd = \frac{\Pi^{ar} \cdot A \cdot \Delta P}{G} \quad (3.4)$$

where  $\Pi^{ar}$  ( $1.95 \times 10^{-10} \text{ kg.m}^{-1}.\text{s}^{-1}.\text{Pa}^{-1}$ ) is the diffusion coefficient for water vapour in air at atmospheric pressure,  $A$  ( $\text{m}^2$ ) the test area of the specimen,  $\Delta P$  (Pa) the vapour pressure differential between the top and bottom surfaces of the specimen and  $G$  (kg/s) the rate of water vapour flow across the specimen in steady state conditions.  $A$  corresponds to the average of the top and bottom exposed areas of the specimen (CEN 2001).

## 4 Results and Discussion

### 4.1 Capillary absorption test

The main objective of this test was accessing the influence that soluble salts may have on liquid capillary transport. This was evaluated by determining the sorptivity, a quantity that can be accurately defined in terms of flow theory. Therefore, these experimental results serve also to validate this theory for the case of salt solutions.

#### 4.1.1 Sorptivity (S)

Fig. 3 shows how sorptivity varies with the concentration of the two types of salt solution for the three stones.

As seen, sorptivity decreases as the salt concentration increases for all materials and salts. The variation is more relevant for the material with higher porosity (CA) than for the less porous material (CC). For the Bentheimer sandstone (B), sorptivity was only determined for two concentrations (pure water and the saturated salt solutions), so, linearity cannot be confirmed in this case.

Nonetheless, its results are consistent with those of the other stones.

To allow comparing the significance of the influence of soluble salts on capillary transport, Table 2 shows how much the sorptivity values obtained for the saturated salt solutions represent in relation to those obtained for pure water. As

seen, sodium nitrate induces the greatest sorptivity reduction for the three materials, although overall the difference among the two salts is not very large.

In Table 3 a summary of the results is shown which include the values of the cumulative volume of liquid absorbed per unit volume  $i$  and the sorptivity  $S$ . Mean values, standard deviation and coefficient of variation are presented.

#### *4.1.2 Verification of the scaling relation*

In Fig. 4, sorptivity  $S$  is scaled as  $(\sigma/\eta)^{1/2}$  for the three stones. Note that each graph includes the different concentrations of the two salt solutions and also pure water (which corresponds to the bold point).

As seen, the model is verified for the three stones since sorptivity scales precisely as  $(\sigma/\eta)^{1/2}$  in all cases. Confirmation of this scaling relation means that the materials are completely wetted by all of these liquids (i.e., the contact angle is null), the materials are inert during liquid absorption and there are no microstructural changes (Hall and Hoff 2002). As it derives from Eq. 3.2, this indicates also that, for the three materials, the changes induced by the salts in liquid capillary transport are due to their effect on the surface tension and viscosity of the liquid, as pointed out by Hall (1994) and Ruíz-Agudo et al. (2007).

## **4.2 Drying test**

The main objective of this test was to access the influence that soluble salts may have on drying. With that purpose, the obtained evaporation curves are analyzed, as well as the decay patterns which aroused due to salt crystallization during drying.

### *4.2.1 Evaporation curve*

The evaporation curves obtained for the Ançã limestone (CA), grey limestone (CC) and Bentheimer sandstone (B) impregnated with pure water and the salt solutions are presented in Fig. 5 and Fig. 6.

Although for the higher salt concentrations the differences are sometimes less clear, a general trend can be observed: the higher the salt concentration the slower the drying. This agrees to what is expected theoretically and observed in practice. However, some isolated specimens deviate from this general trend, depicting a markedly slower drying kinetics. There were occurrences for the three materials and the two salts and they tend to occur at the higher concentrations. The deviant behavior is observed in one specimen of the CA limestone with saturated NaCl solution, one specimen of the CC limestone with the 20% NaCl solution and two specimens of the B sandstone with the 20% NaCl solution. In the beginning, the drying curves of these specimens are similar to the remaining ones but they diverge suddenly, early in the drying process, without any apparent reason (Fig. 7).

#### *4.2.2 Decay patterns*

At the end of drying, efflorescence was observable on the surface of all the specimens. The characteristics of this efflorescence layer depend principally on the type of stone and type of salt, but there are some exceptions, as described below.

##### CA with NaCl

There was formation of a compact white layer of salt (Fig. 8) constituted by vertically oriented crystals (Fig. 9). The thickness of this salt crust increases with the concentration of the salt solution with which there is also an increasingly preferential deposition at the specimen edges. For the maximum concentration (saturated solution), the surface of the specimens was not totally covered by this white efflorescence: a much thinner and vitreous layer of salt with dispersed single large crystals was formed in the centre (Fig. 10).

##### CC with NaCl

There was formation of shrivelled salt crusts with holes at most of the hills (which are hollow), as well as occasional fissures (Fig. 11). These holes tend to develop at areas where the stone possesses dark “clasts” (Fig. 12) which should correspond to a less porous component. “Clasts” of less porous components are relatively common in this type of limestone as in sedimentary rocks in general.

##### B with NaCl

In general, there was formation of nodules of cauliflower-like efflorescence lying on a thin vitreous coat of salt (Fig. 13). As the concentration of the solution increased, the nodules become larger and more scattered. The efflorescence tends to develop preferably at the specimens edges.

There are, however, two exceptions to this general behavior: on the B.20%.1 and B.20%.2 specimens a thick and compact vitreous layer with irregular texture and some isolated massive crystals was formed (Fig. 14 and Fig. 15) instead of the above described white nodular efflorescence. The drying of these two samples was extremely slow (Fig. 5c1) for which reason these tests had to be interrupted before mass stabilization (Fig. 5c2). The occurrence of this different behaviour is hardly explainable because all the specimens were subjected to similar conditions. However, the occurrence of a different decay pattern is consistent with the distinct drying behaviour and vapour permeability of these two specimens (see section 4.4). It looks as the vitreous crust blocked the pores and hindered the drying process.

#### CA with NaNO<sub>3</sub>

There was formation of a compact layer of salt, covering the surface, and whose thickness increases with the concentration of the salt solution (Fig. 16). The crust is quite similar to that observed for the case of NaCl contamination but it is apparently less compact: the crystals appear to be less tightly packed than in the case of NaCl and the surface of the salt crust seems more porous (Fig. 17). The preferential deposition of salt on the edges of the specimens is even more pronounced here (Fig. 18).

#### CC with NaNO<sub>3</sub>

The surface of the CC limestone was covered by a porous coat of whisker-like efflorescence (Fig. 19). The higher the concentration of the salt solution the more compact this salt coat (Fig. 19). For the saturated solution, however, the salt layer presents holes.

For a few specimens, the efflorescence morphology diverges from this general description:

- in one specimen of the 35% concentration solution, a salt crust with very rough texture and holes at most of the hills (Fig. 20) occurred which is quite similar to that observed on the NaCl contaminated CC limestone.



- for two specimens of the saturated solution, the salt crust is more compact and has no holes (Fig. 21); the somewhat slower drying of these specimens during part of the drying test is consistent with this less porous salt coat.

### **4.3 RH above the salt contaminated specimens**

Fig. 22 shows the experimental values of the RH measured above two specimens, of the CA and CC limestones respectively, contaminated with the NaCl solutions of different concentration. As explained in section 3.3, these measurements were performed after 24 h drying. Fig. 22 shows also, in bold, the (theoretical) RH values expected above free surfaces of those solutions. This theoretical RH is the RHeq of the salt solution and was obtained from water activity / molality tables (Robinson and Stokes 2002).

As seen, despite the different RHeq of the salt solution used in the initial contamination, the RH measured above the specimens after 24 h drying has a value similar to that RHeq of a saturated solution. We believe this happened because the salt solutions all had already reached saturation at the evaporation front, regardless of their initial concentration, which is consistent with the fact that efflorescence had already occurred on the specimens at this early point of the drying process (Fig. 23).

There was only one exception to this behaviour, the CA.6% solution, where the RH measured above the material was higher than the RHeq of the saturated salt solution. But this was also the only case where no efflorescence was visible yet when the relative humidity was measured after 24h drying (Fig. 23), which means it too is consistent with our explanation: the lower RH measured above the specimens aroused probably because this less concentrated solution had not saturated yet when the RH measurements were made.

### **4.4 Vapour conductivity test**

The vapour conductivity test was performed to access the influence on vapour transport of the salt deposited in the materials during the drying process. As seen in Fig. 24, a significant amount of salt was deposited in the pores, but an also similarly relevant percentage crystallized as efflorescence.

Fig. 25 shows the results of the vapour conductivity tests which are expressed by the average equivalent air layer thickness ( $Sd$ ). Results are shown for the Ançã limestone (CA) and grey limestone (CC) contaminated with sodium chloride and sodium nitrate, and for the Bentheimer sandstone (B) contaminated with sodium chloride. Average and standard deviation values are always given.

From the analysis of Fig. 25, we can say that, overall in terms of general behaviour, the vapour permeability of the efflorescence-covered materials decreases ( $Sd$  increases) with the concentration of the salt solution. However, these changes are mostly irrelevant, i.e., the  $Sd$  increase is very small. The only exception is the Ançã limestone with sodium chloride where the  $Sd$  has a more relevant significant increase with the salt concentration. This means that only in this case the salt deposited during drying has a relevant hindering effect in relation to vapour transport. This behaviour seems to be related to the morphological characteristics we observed in the efflorescence layer. In fact, this was the case where a more compact efflorescence layer developed, as described in section 4.2.2 (Fig. 8) which is probably blocking vapour transport. In all the other cases the efflorescence layer was more porous, either because it had a less compact packing of the crystals (Fig. 17 and Fig. 19) or because it possessed holes and fissures (Fig. 11 and Fig. 13).

In a more focused analysis, it is seen that some specimens deviate from the general behaviour trend. Three main cases were detected: one for the CA limestone with saturated NaCl solution, one for B sandstone with 20% NaCl solution and one for CC limestone with 35% NaNO<sub>3</sub> solution, whose average  $Sd$  value diverges and/or standard deviation is very high (Fig. 25).

The case of the CC limestone with 35% NaNO<sub>3</sub> solution is difficult to explain since there are no visible differences between efflorescence that allow understanding why is the  $Sd$  in this group so high in relation to the other concentrations. In the drying test we also did not identify anything that could explain this difference. Therefore, we assume this value as an outlier.

In the case of the CA limestone with saturated NaCl solution, the higher standard deviation results probably from the fact that the surface of the stone is not homogeneously covered with salt (Fig. 10).

For the B sandstone with 20% NaCl solution, the high standard deviation is justified by the occurrence of two completely different types of efflorescence (Fig.

14). As seen in section 4.2.1, one of these types of efflorescence gave rise to a much slower drying which is in agreement with its high  $S_d$ .

These observations indicate, therefore, that the influence on vapour transport of the crystalline deposits strongly depends on its morphological characteristics (namely the packing of the crystals and the presence of holes/fissures in the salt layer).

#### **4.5 Overall discussion**

The drying experiments revealed, as a general trend, that for both salts the higher the salt concentration the slower the drying (see section 4.2.1). The four main hypothetical causes for this general behaviour are discussed below.

##### (Hip. 1) Differences in the amount of moisture in the specimens

The amount of water present in the specimens decreases as the concentration of the solution increases. However, what was observed was that the specimens with the lower amount of water, i.e. more concentrated solutions had a much slower drying. So, differences in the amount of moisture could not be a cause of the observed differences.

##### (Hip. 2) Variation of the RH above the materials

The  $RH_{eq}$  of a salt solution decreases as its concentration increases (Table 1) which suggests that a lower RH could exist above the specimens with higher salt concentration, leading to a lower RH gradient between the material and the environment and, therefore, to a slower drying kinetics. However, Fig. 22 shows that this is not true because saturation of the salt solutions at the evaporating front occurred always very early in the drying process, as discussed in section 4.3. The figure shows that although solutions with different concentration have different  $RH_{eq}$ , the RH above the contaminated specimens tested here is, in general, always similar to the  $RH_{eq}$  of the salt. This means that a variation of the RH above the materials is also not the cause of the observed differences in drying kinetics. It may be relevant in situations where salts with different  $RH_{eq}$  are being compared (Gonçalves et al. 2007), but not in this case where that does not happen.

### (Hip. 3) Hindering of vapour transport by the salt crystals

Obstruction of vapour transport by the crystallized salt could delay drying.

Indeed, the higher the concentration of the contaminant solution the higher the amount of crystallized salt at the end of drying. Therefore, this effect could very well justify a slower drying kinetics for the more concentrated solutions.

However, the experimental results (Fig. 25) show that the vapour conductivity of the salt contaminated materials suffers, in general, only minor changes with the increase in the concentration of the salt solution, despite of the differences in drying kinetics. We attribute this non-obstructive character of the salt deposits to the non-dense packing of the crystals or to the presence of holes and fissures in external salt crusts, as discussed in section 4.4.

There was only one case where an apparently more significant variation of the vapour conductivity with the concentration of the salt solution was detected. It was the CA limestone with NaCl (Fig. 25), which presented seemingly more compact efflorescence (section 4.2.2).

To try to find out whether these changes in vapour transport were affecting the drying kinetics in this case, we have looked at the possible correlation between the drying index ( $DI$ ) and the equivalent air layer thickness ( $Sd$ ). As shown in Fig. 26, while in the other four cases the  $DI$  varies despite the  $Sd$  is almost constant, for the CA limestone with NaCl an approximately linear correlation seems to exist between the two quantities. This seems to mean that in this case there was obstruction of vapour by the deposited salt and a consequent delay of drying whose significance increases with the concentration of the contaminant solution. These conclusions are consistent with the hypothesis that blocking of vapour transport by the salt crystals can indeed occur, depending on the morphology (compactness) of the salt deposits, in which case it can give rise to differences in drying kinetics. Alike results were recently achieved by Prat (2012) for glass bead packings, which indicate that the occurrence of two different drying regimes, the “blocking regime” and the “enhanced drying rate regime” correspond to two different types of efflorescence, “crusty” and “patchy”, respectively. The present results also show that the effect on vapour transport cannot, however, fully explain the differences in drying kinetics.

### (Hip. 4) Changes in liquid transport due to sorptivity variation

A lower sorptivity means that equilibrium between the liquid flow and the vapour flow tends to occur at a higher depth in the material. Hence, the drying process will tend to be slower.

As seen before, sorptivity indeed decreases linearly as the salt concentration increases (Fig. 3) due to the differences that arise in surface tension and viscosity (Fig. 4). This was observed for the three tested materials.

Fig. 27 shows that an approximately linear correlation seems to exist also between sorptivity and the drying index for the two limestones. This is consistent with the hypothesis that sorptivity variation is one of the causes of the observed differences in drying kinetics.

In the case of Bentheimer, it was not possible to evaluate a possible correlation since, as explained in section 3.1, the sorptivity was only determined for saturated solution and pure water.

Fig. 27 shows also that there is an important difference between the two materials (CA and CC) that were tested with both salts: for the CC limestone, a single tendency line could encompass both salts whereas for the CA limestone there are clearly distinct tendencies for sodium chloride and sodium nitrate, respectively. We think that this happens because, for the CA limestone, sodium chloride hindered vapour transport whereas for sodium nitrate that did not happen. In the case of CC limestone neither type of salt had an influence on vapour transport. Therefore, for the CA limestone with sodium chloride the drying kinetics (hence, the drying index DI) suffers the influence of two distinct factors, sorptivity and vapour permeability, while in the other cases, it depends only on the sorptivity.

For some specimens, efflorescence morphology deviated from that occurring for the remaining specimens of the same type of stone subjected to similar experimental conditions. This kind of deviant behaviour took place only sporadically, although it tended to occur at the higher concentrations and there were occurrences for both salts and all the materials. The deviant specimens revealed also, usually, tendency to have a slower drying kinetics or lower vapour conductivity. In his drying experiments on glass bead packings, Prat (2012) was able to obtain compact (“custy”) efflorescence which blocked the evaporation process for sufficiently small beads and porous (“patchy”) efflorescence without such an effect when the beads were sufficiently large. In our case, the deviant

cases seem to have an essentially unpredictable nature. Prat's results suggest that they derive possibly from small casual inhomogeneities in the pore network of the natural stone materials tested here.

## 5 Conclusions

This work investigates and discusses the influence of NaCl and NaNO<sub>3</sub> on liquid capillary transport, vapour conductivity and drying kinetics of three porous stones. These two salts are among the most common in decayed buildings, possess only one crystalline form above 0°C and have similar equilibrium relative humidity (RHeq) at 20°C, the temperature at which the experiments were performed. The influence of the salts on liquid capillary transport was evaluated through water absorption tests. These showed that the sorptivity of the three stones decreases as the salt concentration increases and that sodium nitrate induces the greatest sorptivity reduction, although overall the difference among the two salts is not very large. Further, for the three materials, it was confirmed that sorptivity scales as  $(\sigma/\eta)^{1/2}$ , which means that the changes they induce on liquid capillary transport across porous materials are due to their effect on surface tension and viscosity of the liquid.

During the subsequent drying of the specimens, the salt crystallized and formed efflorescence whose morphology, in general, was similar for sodium chloride and sodium nitrate and varied with the type of stone.

After complete drying, the vapour conductivity of the salt contaminated specimens was measured by the dry-cup method. The results showed that the obstructive effect of salt deposits was apparently related to the morphological characteristics of the efflorescence. In most cases the presence of salt did not alter the vapour transport properties of the stones. This is in accordance with the observed non-dense packing of the external deposits or with the presence of holes and fissures in the salt crusts. Only in one case (Ançã limestone with NaCl) the deposited salt had a relevant obstructing effect on vapour flow, which is in accordance with the fact that denser efflorescence was observed in this case. This means that not all types of efflorescence will have an obstructive effect in relation to vapour transport.

The drying kinetics was accessed through gravimetric evaporation curves obtained during the drying process. For both salts, a general tendency was observed to have a slower drying process as the concentration of the salt solution increased.

Two possible causes for this variation in drying kinetics have been dismissed: (i) the lower amount of moisture present in the more concentrated solutions is certainly not a cause because drying is slower in these cases; (ii) lowering of the water activity due to the amount of solute, hence, of the vapour pressure gradient between the material and its environment is also not a cause because the solution saturates at the evaporation front very early in the drying process; this is shown by the fact that the RH above the specimens, measured after 24 hours drying, was always similar to the  $RH_{eq}$  of the salt regardless of the concentration of the contaminating solution.

The major cause for having a slower drying process as the concentration of the salt solution increases seems to be the decrease in the sorptivity of the stones. A lower sorptivity means that, for similar liquid content, equilibrium between the liquid flow and the vapour flow will tend to occur at a higher depth, which will hamper the drying process.

Obstruction of vapour transport by the crystalline deposits can be an additional cause whose significance seems to depend on the morphology of such deposits. Indeed, not all types of deposit will affect vapour transport. In the present experiments, such effect was observed only in one out of the five stone/salt combinations (the Ançã limestone with NaCl). In this case, compact salt crusts were formed on the surface of the specimens. In all the other cases, the non-significant influence on vapour transport is associated to the presence of porous efflorescence or salt crusts with holes and fissures through which vapour can escape. The salt present in the pores as subflorescence, which is relevant also in these cases, did not apparently have any relevant influence on vapour transport. For some specimens, efflorescence morphology deviated from that occurring for the remaining specimens of the same type of stone subjected to similar experimental conditions. The deviant specimens revealed also, usually, tendency to have a slower drying kinetics or lower vapour conductivity. This deviant behaviour tended to occur at the higher concentrations. However, it seems to have an essentially unpredictable nature and derives possibly from small casual

inhomogeneities in the pore network of the tested stones. This component of unpredictability in the crystallization patterns and its consequences in terms of the properties and behaviour of the salt contaminated material requires further research and needs to be considered in future studies on salt decay.

#### ACKNOWLEDGEMENTS

This work was funded by the Portuguese Foundation for Science and Technology (FCT) under the research project DRYMASS (ref. PTDC/ECM/100553/2008). Vânia Brito is supported by a research grant provided under this project.

We acknowledge the contribution of Leo Pel (Technical University of Eindhoven – TU/e) and José Delgado Rodrigues (LNEC) in discussing some aspects of this work in the framework of the mentioned DRYMASS research project. We are also thankful to Veerle Cnudde (Ghent University), and Timo G. Nijland (Netherlands Organization for Applied Scientific Research - TNO) for providing the Bentheimer sandstone samples. We would like to acknowledge also the support of LNEC technicians who helped with different aspects of the experimental work: José Costa and Paula Menezes.

## References

- Beltrán, V., Escardino, A., Feliu, C., Rodrigo, M.D.: Liquid suction by porous ceramic materials. *Brit Ceram Trans J*, 87, 64-69 (1988)
- CEN: Hygrothermal performance of building materials and products. Determination of water vapour transmission properties. EN ISO 12572:2001.
- Commissione NORMAL: Misura dell'indice di asciugamento (drying index). Roma, CNR/ICR. Doc n° 29/88 (1991)
- CRC: Handbook of Chemistry and Physics. Weast RC (eds), CRC Press, Boca Raton (1985).
- Gonçalves, T.D., Pel, L., Rodrigues, J.D.: Drying of salt contaminated masonry: MRI laboratory monitoring. *Environ Geol* 52, 249-258 (2007)
- Gonçalves, T.D., Brito, V., Pel, L.: Water vapour emission from solid mesoporous materials during the constant drying rate period. *Dry Technol*, 30:5, 462-474 (2012)
- Greenspan, L.: Humidity fixed points of binary saturated aqueous solutions. *J. Res. National Bur. Stand-A, Physics and Chemistry* 1 89-96 (1977)
- Gummerson ,R.J., Hall, C., Hoff, W.D.: Water movement in porous building materials - II. Hydraulic suction and sorptivity of brick and other masonry materials. *Building Environ.* 15, 101-108 (1980)
- Hall, C.: Barrier performance on concrete: a review of fluid transport theory. *Mater Struct* 27, 291–306 (1994)



- Hall, C., Hoff, W.D.: Water Transport in Brick, Stone and Concrete. Spon Press, London and New York (2002). ISBN 0-419-22890-X
- Pel, L., Huinink, H., Kopinga, K.: Salt transport and crystallization in porous building materials. *Magn Reson Imaging* 21, 317-320 (2003)
- Petković, J., Huinink, H.P., Pel, L., Kopinga, K., Van Hees, R.P.J.: Salt transport in plaster/substrate layers. *Mater Struct* 40, 475–490 (2007).
- Reda Taha, M.M., El-Dieb, A.S., Shrive, N.G.: Sorptivity: a reliable measurement for surface absorption of masonry brick units. *Mater Struct* 34, number 7, 438-445 (2001)
- RILEM TC 25-PEM: Recommended tests to measure the deterioration of stone and to assess the effectiveness of treatment methods. *Materials and Structures*, 13: 209-209 (1980)
- Robinson, R., Stokes, R.: *Electrolyte Solutions: The Measurement and Interpretation of Conductance, Chemical Potential and Diffusion in Solutions of Simple Electrolytes*. ISBN 0-486-42225-9. Republication of the second revised edition which was originally published in 1970 by Butterworth, London. (2002)
- Rodriguez-Navarro, C., Doehne, E.: Salt weathering: influence of evaporation rate, supersaturation and crystallization pattern. *Earth Surf. Process. Landforms* 24:191–209 (1999)
- Rucker, P., Holm, A., Krus, M.: Determination of moisture and salt content distributions by combining NMR and gamma ray measurements. *Materialsweek. Munich* (2000)
- Ruíz-Agudo, E., Mees, F., Jacobs, C., Rodriguez-Navarro, C.: The role of saline solution properties on porous limestone salt weathering by magnesium and sodium sulfates. *Environ Geol* 52, 269-281 (2007)
- Sghaier, N., Prat, M.: Effect of efflorescence formation on drying kinetics of porous media. *Transp Porous Med* 80, 441-454 (2009)
- Schwarz, H.J., Steiger, M. SaltWiki. <http://www.saltwiki.net> (2011). Accessed 24 September 2012
- Prat, M.: How to make crusty or patchy efflorescence. *Workshop Crispom III – Crystallization in porous media. Book of abstracts* (2012).

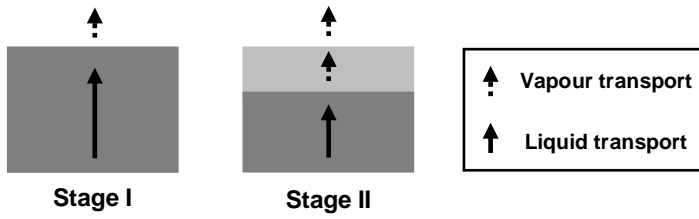


**Fig. 1** Drying of a porous building material

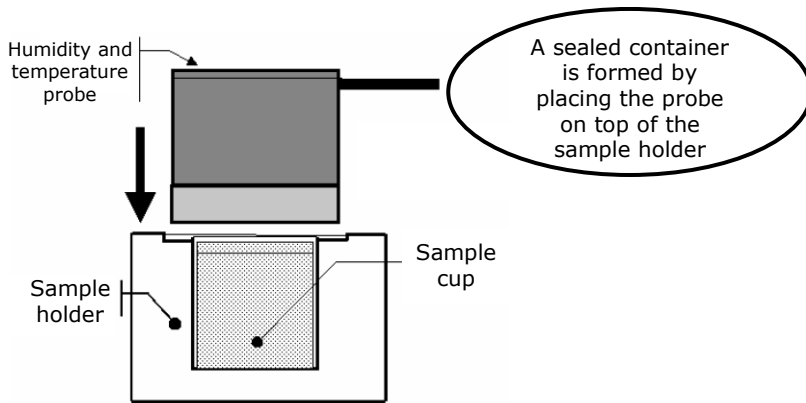


**Fig. 2** Principle of measurement of Hygrolab 3 by Rotronic

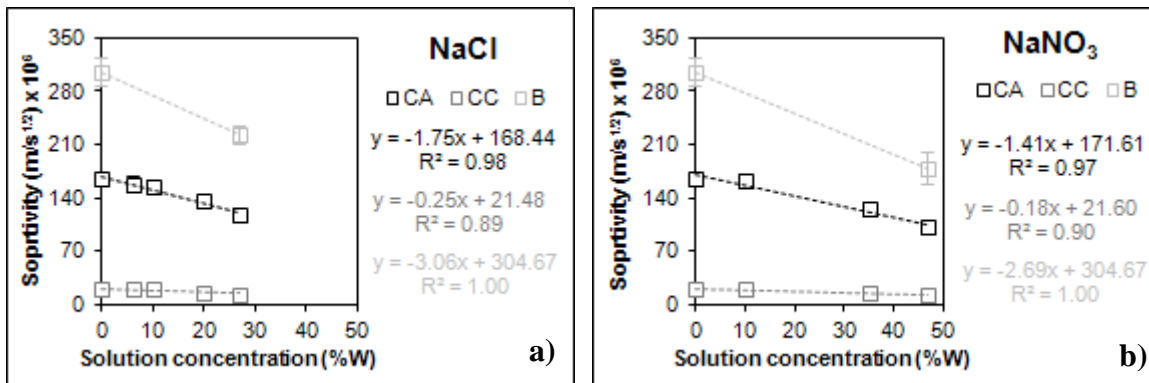


**Fig. 3** Sorptivity as a function of the salt concentration for a) NaCl and b) NaNO<sub>3</sub>, including water

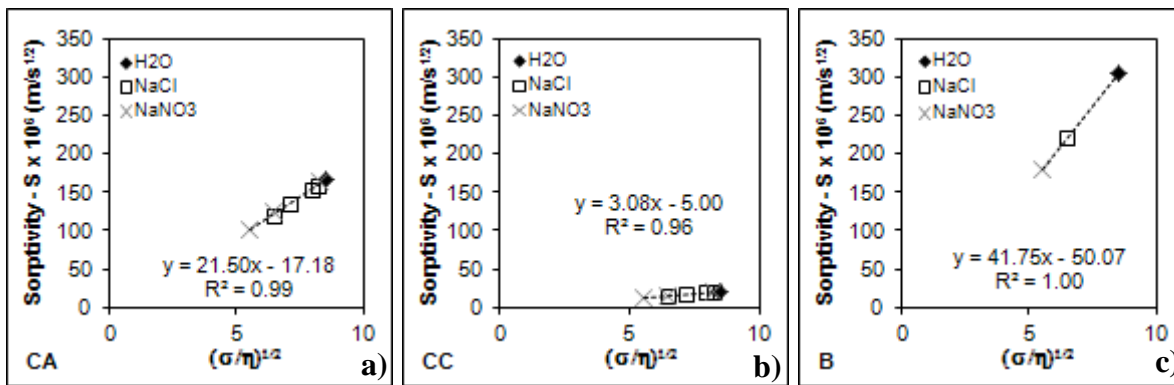


Fig. 4 Sorptivity scaled as  $(\sigma/\eta)^{1/2}$  for a) Anca limestone, b) grey limestone and c) Bentheimer sandstone

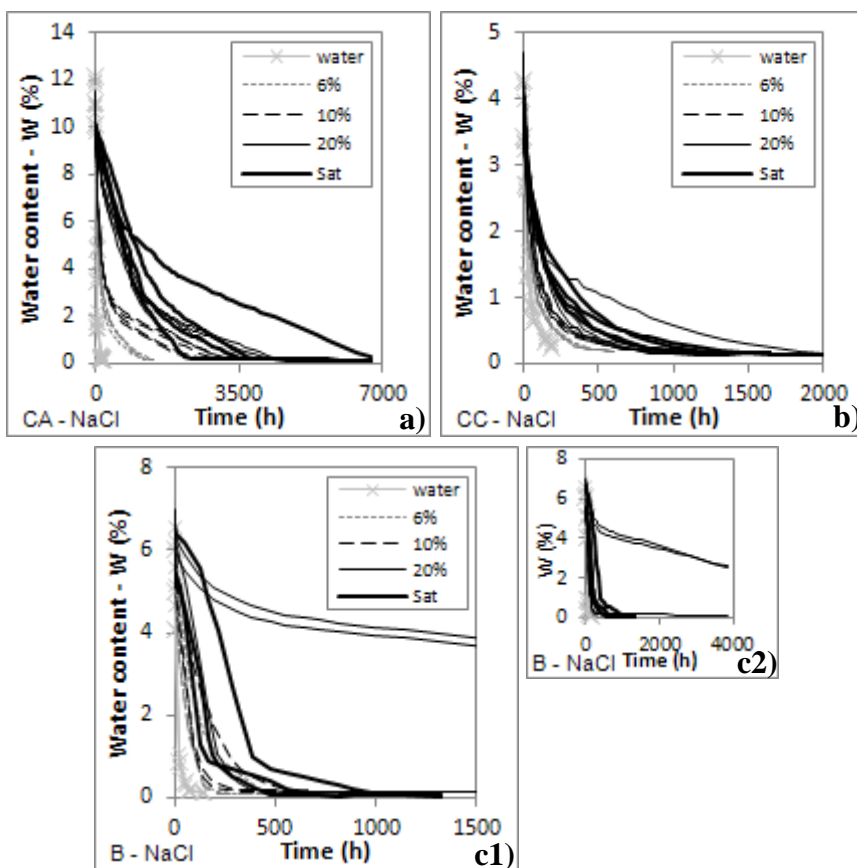
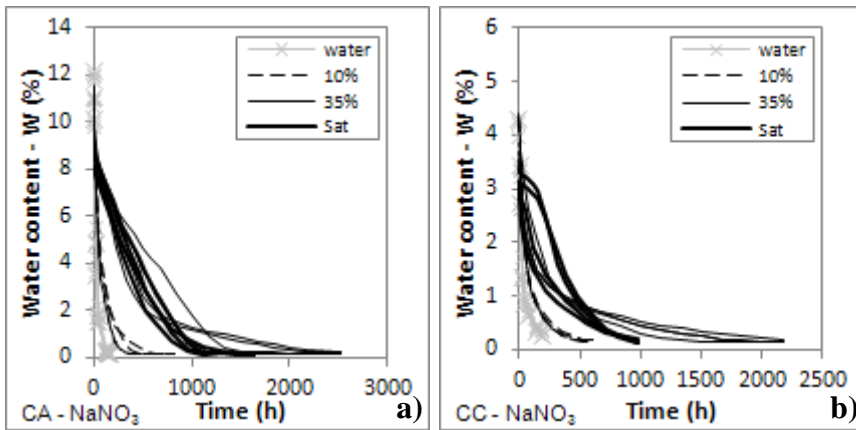
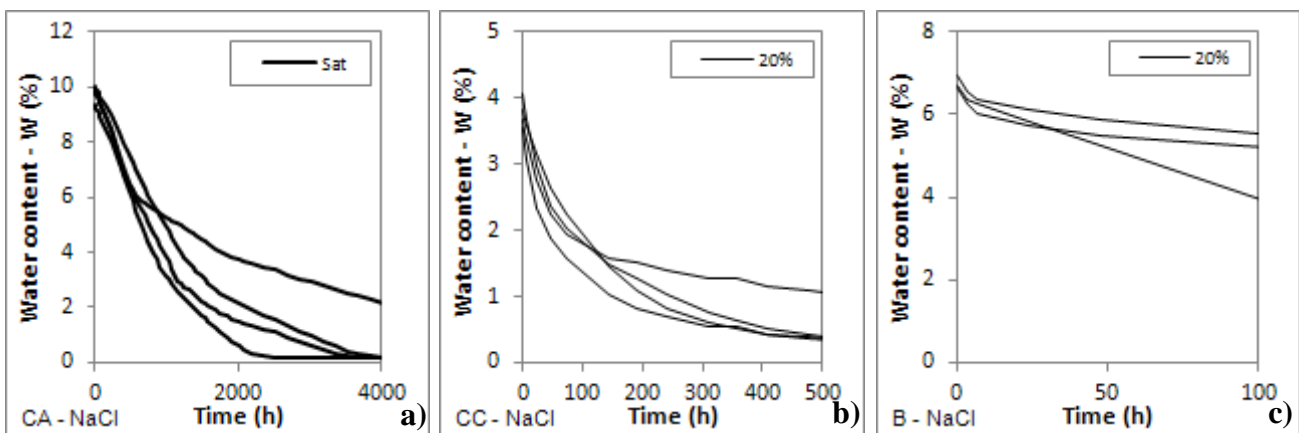


Fig. 5 Drying curves obtained with NaCl and pure water for: a) Anca limestone, b) "grey" limestone; c) Bentheimer sandstone whose results are presented at two different scales



**Fig. 6** Drying curves for  $\text{NaNO}_3$  and pure water in the case of: a) Ançã limestone and b) “grey” limestone



**Fig. 7** Drying curves of the groups which include one or more specimens with deviant behaviour: a) Ançã limestone with saturated  $\text{NaCl}$  solution, b) “grey” limestone with the 20%  $\text{NaCl}$  solution and c) Bentheimer sandstone with the 20%  $\text{NaCl}$  solution

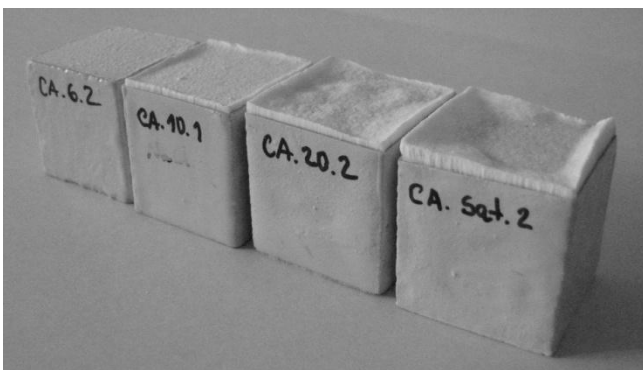


**Fig. 8** The thickness of the  $\text{NaCl}$  crust on Ançã limestone increases with the concentration of the salt solution (from left to right) and shows a preferential deposition at the edges of the specimens

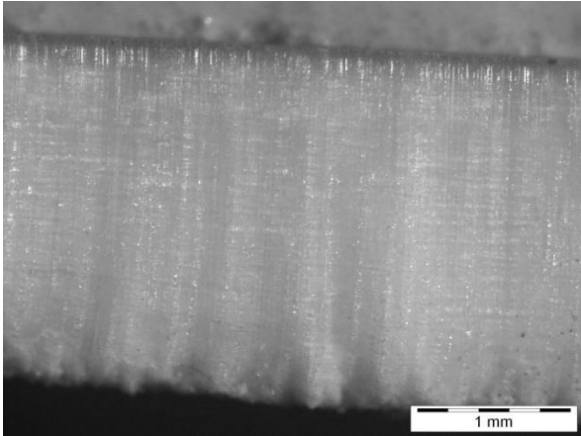


**Fig. 9** NaCl crystals with a clear vertical orientation on a CA.20% specimen: 30x magnification

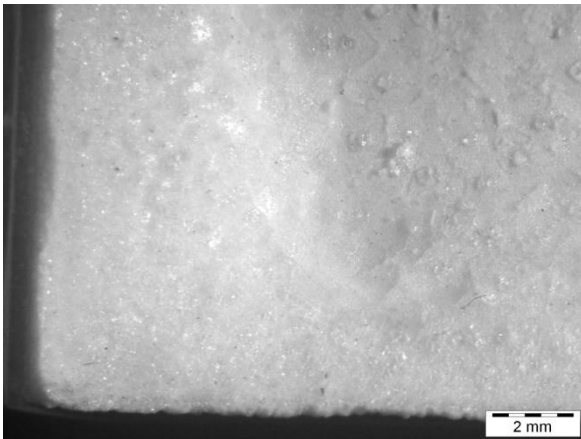


**Fig. 10** Preferential deposition of NaCl at the edges of a CA.Sat specimen and thinner vitreous layer with dispersed large single crystals on the center: 7.5x magnification

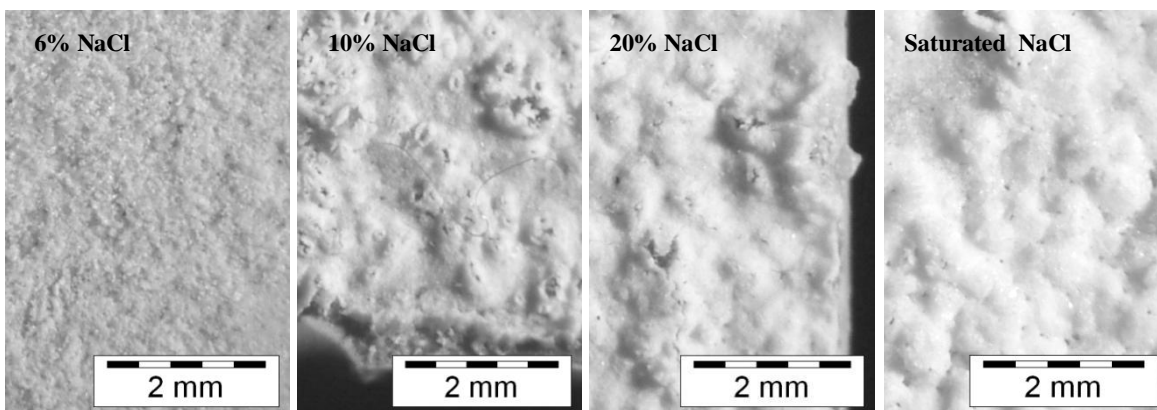


**Fig. 11** Shrivelled salt crusts of NaCl with holes at most of the hills on the "grey limestone" (concentration of the salt solution increases from left to right): 7.5x magnification

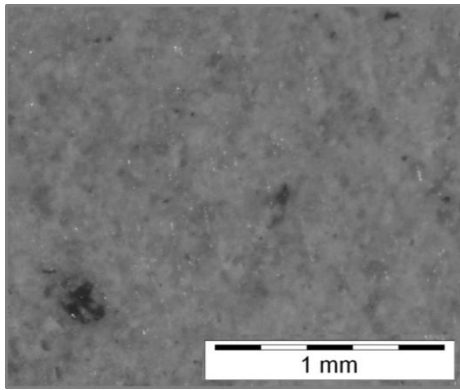


**Fig. 12** Dark “clasts” visible on the surface of the “grey” limestone: 30x magnification

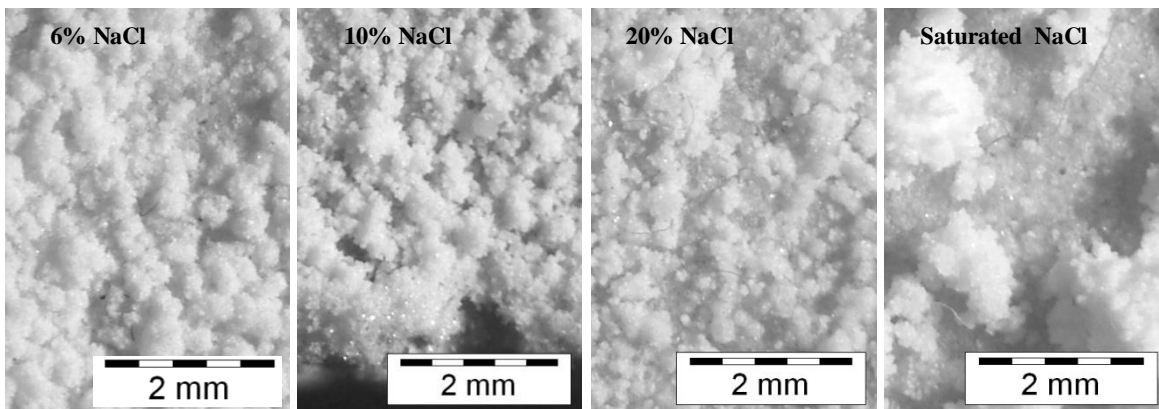


**Fig. 13** Nodules of cauliflower-like NaCl efflorescence lying on a thin vitreous coat of salt in Bentheimer sandstone (salt concentration increases from left to right): 7.5x magnification

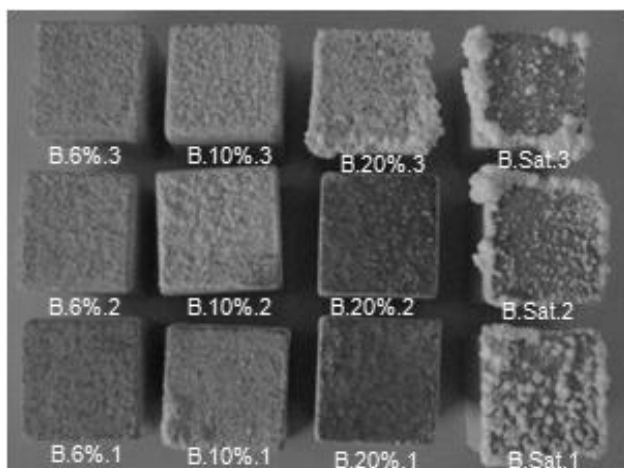


**Fig. 14** Bentheimer specimens contaminated with NaCl solutions with concentrations of 6%, 10%, 20% and saturated (from left to right)

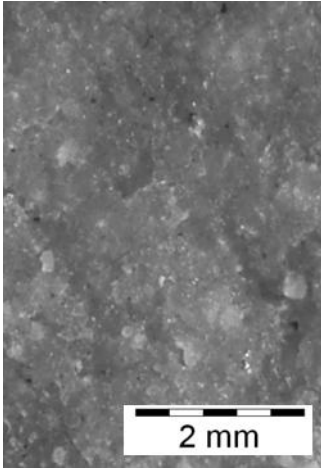


**Fig. 15** Thick, compact and vitreous NaCl crust of irregular texture with isolated salt crystals: 30x magnification of B.20.2 specimen

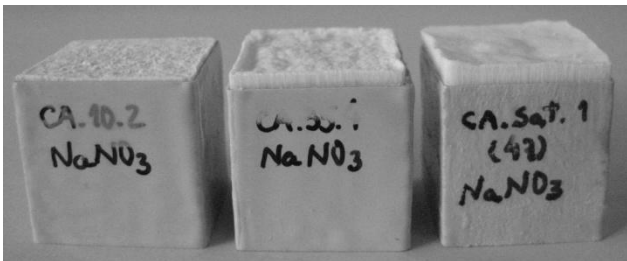


**Fig. 16** Thickness of NaNO<sub>3</sub> layer increases with the concentration of salt in Ançã limestone (from left to right)

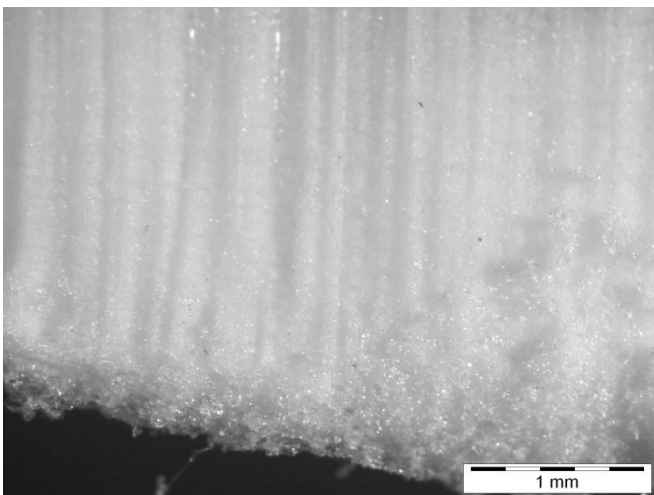


**Fig. 17** Porous surface layer of NaNO<sub>3</sub>: 30x magnification of CA.Sat specimen

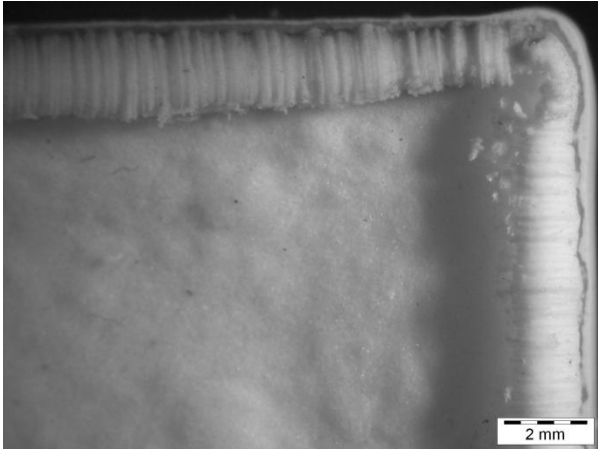


**Fig. 18** Preferential deposition of  $\text{NaNO}_3$  at the edges: 7.5x magnification of CA.35% specimen

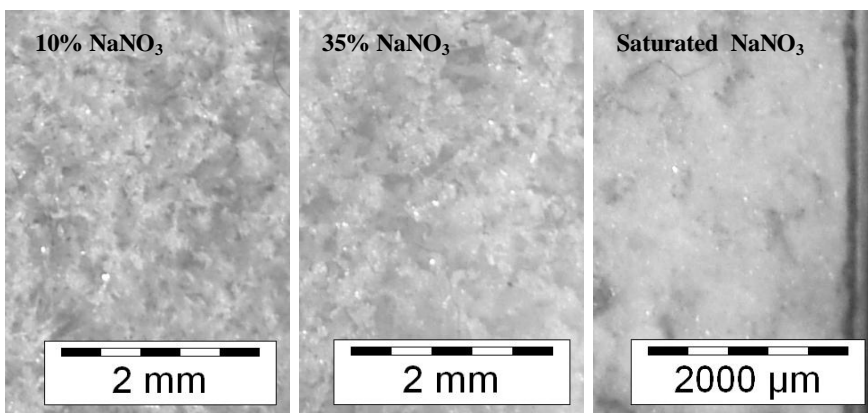


**Fig. 19** Porous coat of whisker-like  $\text{NaNO}_3$  efflorescence in "grey limestone" (salt concentration increases from left to right): 7.5x magnification

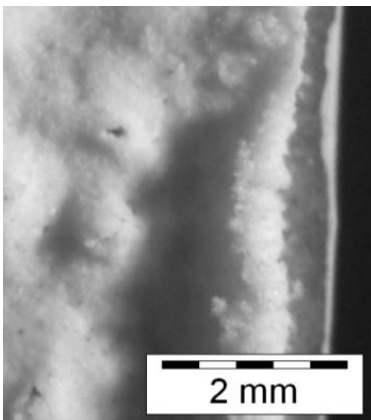


**Fig. 20** Different  $\text{NaNO}_3$  efflorescence morphology: 7.5x magnification of one CC.35 specimen



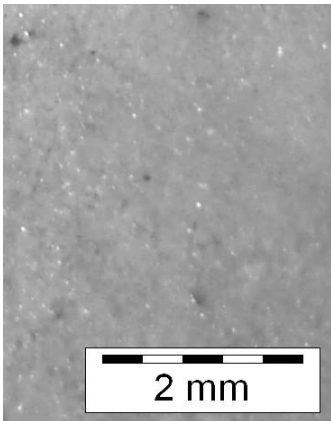


**Fig. 21**  $\text{NaNO}_3$  crust more compact and without holes: 7.5x magnification of one CC.Sat specimen

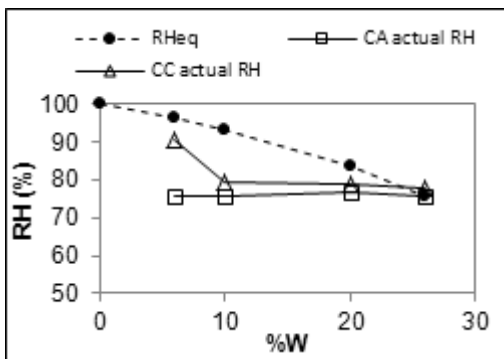


**Fig. 22** RH above the CA and CC limestones contaminated with sodium chloride solutions of different concentration (in bold, the RHeq of the salt solutions is presented as a reference)

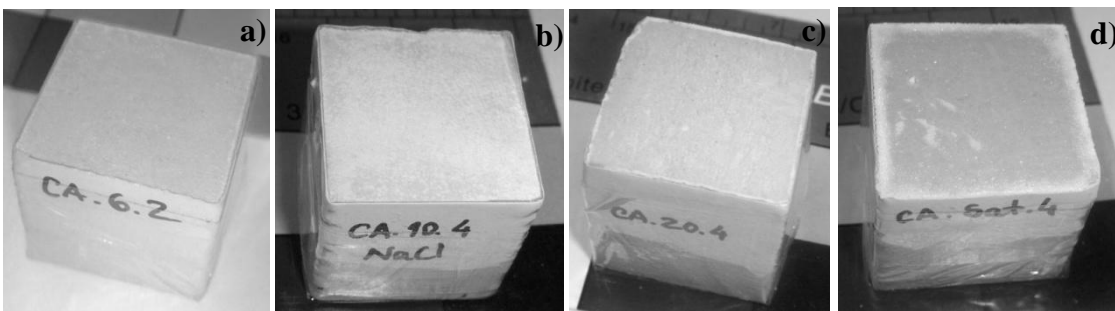


**Fig. 23** Specimens showing efflorescence during RH measurements: a) 6% NaCl, b) 10% NaCl, c) 20% NaCl and d) saturated NaCl

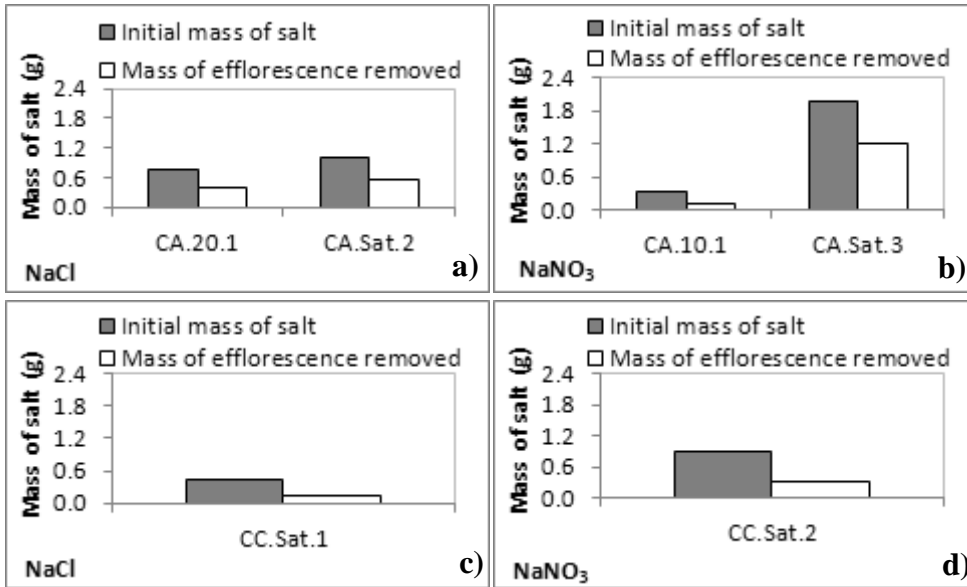


**Fig. 24** Total amount of salt introduced in the specimens and total amount that crystallized as efflorescence (for the purpose of its quantification, efflorescence was removed from the surface of these specimens by scraping): a) two CA-NaCl specimens, b) two CA-NaNO<sub>3</sub> specimens, c) one CC-NaCl specimen and d) one CC-NaNO<sub>3</sub> specimen

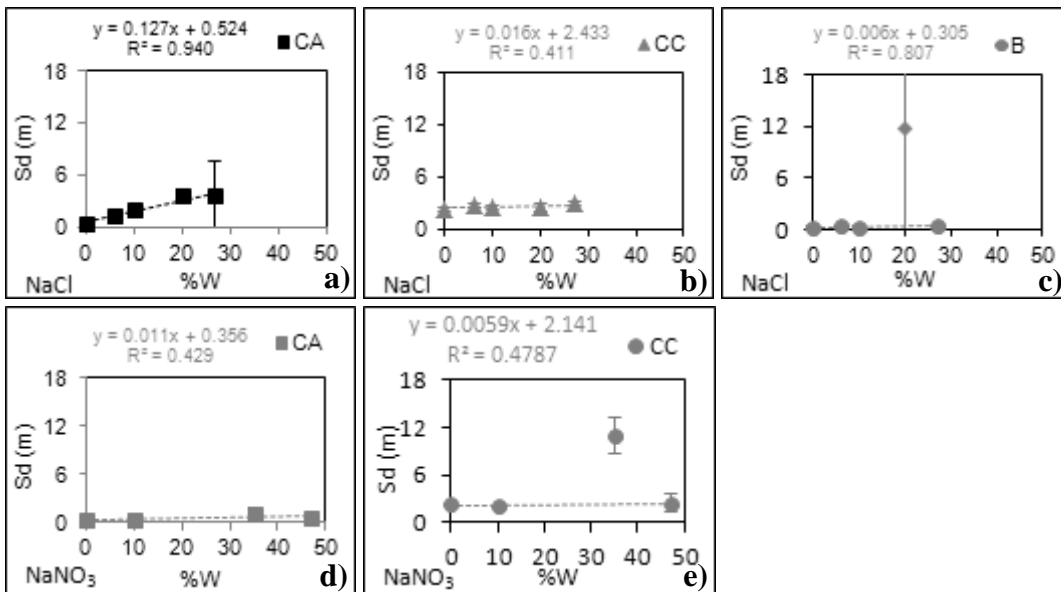


**Fig. 25** Equivalent air layer thickness (Sd) as a function of the solution's concentration of the salt solutions: a) CA-NaCl, CC-NaCl, c) B-NaCl, d) CA-NaNO<sub>3</sub> and e) CC-NaNO<sub>3</sub>

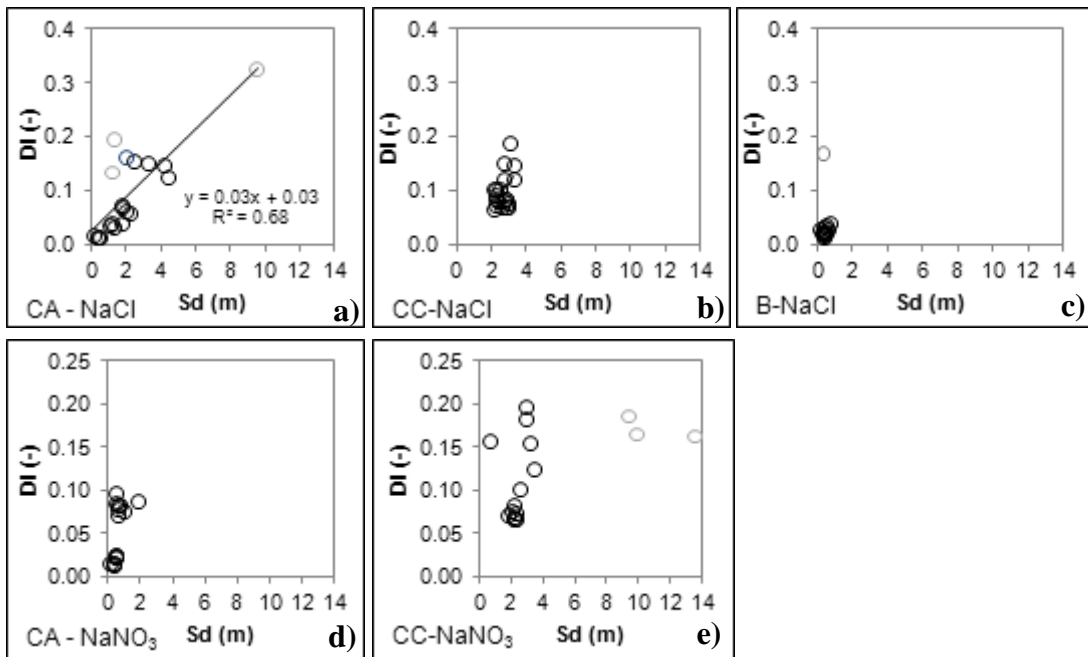


**Fig. 26** Correlation between drying index (DI) and equivalent air layer thickness (Sd); the grey bullets are the specimens with deviant vapour permeability behaviour and different efflorescence morphology. a) CA with NaCl, b) CC with NaCl, c) B with NaCl, d) CA with NaNO<sub>3</sub> and d) CC with NaNO<sub>3</sub>

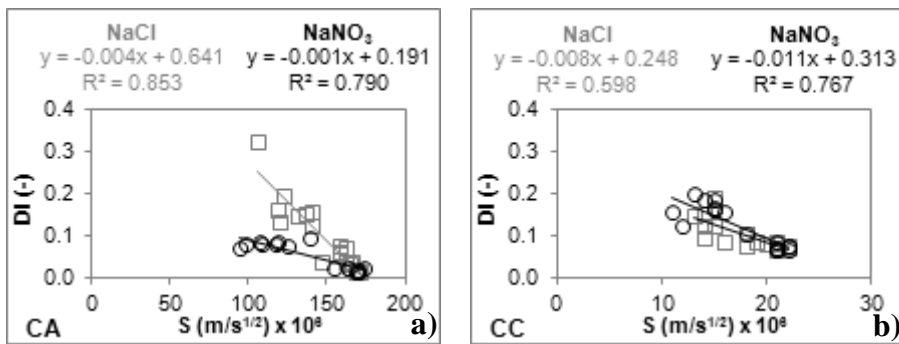


**Fig. 27** Correlation between drying index (DI) and sorptivity (S) for: a) CA and b) for CC

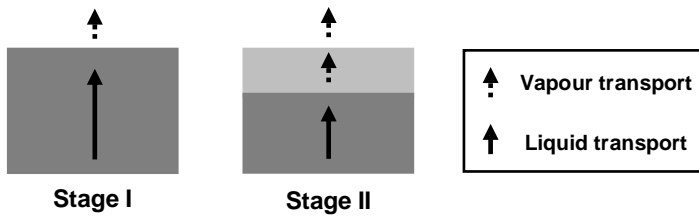


**Fig. 1** Drying of a porous building material

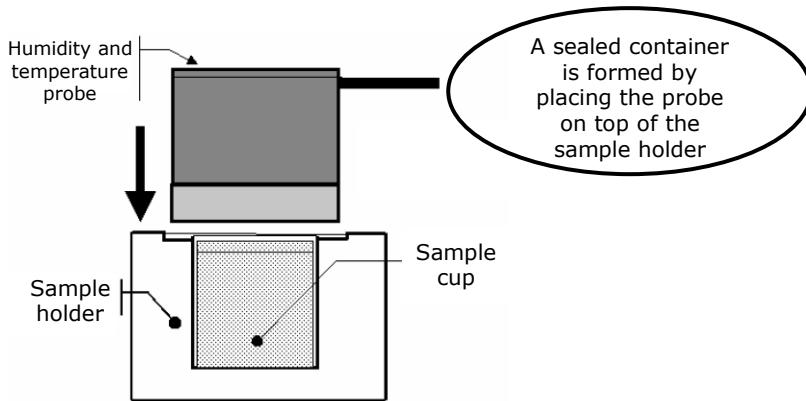


**Fig. 2** Principle of measurement of Hygrolab 3 by Rotronic

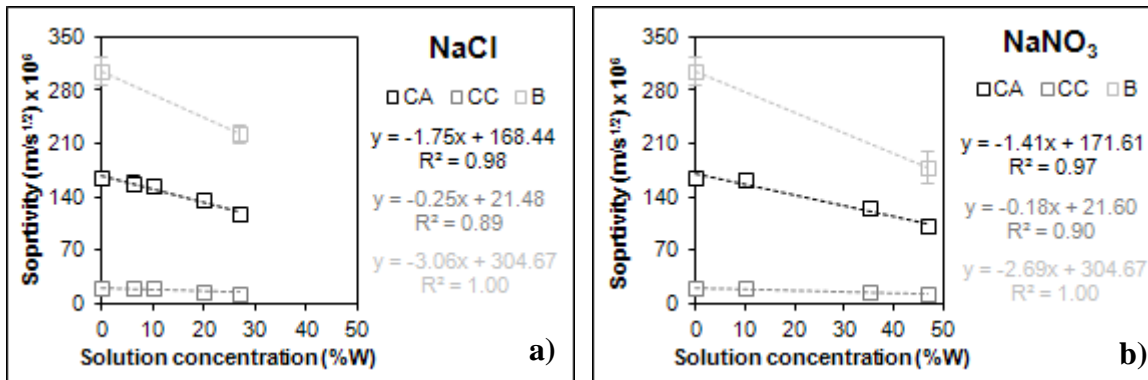


**Fig. 3** Sorptivity as a function of the salt concentration for a) NaCl and b) NaNO<sub>3</sub>, including water

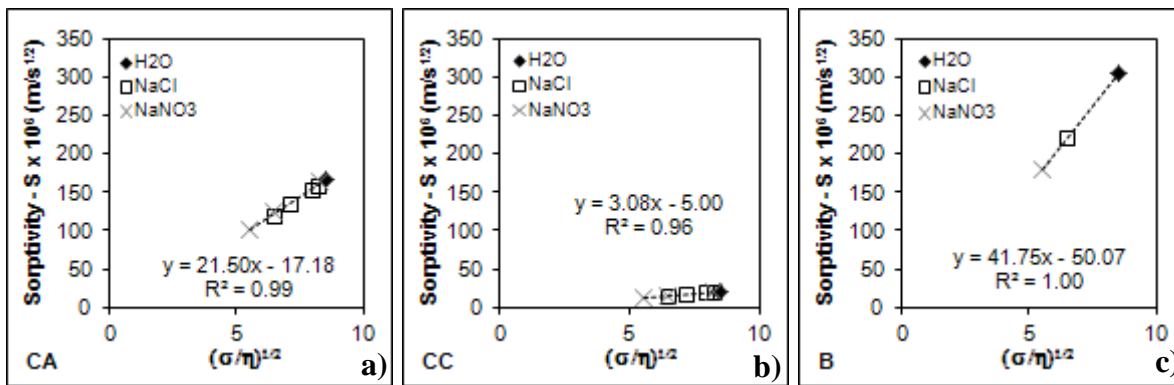


Fig. 4 Sorptivity scaled as  $(\sigma/\eta)^{1/2}$  for a) Anca limestone, b) grey limestone and c) Bentheimer sandstone

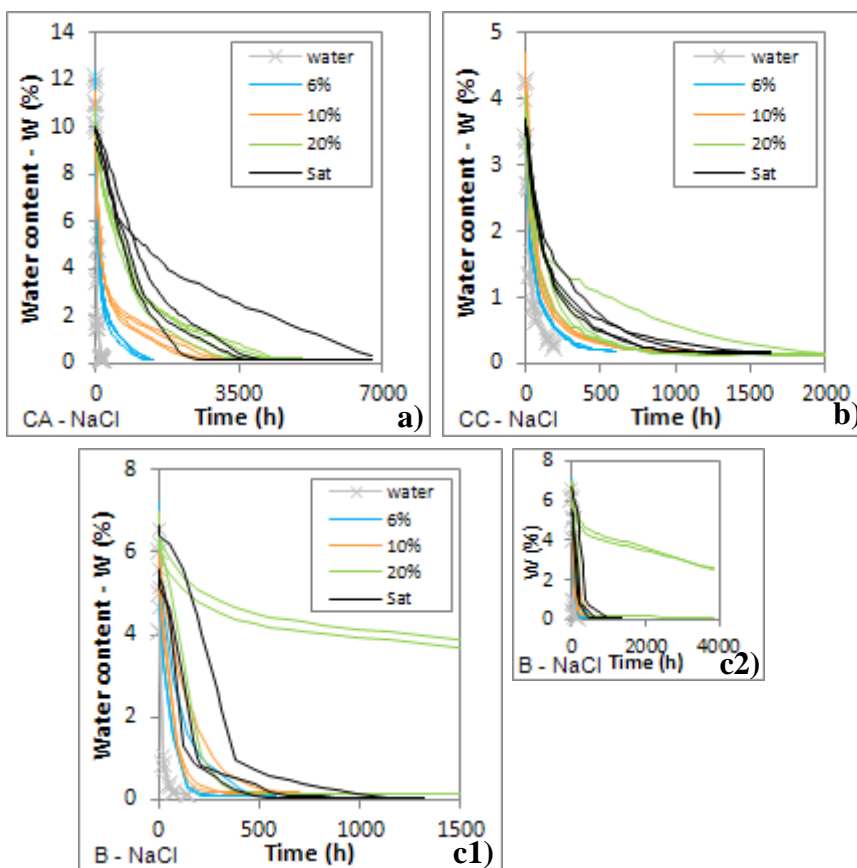
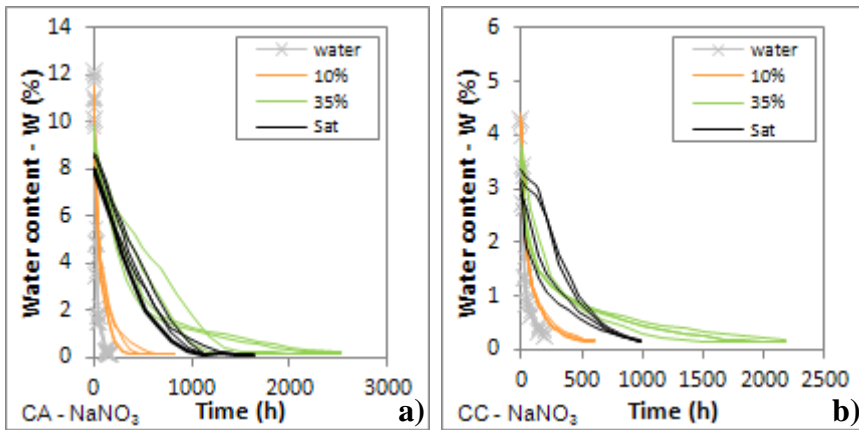
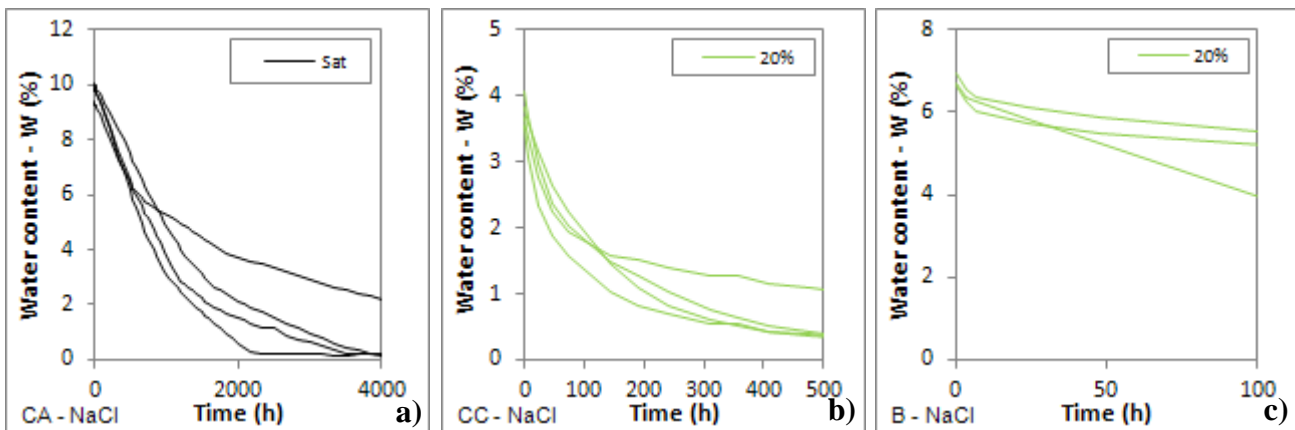


Fig. 5 Drying curves obtained with NaCl and pure water for: a) Anca limestone, b) "grey" limestone; c) Bentheimer sandstone whose results are presented at two different scales



**Fig. 6** Drying curves for  $\text{NaNO}_3$  and pure water in the case of: a) Ançã limestone and b) “grey” limestone



**Fig. 7** Drying curves of the groups which include one or more specimens with deviant behaviour: a) Ançã limestone with saturated  $\text{NaCl}$  solution, b) “grey” limestone with the 20%  $\text{NaCl}$  solution and c) Bentheimer sandstone with the 20%  $\text{NaCl}$  solution



**Fig. 8** The thickness of the  $\text{NaCl}$  crust on Ançã limestone increases with the concentration of the salt solution (from left to right) and shows a preferential deposition at the edges of the specimens

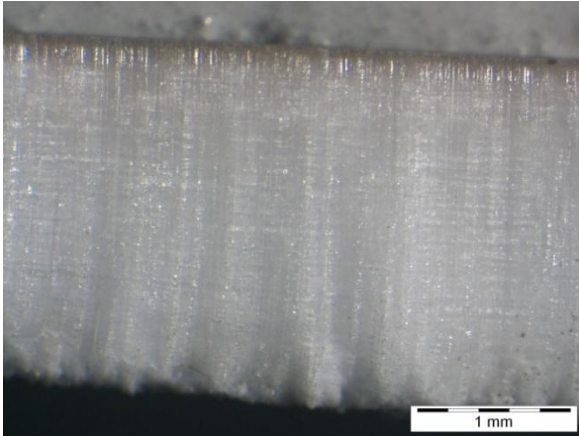


**Fig. 9** NaCl crystals with a clear vertical orientation on a CA.20% specimen: 30x magnification

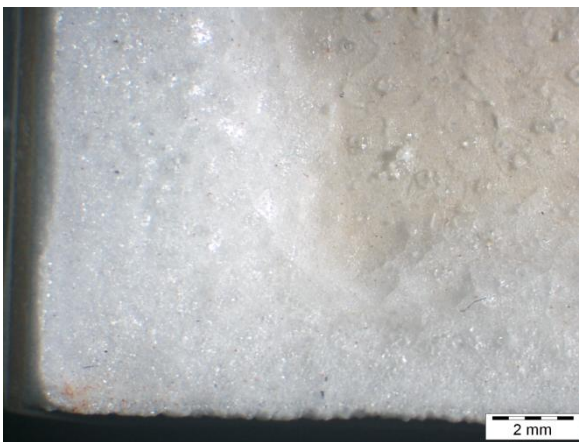


**Fig. 10** Preferential deposition of NaCl at the edges of a CA.Sat specimen and thinner vitreous layer with dispersed large single crystals on the center: 7.5x magnification

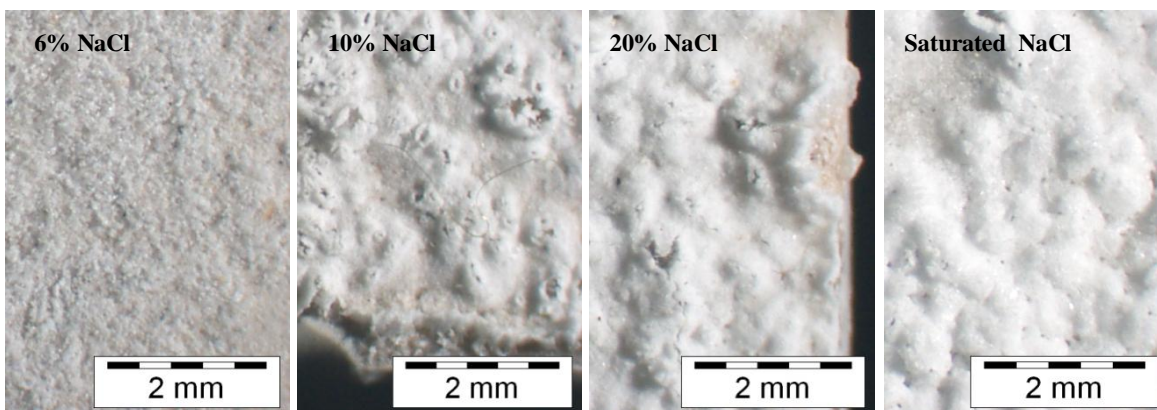


**Fig. 11** Shrivelled salt crusts of NaCl with holes at most of the hills on the "grey limestone" (concentration of the salt solution increases from left to right): 7.5x magnification



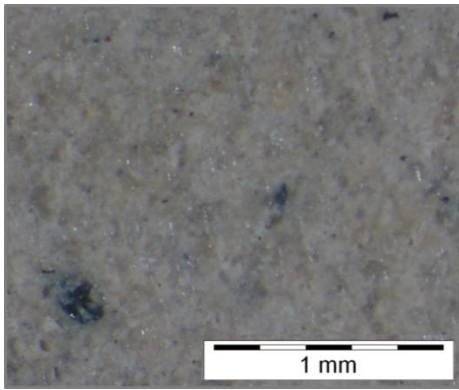


**Fig. 12** Dark “clasts” visible on the surface of the “grey” limestone: 30x magnification

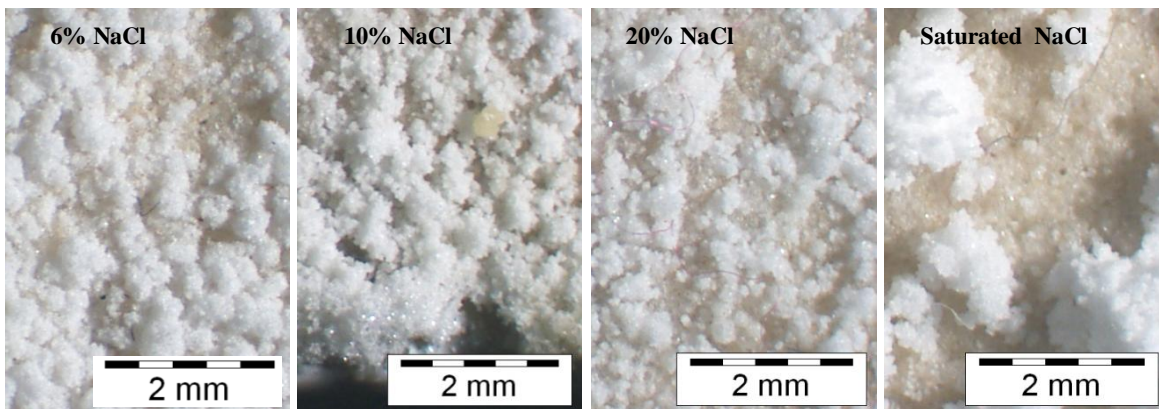


**Fig. 13** Nodules of cauliflower-like NaCl efflorescence lying on a thin vitreous coat of salt in Bentheimer sandstone (salt concentration increases from left to right): 7.5x magnification

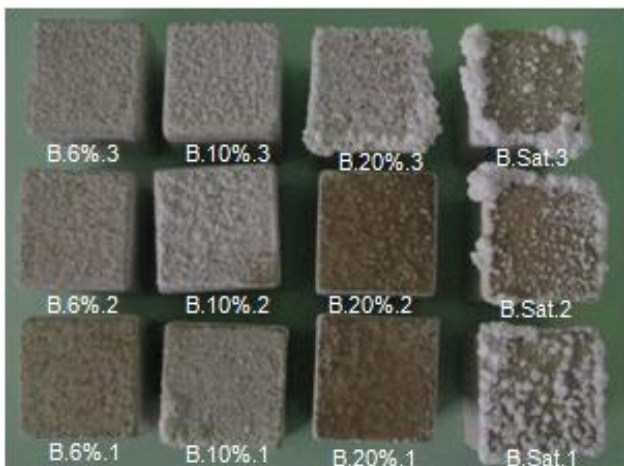


**Fig. 14** Bentheimer specimens contaminated with NaCl solutions with concentrations of 6%, 10%, 20% and saturated (from left to right)





**Fig. 15** Thick, compact and vitreous NaCl crust of irregular texture with isolated salt crystals: 30x magnification of B.20.2 specimen

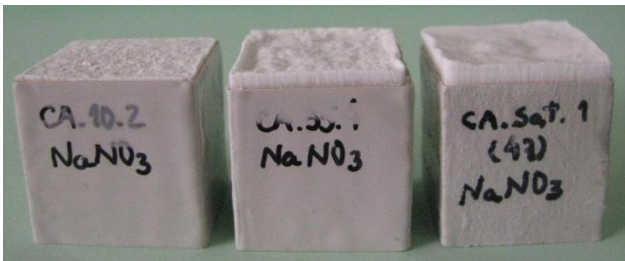


**Fig. 16** Thickness of NaNO<sub>3</sub> layer increases with the concentration of salt in Ançã limestone (from left to right)

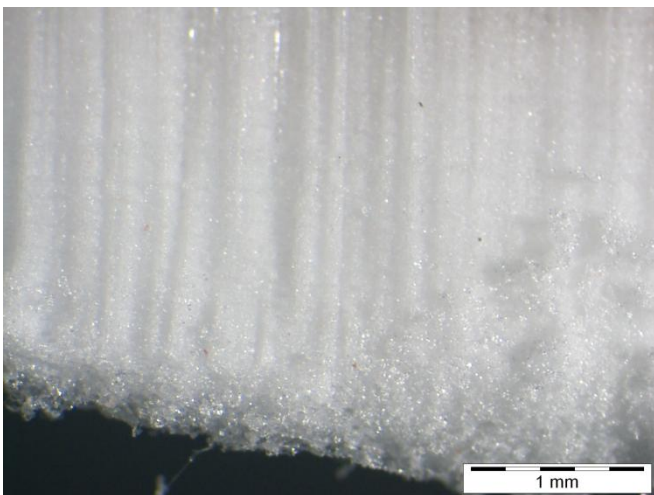


**Fig. 17** Porous surface layer of NaNO<sub>3</sub>: 30x magnification of CA.Sat specimen

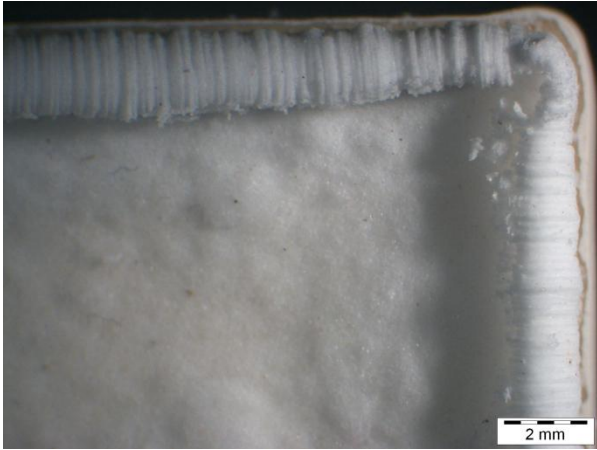


**Fig. 18** Preferential deposition of  $\text{NaNO}_3$  at the edges: 7.5x magnification of CA.35% specimen

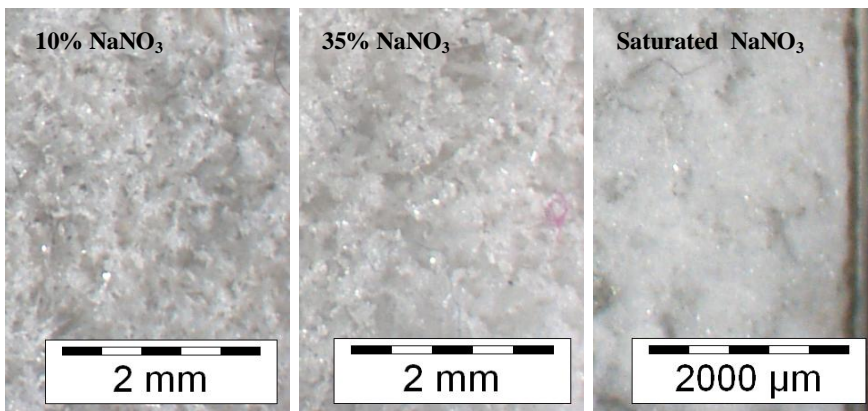


**Fig. 19** Porous coat of whisker-like  $\text{NaNO}_3$  efflorescence in "grey limestone" (salt concentration increases from left to right): 7.5x magnification

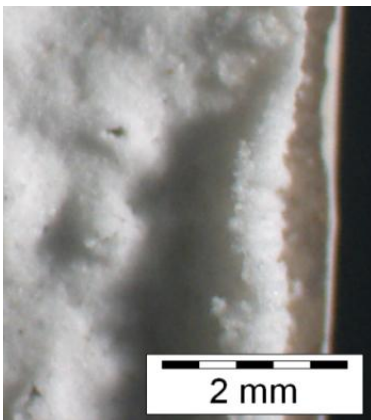


**Fig. 20** Different  $\text{NaNO}_3$  efflorescence morphology: 7.5x magnification of one CC.35 specimen

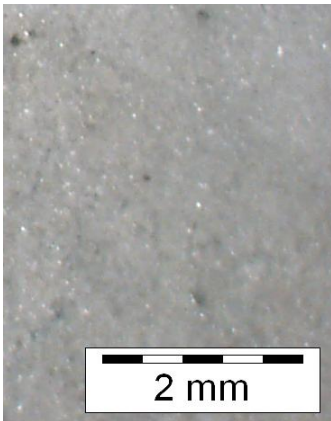


**Fig. 21**  $\text{NaNO}_3$  crust more compact and without holes: 7.5x magnification of one CC.Sat specimen

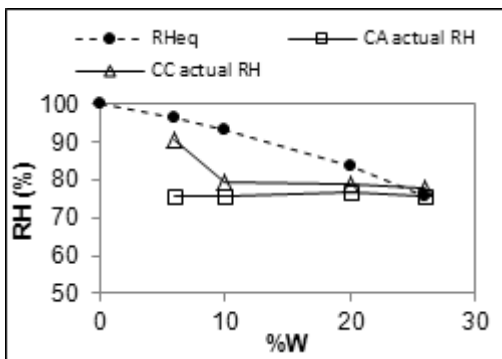


**Fig. 22** RH above the CA and CC limestones contaminated with sodium chloride solutions of different concentration (in bold, the RHeq of the salt solutions is presented as a reference)

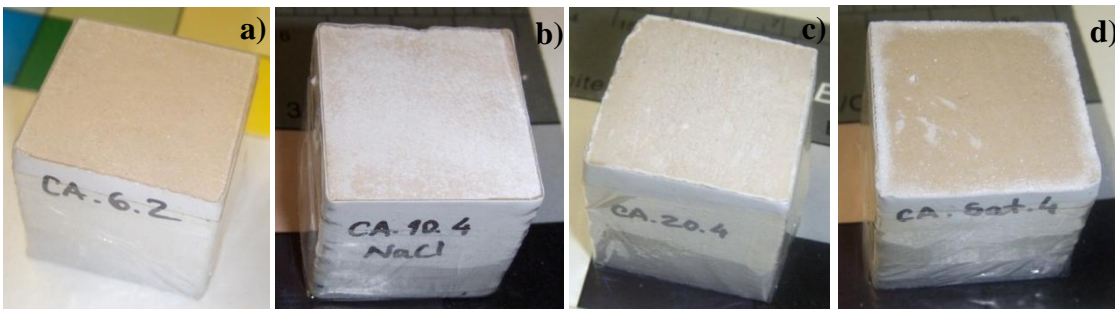


**Fig. 23** Specimens showing efflorescence during RH measurements: a) 6% NaCl, b) 10% NaCl, c) 20% NaCl and d) saturated NaCl

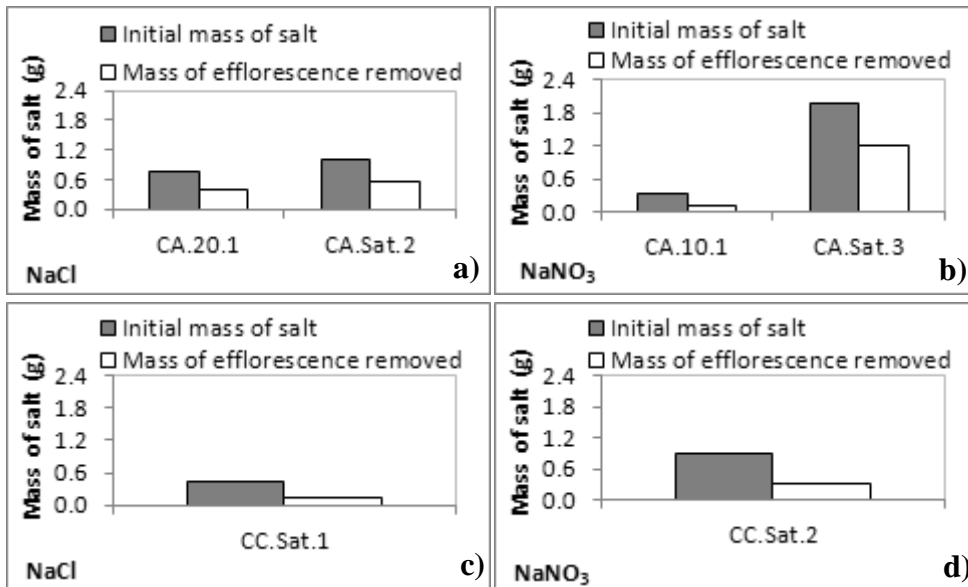


**Fig. 24** Total amount of salt introduced in the specimens and total amount that crystallized as efflorescence (for the purpose of its quantification, efflorescence was removed from the surface of these specimens by scraping): a) two CA-NaCl specimens, b) two CA-NaNO<sub>3</sub> specimens, c) one CC-NaCl specimen and d) one CC-NaNO<sub>3</sub> specimen

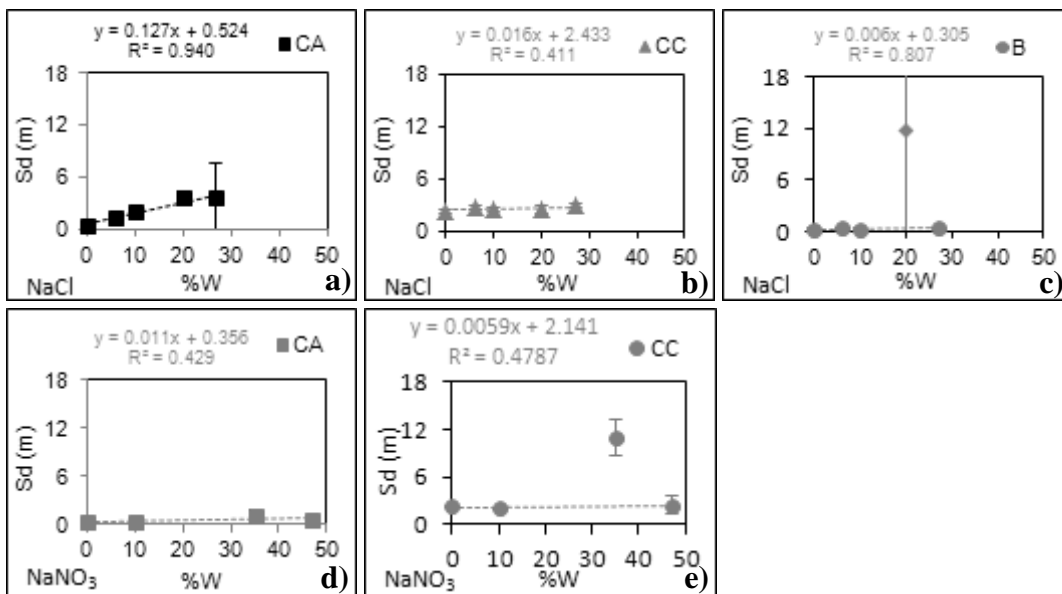


**Fig. 25** Equivalent air layer thickness (Sd) as a function of the solution's concentration of the salt solutions: a) CA-NaCl, CC-NaCl, c) B-NaCl, d) CA-NaNO<sub>3</sub> and e) CC-NaNO<sub>3</sub>

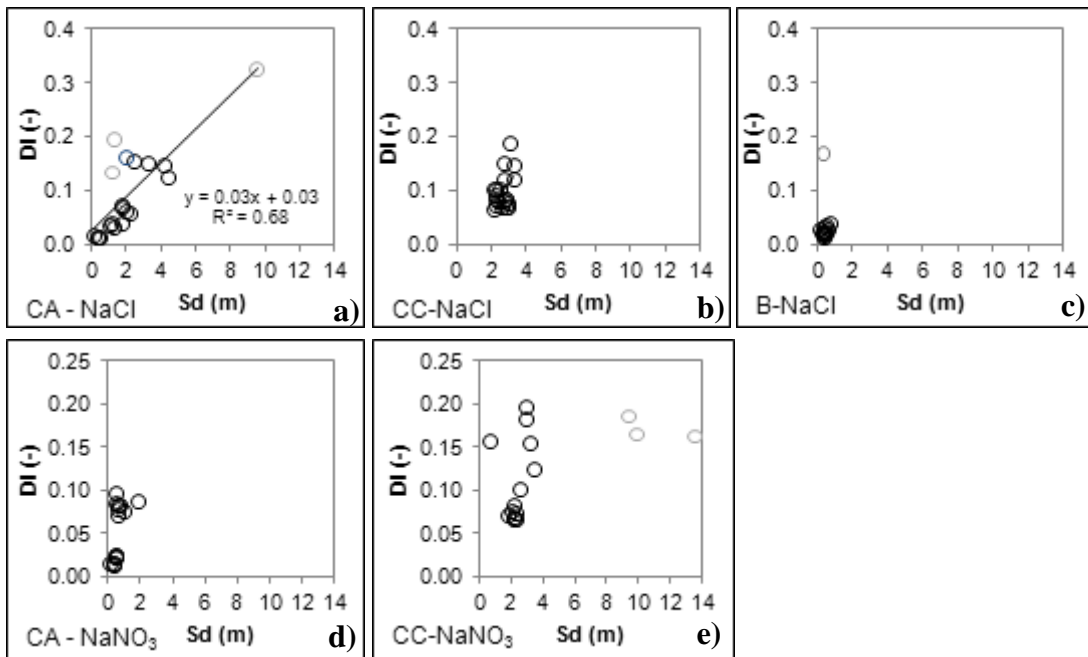


**Fig. 26** Correlation between drying index (DI) and equivalent air layer thickness (Sd); the grey bullets are the specimens with deviant vapour permeability behaviour and different efflorescence morphology. a) CA with NaCl, b) CC with NaCl, c) B with NaCl, d) CA with NaNO<sub>3</sub> and d) CC with NaNO<sub>3</sub>

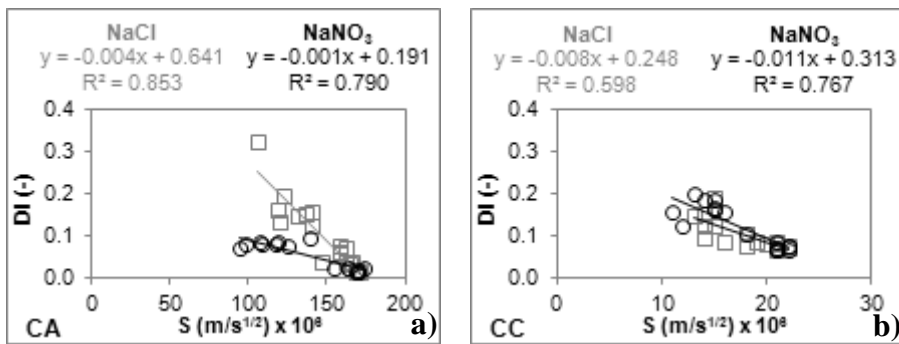


**Fig. 27** Correlation between drying index (DI) and sorptivity (S) for: a) CA and b) for CC

**Table 1** Physical characteristics of the salt solutions

Salt solution	Concentration W%	Equilibrium relative humidity (%) at 25°C (Robinson and Stokes 2002)	Density (kg/l) at 20°C (CRC 1986)	Surface tension (mN/m) at 20°C (CRC 1986)	Absolute viscosity (cP) at 20°C (CRC 1986)
NaCl	6	96.4 <sup>a</sup>	1.0413	74.82 <sup>a</sup>	1.104
	10	93.5 <sup>a</sup>	1.0707	75.92 <sup>a</sup>	1.194
	20	83.9 <sup>a</sup>	1.1478	79.51 <sup>a</sup>	1.558
	26	76.0 <sup>a</sup>	1.1972	82.55	1.990
NaNO <sub>3</sub>	10	96.1 <sup>a, c</sup>	1.0674	74.24 <sup>a</sup>	1.081
	35	83.2 <sup>b, c</sup>	1.2704 <sup>a</sup>	79.52 <sup>a</sup>	1.884 <sup>a</sup>
	47	72.7 <sup>b, c</sup>	1.3586 <sup>b</sup>	87.05	2.853 <sup>b</sup>

Concentration = (mass of solute / mass of solution) x 100; W% – weight percent

<sup>a</sup> Data obtained by interpolation.

<sup>b</sup> Data obtained by extrapolation.

<sup>c</sup> The equilibrium relative humidity of the salt solutions was determined using equation

$\ln a_w = -\Phi \cdot M_w \cdot v \cdot m$ . This equation relates the water activity,  $a_w$  (dimensionless), of a solution to its molal osmotic coefficient  $\Phi$  (dimensionless).  $M_w$  (kg/mol) is the molar mass of pure water,  $v$  (dimensionless) is the stoichiometric parameter and  $m$  (mol/kg) is the molality of the solution.

**Table 2** Percentage of sorptivity of saturated salt solutions in relation to the pure water sorptivity

Material	CA	CC	B
Salt solution	Sorptivity (% of the value obtained for pure water)		
NaCl	71	69	73
NaNO <sub>3</sub>	61	62	59

**Table 3** Summary of capillary absorption results

Solution	Concentration (% w/w)	CA				CC				B									
		Sorptivity (m/s <sup>1/2</sup> ) x 10 <sup>6</sup>		CV	i <sub>max</sub> (m) x 10 <sup>3</sup>		CV	Sorptivity (m/s <sup>1/2</sup> ) x x 10 <sup>6</sup>		CV	i <sub>max</sub> (m) x 10 <sup>3</sup>		CV						
		Mean	SD		Mean	SD		Mean	SD		Mean	SD		Mean	SD				
water	0	<b>166.2</b>	4.6	2.8	5.6	0.1	1.8	<b>20.2</b>	1.6	8.1	2.3	0.1	3.8	<b>304.7</b>	17.7	5.8	14.8	0.4	2.7
	6	<b>157.5</b>	10.3	6.5	5.5	0.3	5.5	<b>20.8</b>	1.5	7.1	2.4	0.1	4.3	-	-	-	-	-	-
NaCl	10	<b>154.3</b>	8.0	5.2	5.3	0.3	5.3	<b>19.8</b>	2.3	11.7	2.4	0.1	5.9	-	-	-	-	-	-
	20	<b>135.5</b>	5.0	3.7	5.4	0.1	2.8	<b>16.7</b>	1.8	10.5	2.4	0.1	4.6	-	-	-	-	-	-
	27 (Sat)	<b>118.7</b>	7.4	6.3	5.2	0.2	3.5	<b>14.0</b>	0.9	6.4	2.3	0.0	1.6	<b>222.0</b>	11.4	5.1	14.5	0.2	1.5
	10	<b>163.5</b>	8.2	5.0	5.3	0.2	3.2	<b>21.5</b>	0.6	2.7	2.5	0.0	1.2	-	-	-	-	-	-
NaNO <sub>3</sub>	35	<b>125.3</b>	9.7	7.7	5.2	0.2	3.0	<b>15.3</b>	0.5	3.3	2.4	0.1	2.6	-	-	-	-	-	-
	47 (Sat)	<b>102.0</b>	6.5	6.4	5.4	0.1	2.4	<b>12.5</b>	1.3	10.3	2.4	0.1	5.1	<b>178.3</b>	20.4	11.4	14.6	0.3	2.1

SD – standard deviation CV - coeficiente of variation